



National Library
of Canada

Bibliothèque nationale
du Canada

Canadian Service Service des thèses canadiennes

Ottawa, C
K1A 0N4

NOTICE

The quality of this microform is heavily dependent upon the quality of the original thesis submitted for microfilming. Every effort has been made to ensure the highest quality of reproduction possible.

If pages are missing, contact the university which granted the degree.

Some pages may have indistinct print especially if the original pages were typed with a poor typewriter ribbon or if the university sent us an inferior photocopy.

Previously copyrighted materials (journal articles, published tests, etc.) are not filmed.

Reproduction in full or in part of this microform is governed by the Canadian Copyright Act, R.S.C. 1970, c. C-30.

AVIS

La qualité de cette microforme dépend fondamentalement de la qualité de la thèse soumise au microfilmage. Nous avons tout fait pour assurer une qualité supérieure de reproduction.

Si manque des pages, veuillez communiquer avec l'université qui a conféré le grade.

La qualité d'impression de certaines pages peut laisser à désirer, surtout si les pages originales ont été dactylographiées à l'aide d'un ruban usé ou si l'université nous a fait parvenir une photocopie de qualité inférieure.

Les documents qui font déjà l'objet d'un droit d'auteur (articles de revue, tests publiés, etc.) ne sont pas microfilmés.

La reproduction, même partielle, de cette microforme est soumise à la loi canadienne sur le droit d'auteur, SRC 1970, c. C-30.

THE UNIVERSITY OF ALBERTA

EPITHELIAL INVOLVEMENT IN CHOLELITHIASIS IN GROUND SQUIRRELS

BY

RAMJEET SINGH ~~PENSINGH~~

A THESIS

SUBMITTED TO THE FACULTY OF GRADUATE STUDIES AND RESEARCH

IN PARTIAL FULFILMENT OF THE REQUIREMENTS FOR THE DEGREE

OF DOCTOR OF PHILOSOPHY

DEPARTMENT OF ANATOMY AND CELL BIOLOGY

EDMONTON, ALBERTA

(FALL 1987)

Permission has been granted to the National Library of Canada to microfilm this thesis and to lend or sell copies of the film.

The author (copyright owner) has reserved other publication rights, and neither the thesis nor extensive extracts from it may be printed or otherwise reproduced without his/her written permission.

L'autorisation a été accordée à la Bibliothèque nationale du Canada de microfilmer cette thèse et de prêter ou de vendre des exemplaires du film.

L'auteur (titulaire du droit d'auteur) se réserve les autres droits de publication; ni la thèse ni de longs extraits de celle-ci ne doivent être imprimés ou autrement reproduits sans son autorisation écrite.

ISBN 0-315-41065-5

THE UNIVERSITY OF ALBERTA

RELEASE FORM

NAME OF AUTHOR:..... Ramjeet S. Pemsingh.....
TITLE OF THESIS:..... Epithelial Involvement in Cholelithiasis
..... in Ground Squirrels.....
DEGREE:..... Doctor of Philosophy in Anatomy & Cell Biology.....
YEAR THIS DEGREE GRANTED:..... Fall, 1987.....

Permission is hereby granted to THE UNIVERSITY OF ALBERTA LIBRARY to reproduce single copies of this thesis and to lend or sell such copies for private, scholarly or scientific research purposes only.

The author reserves other publication rights, and neither the thesis nor extensive extracts from it may be printed or otherwise reproduced without the author's written permission.

Ramjeet S. Pemsingh
.....
(Student's signature)

407 Michener Park, Edmonton, Alberta.....
(Student's permanent address)

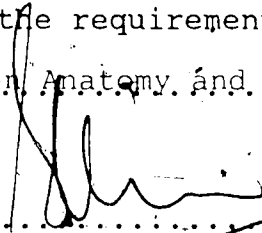
Canada, T6H 4M5.....

Date: June 25, 1987

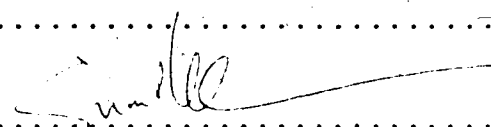
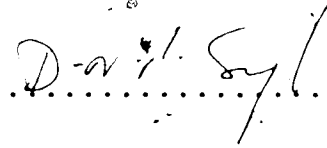
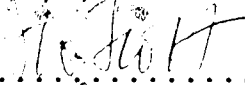
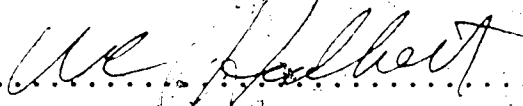
THE UNIVERSITY OF ALBERTA

FACULTY OF GRADUATE STUDIES AND RESEARCH

The undersigned certify that they have read, and recommend to the Faculty of Graduate Studies and Research for acceptance, a thesis entitled. Epithelial Involvement in Cholelithiasis in Ground Squirrels..... submitted by.. Ramjeet S. Pemsingh..... in partial fulfilment of the requirements for the degree of Doctor of Philosophy in Anatomy and Cell Biology.....



(Supervisor)



(External examiner)

To my two sons, Navendra K. and Sachin N.

ABSTRACT

The search for an appropriate animal model to study cholelithiasis is ongoing. The present study was designed to determine whether the Richardson's ground squirrel (Spermophilus richardsonii) would be a suitable model in which to study cholesterol precipitation, the formation of biliary concretions, mucosal changes occurring prior to, during and after stone formation, and compare these findings with those in humans and in other models.

Two hundred and thirty-eight ground squirrels of both sexes were divided into control and experimental groups. Each group contained at least four animals. The experimental groups were fed a 2% cholesterol-enriched rat chow diet for intervals of 6, 12, 18, 24 hours, 3, 5, 7 days, 2, 3, 10, 20 weeks, and 3 weeks on cholesterol-enriched diet followed by 3 weeks on normal rat chow diet.

The results indicated that in control animals, the gallbladder epithelium was composed of three types of cells: light, dark and edematous, the latter being extruded from the epithelial sheet. Normal columnar epithelial cells underwent mitoses. The basal lamina formed peg and socket interdigitations with the basal plasma membrane, and desmosomes were seen throughout the lateral membranes.

Noradrenergic nerve fibers were seen beneath the lining epithelium and between muscle bundles. A basal level of both sialylated and sulphated mucins was exocytosed in membrane-bound granules by merocrine secretion.

In experimental animals, mucus hypersecretion and bile lithogenicity occurred as early as 18 hours and continued throughout the experimental period. Cholesterol monohydrate crystal precipitation occurred in 24 hours, microliths were formed in 2-3 weeks and mulberry stones occurred within 10 weeks. The larger stones contained 61-74% cholesterol. Mucosal changes observed include increased cellular proliferation in one week, cellular damage and extrusion, hypertrophy and hyperplasia in 10 weeks, plasma cell infiltration and Rokitansky-Aschoff sinuses in 20 weeks. Other mucosal changes observed were lipid accumulation intercellularly and intracellularly in 12 hours, deposition of cholesterol and neutral lipid supranuclearly and basally by 7 days and in the lamina propria and its macrophages by 20 weeks.

The present study demonstrated that the Richardson's ground squirrel is an excellent model to study the pathogenesis of cholesterol gallstone disease.

ACKNOWLEDGEMENTS

I wish to express my gratitude to Dr. Brian R. MacPherson for agreeing to be my supervisor and for his constant advice and support during the course of this study.

I would also like to express my deep appreciation to Dr. D.N.P. Singh, Dr. G.W. Scott and Dr. T.S. Leeson for their advice and valuable criticisms in the preparation of this thesis.

I wish to extend special thanks to Ms C. Long, Ms D. Colwell, G. Morrison and G. Higgs for their technical assistance.

I wish to thank all my colleagues, faculty and staff of the Department of Anatomy and Cell Biology for their help and cooperation in various capacities.

I wish to acknowledge the financial support of the Alberta Heritage Foundation for Medical Research for awarding me a Studentship and the Medical Research Council of Canada and Central Research Fund of the University of Alberta for supporting this project.

Finally, I wish to thank my wife, Jasmin and my two sons, Navendra and Sachin, for their perseverance, understanding and encouragement throughout the period of study.

TABLE OF CONTENTS

Chapter	Page
1. INTRODUCTION.....	1
2. LITERATURE REVIEW.....	4
Uptake of dietary cholesterol.....	4
Cholesterol in the liver.....	7
Bile.....	8
Mucus.....	10
Function of mucus.....	11
Role of mucus in gallstone formation.....	12
Factors regulating mucus secretion.....	14
Crystal and stone formation.....	16
Mucosal changes.....	18
Animal models of gallstone disease.....	22
Pigment stones.....	24
Cholesterol stones.....	24
Objectives.....	27
3. MATERIALS AND METHODS.....	33
4. RESULTS.....	43
Controls.....	43
Light cells.....	46
Mucus secretion.....	46
Dark cells.....	48
Edematous cells.....	48
Experimental animals.....	51
Mucus secretion.....	51

Crystal precipitation and stone formation....	53
Mucosal changes.....	57
Cell proliferation and damage.....	57
Cholesterolosis-like lesion.....	60
5. DISCUSSION.....	70
Controls.....	70
Mucus.....	76
Experimental animals.....	80
Mucus secretion.....	80
Crystal precipitation and stone formation....	81
Mucosal changes.....	88
Cell proliferation and damage.....	88
Cholesterolosis-like lesion.....	94
6. SUMMARY AND CONCLUSION.....	100
BIBLIOGRAPHY.....	164
APPENDIX I-VI.....	183

TABLES

page

Table I. Mucus secretion..... 64

Table II. Bile lithogenicity..... 65

Table III. Mitotic and labelling indices..... 66

LIST OF FIGURES

	Page
Figure 1. A TEM micrograph of a control animal showing light and dark cells.....	104
Figure 2. A TEM micrograph of a control animal showing a fenestrated capillary.....	104
Figure 3. Unmyelinated nerve in a control animal.....	104
Figure 4. Adrenergic nerve between muscle bundles.....	106
Figure 5. Adrenergic nerve beneath the basal lamina....	106
Figure 6. A TEM micrograph of a control animal showing organelles and junctional complex.....	106
Figure 7. A TEM micrograph showing microfilaments near a centriole.....	108
Figure 8. A lipid droplet in an epithelial cell of a control animal.....	108
Figure 9. An actively secreting epithelial cell.....	108
Figure 10. A LM micrograph showing both sialylated and sulphated mucins in control gallbladder.	110
Figure 11. A LM micrograph showing sialylated mucin with side chain substitution.....	110
Figure 12. An EM autoradiograph of a control animal.....	112
Figure 13. An EM autoradiograph of a treated animal.....	114
Figure 14. An EM autoradiograph of a control animal.....	114
Figure 15. Secretory granules in subapical region.....	114
Figure 16. Secretory granule extrusion.....	116
Figure 17. An apical bulla in a control animal.....	116
Figure 18. An EM micrograph of mitosis in a control animal.....	116
Figure 19. An EM micrograph of a dark cell.....	118

Figure 20. An EM micrograph of a dark cell.....	118
Figure 21. An EM micrograph of an edematous cell.....	118
Figure 22. An EM micrograph of an edematous cell.....	120
Figure 23. An EM micrograph showing peg and socket interdigitations.....	120
Figure 24. An EM micrograph showing intercellular spaces distention.....	120
Figure 25. An EM micrograph of an intact desmosome.....	122
Figure 26. Reduction of peg and socket interdigitations under actively transporting cells.....	122
Figure 27. A leucocyte migrating through the basal lamina.....	122
Figure 28. A leucocyte near junctional complex.....	124
Figure 29. A SEM micrograph of control gallbladder.....	124
Figure 30. A SEM micrograph of filled gallbladder.....	124
Figure 31. SEM of mucus release in control gallbladder..	126
Figure 32. SEM of control gallbladder showing lateral interdigitations.....	128
Figure 33. SEM micrograph showing oval nuclei in cells..	128
Figure 34. SEM micrograph of basal lamina.....	128
Figure 35. Mucus secretion at 18 hours.....	130
Figure 36. Mucus secretion at one day.....	130
Figure 37. Sludge-like material at 3 days.....	130
Figure 38. Sludge and lamination of crystals at 5 days..	130
Figure 39. A micrograph of mucus granules at 7 days.....	132
Figure 40. A TEM micrograph of an apical bulla.....	132
Figure 41. Sludge material at 2 weeks.....	134
Figure 42. Sludge material at 0 weeks.....	134
Figure 43. SEM of apical bulla in 5 days animals.....	134

Figure 44. Mucus secretion in 3W3R animals.....	134
Figure 45. Small cholesterol crystals at one day.....	136
Figure 46. Small cholesterol crystals at 7 days.....	136
Figure 47. Platelets at 2 weeks.....	136
Figure 48. Platy units with biliary material.....	136
Figure 49. Microlith at 3 weeks.....	138
Figure 50. Concrements of 10 week animal.....	138
Figure 51. Lobular subunits of 10 week stones.....	138
Figure 52. Multilobular shape of 10 week stone.....	138
Figure 53. SEM of component lobules.....	140
Figure 54. Biliary sludge of component lobules.....	140
Figure 55. Mulberry stone at 20 weeks.....	140
Figure 56. Polished regions of mulberry stone.....	140
Figure 57. Fractured edge of stones showing capsule and septum.....	142
Figure 58. Central region of fractured stone.....	142
Figure 59. TEM micrograph of mitosis at 2 weeks.....	144
Figure 60. LM autoradiograph of 2 week animal.....	144
Figure 61. SEM micrograph showing defects in the epithelial sheet.....	146
Figure 62. TEM micrograph showing no defect in the epithelial sheet.....	146
Figure 63. SEM of hypertrophy at 10 weeks.....	148
Figure 64. LM showing hyperplasia.....	148
Figure 65. Rokitansky-Aschoff sinuses at 20 weeks.....	148
Figure 66. Inflammatory cells in lamina propria at 20 weeks.....	150
Figure 67. Inflammatory cells between epithelial cells and basal lamina at 20 weeks.....	150

Figure 68. LM autoradiograph showing labelled fibroblasts in lamina propria.....	152
Figure 69. LM autoradiograph showing labelled fibroblasts in adventitia at 2 weeks....	152
Figure 70. Lipid accumulation at 12 hours.....	154
Figure 71. Residual bodies at one day.....	154
Figure 72. Lipid accumulation at 7 days.....	156
Figure 73. Lipid accumulation at 7 days.....	156
Figure 74. Control gallbladder stained with oil red O...	158
Figure 75. Frozen section stained with oil red O.....	158
Figure 76. Lipid droplets in basal regions of cells.....	160
Figure 77. Digitonin complexed gallbladder at 7 days showing cholesterol in cisternae.....	160
Figure 78. Digitonin complexed gallbladder showing free cholesterol in residual bodies.....	162
Figure 79. Digitonin revealing free cholesterol on epithelial surface.....	162
Figure 80. Osmiophilic droplets in lamina propria at 20 weeks.....	162
Figure 81. Macrophage in lamina propria with inclusions at 20 weeks.....	162

INTRODUCTION

Gallstones, although recognised for centuries, have commanded special attention over the past few decades. This has occurred because gallstone disease now represents a major health problem in Canada, affecting some 130,000 adults per year. It is the most common abdominal surgical problem in Canada with about 80,000 cholecystectomies per year performed at a cost of some \$280,000,000 (Shaffer, 1980; Vayda, 1973).

The presence of gallstones in the human population is higher because about 90% of the affected people with some form of gallbladder disease displayed minor or no symptoms (silent stones) (Bouchier, 1984).

The formation of gallstones depends on a number of factors. The presence of a lithogenic bile in the gallbladder is not sufficient to produce cholelithiasis. In addition the gallbladder mucosa (mucus hypersecretion), muscularis (stasis) and nucleating factor(s) are involved. The nucleating factor(s) have not been fully identified but there is increasing evidence that mucus is involved (LaMont et al., 1984).

Human gallbladder tissue obtained from

cholecystectomies are generally in the end stage of the disease process and as such it is difficult to chronologically evaluate hepatobiliary physiology, gallstone formation or other disease of the gallbladder. This results in major gaps in our knowledge and the need for animal models to fill these gaps.

A number of animal models have been developed to study gallbladder disease (Malet, 1985; Holzbach, 1984; Hoffmann, 1984). Freston and Bouchier (1968) listed eight features that are optimal for an ideal model. (see literature review). A number of these models such as: dog, rabbit, mouse, hamster and guinea pig failed to fulfill these criteria either because of the diet used, type of stone formed, length of time needed for stone formation or pathological changes occurring in other organs besides the gallbladder.

The prairie dog model most closely fulfills the criteria of Freston and Bouchier (1968). The caloric distribution of the diet is similar to man, the type of stone formed, rapid development of stones, and an adequate amount of tissue and bile make this model ideal to study gallbladder disease.

The scarcity and protected status of the prairie dog

in Canada led Davison et al. (1982) and Fridhandler et al. (1983) to further developed Patton et al.'s (1961) ground squirrel model. The Richardson's ground squirrel, when fed a 1% cholesterol-enriched rat chow diet, secreted bile with an increased lithogenic index close to saturation levels within two weeks and defective gallbladder contractility before crystal precipitation (Fridhandler et al., 1983). A thorough systematic investigation of this model in the cholelithiasic process however was lacking. This study was designed to:

- (a) describe the morphology of the normal ground squirrel gallbladder
- (b) identify the chronology of crystal and stone formation
- (c) describe the morphology and method of formation of these biliary concretions
- (d) describe intraepithelial and mucosal changes occurring prior to, during and after stone formation.

LITERATURE REVIEW

Uptake of dietary cholesterol

The source of cholesterol is twofold. As much as 10% is manufactured by the liver at a rate of 1000mg a day. The other source is dietary intake. Some foods have a high cholesterol content: beef kidney(90g)- 633mg; beef liver (90g)- 372mg; one egg- 275mg; doughnut(90g)- 10mg; french fries(90g)- 20mg (Langone, 1984).

Cholesterol, which is present in all diets chiefly as free alcohol, is hydrolyzed by pancreatic cholesterol esterase before it is absorbed. Bile and fat are necessary for cholesterol absorption. Bile, phospholipids, triglycerides (fat) and cholesterol form micelles which are taken into the columnar epithelial cells of the small intestine by passive diffusion and active absorption in the terminal ileum. In the absence of bile and fat, no cholesterol is absorbed. Cholesterol fed in a fat-free diet may also be absorbed because endogenous fat, sufficient for micelle formation, is always present in the intestinal contents. Cholesterol is rapidly absorbed by the intestinal mucosa, reaching a peak 3 hours after a meal in man, and then is slowly released into the lymph with a peak at 9 hours after the meal (Davenport, 1971).

Cholesterol in the intestinal epithelial cells comes from three sources: (1) bile (60%), (2) dietary (20%), (3) desquamated mucosal cells (20%). These pools of cholesterol in the mucosal epithelium do not mix. The mechanism of separation is unknown (Davenport, 1971; Turley and Dietschy, 1982).

Lipid droplets in the lumen, emulsified by the action of bile salts, are broken down by pancreatic lipase. This process releases free fatty acids and monoglycerides that diffuse across the apical membrane and accumulate in the apical cytoplasm. Short chain fatty acids diffuse through the cell and enter the capillaries. Long chain fatty acids and monoglycerides serve as substrates for triglyceride-synthesizing enzymes located in the smooth endoplasmic reticulum (SER). The resynthesized triglyceride, combined with cholesterol esters, phospholipid and a glycoprotein component (apoprotein) are synthesized in the rough endoplasmic reticulum (RER) to form a chylomicron. Chylomicrons are transported in vesicles, whose membrane is derived from the Golgi complex, to the lateral cell surfaces and are discharged by exocytosis into the intercellular spaces (Davenport, 1971; Turley and Dietschy, 1982; Davidson and Glickman, 1971).

Chylomicrons cannot pass through the basement

membrane and therefore do not enter capillaries. Only short and medium size fatty acids (10%) enter the portal system and are taken to the liver. On the other hand, chylomicrons can enter lymphatic lacteals through the open channels between the interstitial spaces to the lymphatic lumen. The endothelial walls of the lacteal are thick but there is no enveloping basement membrane. The droplets pass the endothelial separations. The cells forming the walls of lacteals contain many pinocytotic vesicles capable of carrying fat droplets across them. Once within the lacteals, the fat droplets are carried centrally by the tidal flow of the lymph caused by contraction of smooth muscle fibers of the villi or the gross movements of the mucosa. Once delivered to the blood, chylomicrons do not recirculate in the lymph. In the capillaries of adipose and muscle tissue, the triglyceride bonds are cleaved by the enzyme lipoprotein lipase and the fatty acids are removed either to be stored as adipose tissue or used in muscle for oxidation to supply energy (Davenport, 1971; Davidson and Glickman, 1971).

The remnant of the chylomicron containing the cholesteryl esters is removed from the circulation by receptors at sites present only in the liver (Brown and Goldstein, 1984; 1986).

Cholesterol in the liver

The cholesterol pool in the liver is fairly constant. It is maintained by either dietary absorption and synthesis or excretion (Paumgartner and Paumgartner, 1984). Cholesterol in the liver is derived from three different sources. (1) Dietary cholesterol or cholesterol synthesized in the intestinal mucosa that reached the liver. (2) Cholesterol that is synthesized in extrahepatic tissues (skin, muscles) that reached the liver via high density lipoprotein (HDL) and very low density lipoprotein (VLDL). (3) Synthesis of cholesterol in the liver itself (Turley and Dietschy, 1982).

The loss of cholesterol from the liver pool is by:
(1) loss directly from the body pool by sloughing of oily secretions and cells from the skin, through desquamation of cells from the stomach, small intestine and colon. (2) Cholesterol molecules may be metabolized to other products such as testosterone and adrenocorticosteroids which may in turn be excreted from the body through urine or the gastrointestinal tract. (3) Synthesis of bile acids from cholesterol into bile. (4) Secretion of cholesterol into bile (supersaturation) (Turley and Dietschy, 1982).

Bile

Bile is an aqueous solution continuously secreted at a variable rate by parenchymal cells of the liver into bile canaliculi from which it flows to the hepatic duct. Bile secretion is under nervous, hormonal and chemical control. Stimulation of the vagus nerve, injection of secretin and administration of cholergics increase bile flow (Van der Linden and Bergman, 1977; Paumgartner and Sauerbruch, 1983).

Bile is used as an excretory mechanism by the liver to rid itself of endogenous and exogenous products and maintain homeostasis by excretion of organic ions and cations, neutral compounds, heavy metals and bilirubin. Bile also contains IgA from blood (vesicular transport), lysosomal enzymes (exocytosis) and Na^+ with water from intercellular spaces. Bile ductules and ducts alter the composition and volume of canalicular bile by reabsorption and secretion of water and electrolytes (bicarbonate). Secretion of ductular bile is stimulated by secretin and other gastrointestinal hormones (Paumgartner and Paumgartner, 1984; Paumgartner and Sauerbruch, 1983).

Bile is composed of bile acids: cholic acid, chenodeoxycholic acid (primary), deoxycholic and

9

lithocholic acid (secondary), phospholipids (lecithin) and cholesterol. The primary bile acids are synthesised from cholesterol. Thus, cholesterol is a normal constituent of bile and biliary excretion is the only significant excretory route for this lipid. The mechanism of controlling the secretion of cholesterol in bile is not fully known (Van der Linden and Bergman, 1977; Turley and Dietschy, 1982).

Biliary cholesterol is derived from cholesterol synthesized in the liver, from extrahepatic tissue and from dietary absorption. Under normal conditions, the secretion of cholesterol into bile is closely linked to phospholipids and bile acid secretion. This coupling is brought about by the capacity of bile acids to form micelles. These structures incorporate relatively large amounts of phospholipids to form mixed micelles, which normally facilitate the complete solubilization of all cholesterol secreted into the bile. Recently, it has been shown that phospholipid vesicles existed in bile which contributed significantly to the solubilization and transport of cholesterol (Holzbach, 1986). For reasons that are poorly understood, this coupling reaction can become disrupted, so that more cholesterol enters the bile than can be solubilized by the bile acids and phospholipid present. The production of such a lithogenic bile is the initiating event in the

pathogenesis of cholesterol gallstone disease. It can involve a variety of secretory defects ranging from excessive cholesterol secretion without any change in bile acid and phospholipid secretion rates to decreased bile acids and phospholipid secretion without any change in cholesterol output (Goldstein and Brown, 1984; Turley and Dietschy, 1982).

Mucus

Mucus also called mucin, mucoprotein, mucopolysaccharide and glycoprotein is the slimy secretion of epithelial membranes which contains water, salts and immunoglobulins (LaMont et al., 1984; Freston et al., 1969). The structure and composition of mucus from various organs and mammalian species appeared to vary only slightly. It is a high molecular weight substance with 75% carbohydrate, 20% peptide core and the remainder consisting of variable amount of sulphate, bound counter ions and water. Only 5 monosaccharides occur in mucus: (1) fucose, (2) galactose, (3) sialic acid; (4) N-acetyl glucosamine and (5) N-acetyl galactosamine. These are branching side chains of 5 to 15 residues per chain linked to the peptide core via an O-glycosidic bond to either serine or threonine (LaMont et al., 1984; Allen, 1981; Smith and LaMont, 1985a).

Mucus secretions can be classified into 3 groups on the basis of their histochemical staining: (a) Neutral mucins which stain only with the PAS technique. (b) Sialic acid-containing mucin. Sialic acid is a generic name for various neuraminic acids which differ from each other in whether they are substituted with an acetyl or glycolyl residue on their amino acid group and the number of O-acetyl substitutions on the hydroxyl group. (c) Ester sulphate containing mucin. The acidic mucin stains with basic dyes like alcian blue and/or high iron diamine. The distinction between sialic acid and sulphate groups is achieved by varying the salt concentration or the pH of the staining solution. The specificity of these techniques is increased by the use of enzymes to remove the sugar moieties; *ie.* neuraminidase selectively removes sialic acid (Reid *et al.*, 1985; Pearse, 1968; Spicer, 1965). It is therefore possible to specifically characterize the various types of mucins secreted based on their staining properties.

Function of mucus in the G.I. tract

There are three main functions of mucus secreted by epithelial cells of the gastrointestinal tract.

- (1) Protect the delicate mucosal epithelium of the G.I. tract from damage by food, fecal contents and vigorous

forces that accompany digestion.

(2) Provide slimy lubrication for the passage of solid material and a diffusion barrier to noxious substances.

(3) Retain water and provide a perpetual aqueous environment for the mucosal surface (Allen, 1981; Smith and LaMont, 1985b).

Role of mucus in gallstone formation

Mucin, a high molecular weight glycoprotein, is secreted by the gallbladder and biliary duct epithelium. It exists as a sol phase of monomers in the luminal secretion and gel phase of polymers adherent to the epithelial surface. A common feature in all animal models of gallstone formation has been mucus hypersecretion and/or concentration in all cholesterol stones (LaMont et al., 1984). Mucus increases the viscosity of bile. Gallbladder mucus shares with other epithelial mucins the ability to bind lipids, bile pigments and calcium (Smith and LaMont, 1983; Forstner and Forstner, 1975). It is the protein core of mucin which provides a hydrophobic domain that does the actual binding. The lipid binding properties of mucin may contribute to the nucleation process by providing a hydrophobic microenvironment in the mucus gel which will be favourable to nucleation of cholesterol monohydrate.

crystals either from the micellar phase or from a mesophase of lecithin-cholesterol liquid crystal (LaMont et al., 1984). Womack et al. (1963, 1971) demonstrated the presence of mucus at the center of human gallstones and showed histochemically that there was a thin layer of mucoid substance at the surface of the diseased gallbladder epithelium. Previous studies have shown that mucus hypersecretion actually precedes stone and crystal formation and is an integral part of the nucleating process (Lee et al. 1981b; Freston et al., 1969).

Mucin may also be involved in the pathogenesis of pigmented stones. Maki et al. (1971) reported the presence of sulphated glycoprotein in human pigmented stones. These concretions have a 3-20% glycoprotein-mucin-bilirubin complex (Smith and LaMont, 1985a).

Previous studies have shown that it is difficult to measure mucus synthesis and secretion directly. Indirect measurements were done by estimating mucus gland hyperplasia or the viscosity of gallbladder bile (LaMont et al., 1984). Recent studies using organ culture explants from prairie dogs with radiolabelled glucosamine and autoradiography found that 80% or more of this precursor was incorporated into synthesized mucus granules. This technique appears to provide a convenient and quantitative method to

measure the rate of mucus synthesis and secretion (Lee et al., 1981b; LaMont et al., 1983).

The stimulus for mucus secretion in the presence of lithogenic bile is unknown. However, bile duct ligation appears to prevent hypersecretion in the cholesterol-fed prairie dog suggesting that the stimulus is present in hepatic bile (Lee et al., 1981b). Interestingly, gallbladder mucin release increased with age, an observation which may explain the increase in gallstone formation with age in experimental animals and man (LaMont et al., 1983).

Factors regulating mucus secretion

Mucus is released by exocytosis of secretory granules in the apical portion of the gallbladder epithelial cell (Wahlin et al. 1974; Lee 1980).

(1) Cholecystokin¹ causes a rapid increase of mucus release from its normal basal rate (Wahlin et al., 1976).

(2) Prostaglandins are known to stimulate mucin release in the stomach and may also be involved in the release of gallbladder mucin (LaMont et al., 1983).

(3) Arachidonic acid causes a 2 to 5 fold increase in mucin release in prairie dog gallbladder while indomethacin and aspirin block such a release by inhibiting the synthesis of prostaglandins (LaMont et al., 1983; Lee et

al., 1981a).

(4) Hydrocortisone and related steroid hormones inhibit gallbladder mucin release by inhibiting phospholipase A₂ and thereby reducing the availability of arachidonate for prostaglandin synthesis.

(5) Lysolecithin, a membrane bound cation, is a potent stimulator of gallbladder mucin release and hypersecretion (Neiderhiser et al., 1983).

Crystal and stone formation:

Cholesterol gallstones are formed from cholesterol monohydrate crystals which are found in lithogenic bile (Small, 1980; Sedaghat and Grundy, 1980). There are five stages in the formation of symptomatic gallstone disease.

- (1) There is a genetic trait or metabolic abnormality that leads to the production of a supersaturated bile;
- (2) a chemical stage involving the production of a supersaturated bile;
- (3) a physical stage when cholesterol monohydrate crystals precipitate out from supersaturated bile;
- (4) precipitated crystals aggregate to form macroscopic stones;
- (5) macroscopic stones cause symptoms by initiating cholecystitis or block the cystic duct.

Before cholesterol crystal precipitation can occur nucleation must take place. There are two types of

nucleation: Homogenous nucleation takes place when crystals precipitate out from a highly supersaturated bile.

Heterogenous nucleation can occur from a less supersaturated bile and is induced by other substances such as mucus (Small, 1980; Whiting and Watts, 1984; Levy et al., 1984).

Cholesterol monohydrate crystals are described as colorless, transparent and thin with parallel edges, often having a notched corner and resembling pieces of broken windowpane (Juniper and Burson, 1957). They have also been described as being flat, plate-like parallelograms (Small, 1980), or rhomboidal (Osuga et al., 1974; Ogata and Murata, 1971).

Not that many years ago no generally accepted theory of formation and growth of cholesterol gallstones existed. The major point of disagreement centered on the process of growth, whether it occurred from the nucleus outward (Naunyn, 1921), or from the periphery inward (Sweet, 1935; Tamura, 1943). Observations made on human stones (Ogata and Murata, 1971), human stone development (Osuga et al., 1974) and development of experimentally-induced stones in the squirrel monkey (Osuga et al., 1974) have clarified this question and confirmed the initial theory put forward by Naunyn (1921) that growth occurred from the center.

outwards.

The morphology of human cholesterol gallstones was described in two studies using light and scanning electron microscopy (Ogata and Murata, 1971; Osuga et al., 1975). The latter study proposed a chronological model for the development of macroscopic stones. Rhomboidal cholesterol monohydrate crystals form platy units either by layered growth or random aggregation. These platy units are the basic building units for macroscopic stones which may be either spherical, multilobar or mulberry. The central area of macroscopic stones contained crystals in platy unit form as well as amorphous substance and is connected to the outer capsule by radially arranged plates.

There has been only one study on an animal model to chronologically follow the development of cholesterol gallstones. The squirrel monkey when fed a diet of butter and cholesterol for nine months developed multilobar and mulberry gallstones. The pattern of stone development included the lamination or random aggregation of crystals into platy units. These platy units were the basic building blocks of microliths or macroscopic stones. An alternative route of stone development was the aggregation of wagon wheel shaped concretions into microliths and macrostones.

The basic sequence of crystal precipitation and stone formation was similar in man and the squirrel monkey. However, there were some noticeable differences such as: (1) fragmented crystals seen frequently in squirrel monkeys were only occasionally observed in man; (2) a tiny hole filled with air in the center of squirrel monkey's stone was not seen in human concrements; (3) finally, the presence of microliths with a wagon wheel design common in the squirrel monkey gallbladder and hepatic bile was not a feature of human gallstones.

Mucosal changes

Even though there is no statistical evidence to link gallstones with carcinoma of the gallbladder, a causal relationship has been postulated (Diehl, 1980). The turnover rate of normal gallbladder epithelium is very slow (Bargmann, 1959; Dyban, 1973; Scott, 1978). In a number of studies of cholelithiasis utilizing animal models, an increased cell proliferation was observed before the presence of stones (Scott, 1978; Putz and Willems, 1981; Scott, 1976; Marsch-Zeigler and Palme, 1982; Lee and Scott, 1982). Scott (1978) examined the labelling indices of rabbits fed dihydrocholesterol diet, mice fed a cholesterol-cholic acid diet, and guinea pigs injected with lincomycin. showed labelling indices of 15-21% within the first week of

the cholelithiasic process. Increased mitotic and DNA synthetic activities also were observed in human lithiasic gallbladders (Lamote et al., 1983; Putz and Willems, 1978).

Kaye et al. (1966) examined cell replication in rabbit gallbladder and described proliferative zones in the valleys of mucosal folds. However, Mueller et al. (1972) demonstrated that valleys and folds were transient structures depending on the fullness of the gallbladder when fixed and Scott (1974) found no defined proliferative zones in the guinea pig gallbladder.

There have been three studies that systematically investigated the later stages of cell proliferation and accompanying mucosal changes, correlating them with stone formation (Marsch-Zeigler and Palme, 1982; Lee and Scott, 1982; Lee et al., 1986). In the mouse cholesterol-choleic acid model, hyperplasia occurred within 6-8 days together with increased mitotic and fibroblast labelling indices (Marsch-Zeigler and Palme, 1982; Lee and Scott, 1982). The latter authors also demonstrated muscle thickening and glandular metaplasia by 21-28 days and distinct Rokitansky-Aschoff sinuses by 29-56 days. All these mucosal changes occurred long before the presence of stones. The gallbladder epithelium of rabbits fed a 15% oleic acid diet for 1-5 weeks showed interepithelial cell vacuoles and by

16 weeks Rokitansky-Aschoff sinuses were observed.

Scanning electron microscopy of pathological human gallbladders revealed defects in the epithelial sheet which were interpreted as empty goblet cells or the result of chronic cholecystitis (Myllarniemi and Nickels, 1977; William and Smith, 1978).

Cholesterolosis lesions occur quite frequently in human gallbladders (Miettinen and Tilvis, 1985). There is only one study on the dog cholesterol-choleic model that examined the induced lesion (Holzbach et al., 1977). Both human and the dog studies used a single sampling interval.

Previous studies on the guinea pig gallbladder in situ using radiolabelled oleic acid, cholesterol and lecithin, have demonstrated that this organ is capable of absorbing materials other than water and electrolytes (Neiderhiser et al., 1971; Neiderhiser et al., 1973; Neiderhiser et al., 1976; Hopwood et al., 1983). Studies on human gallbladder cholesterolosis have shown that lipid accumulation can occur either in epithelial cells, the lamina propria or both (Kouroumalis et al., 1984; Koga et al., 1986; Koga, 1985; Nevalainen and Laito, 1972; Boyd, 1922; Illingworth, 1929; Hora and Schulz, 1979; English and Hopwood, 1985).

Koga (1985) demonstrated a massive accumulation of lipids in the epithelial cells and also in macrophages found in the lamina propria of human gallbladders while Nevalainen and Laito (1972) showed lipid accumulation in epithelial cells only. In dogs fed cholesterol-cholic acid for nine months, lipid accumulation was seen only in the epithelial cells and not in macrophages (Holzbach et al., 1977).

Previous studies have proposed that absorbed lipids reached the lymphatic or venous system via the intercellular spaces and passed to the lamina propria where they were engulfed by macrophages which then entered the general circulation (Niderhiser et al., 1976; Kouroumalis et al., 1984; Koga, 1985; English and Hopwood, 1985).

Cells may also rid themselves of the absorbed lipid by heterophagocytosis, which resulted in the formation of residual bodies (Nevalainen and Laito, 1972; Hora and Schultz, 1970), or esterification of the absorbed lipid to give discrete lipid droplets (Miettinen and Tilvis, 1985; Subbiah and Dicke, 1977; Tilvis et al., 1982).

Characterization of lipid accumulation in the mucosa was done histochemically (English and Hopwood, 1985; Koga, 1985; Koga et al., 1975; Williamson, 1969; Okros, 1968):

Frozen sections stained with oil red O demonstrated neutral lipids while digitonin complexed experiments revealed free cholesterol.

Animal model of gallstone disease

It is difficult to chronologically evaluate hepatobiliary physiology or gallstone formation in humans because cholecystectomized gallbladders are generally in the end stage of the disease process. There is little if any, normal tissue. This results in major gaps in our understanding of the disease process and hence the use of animal models to fulfil this role.

The search for animal models to study gallbladder disease is ongoing. There is no existing animal model that perfectly parallels human gallstone disease as cholelithiasis is multifactorial and involves: (a) biliary cholesterol supersaturation, (b) abnormality of biliary proteins, (c) relative gallbladder stasis, (d) hypersecretion of mucus and (e) other potential defects.

In all the models, induction of cholelithiasis requires manipulation of the exogenous factors i.e. cholesterol overload which in turn profoundly alters the normal metabolic state resulting in the supersaturation of

bile.

Freston and Bouchier (1968) listed a number of characteristics for the ideal model of experimental cholelithiasis against which all available models may be compared. The criteria were: (1) simple and reproducible method for induction; (2) a diet comparable to a typical human diet if dietary method of induction is used; (3) animals should be easy to procure and reasonably inexpensive; (4) reasonably rapid stone formation, for example within several weeks rather than months; (5) gallstone composition similar to that of human, whether cholesterol or pigment stones are induced; (6) adequate amounts of tissue, bile, blood and adequately sized bile duct to allow for cannulation to sample hepatic bile and enough stones for complete quantitative analysis; and (7) other than the production of gallstones, there should be no other difference between experimental and control animals. A number of animal models have been developed to study both pigment and cholesterol gallstones; each one had an identifiable deficiency (Freston and Bouchier, 1968; Gurl and DenBesten, 1978; Hoffmann, 1984; Holzbach, 1984; Schoenfield, 1972; Tepperman and Weiner, 1963; Van der Linden and Bergman, 1977; Patton et al., 1961; Malet, 1985).



Pigment stones

Mongrel dogs

A 1% cholesterol diet supplemented with 10% casein, 50% sucrose, 26% starch, and 5% lard induced pigmented stones in dogs within one week and after 12 weeks on the diet all animals developed stones. The stones induced consisted of cholesterol, bilirubin and protein. Some calcium and bile acids were also contained within the concretions. The cost and size of the animals suggest that this model is not ideal for the study of cholelithiasis (Malet, 1985; Van der Linden and Bergman, 1977).

Hamster

Pigment stones consisting of calcium, phosphate, bile salts and pigment are developed in females and older hamsters. A number of diets including the addition of 30% ethanol to drinking water, lithogenic diets supplemented with thyroxine, and a 1% cholesterol-enriched diet induced pigment stone formation. These stones were basically similar to those in man (Malet, 1985; Van der Linden and Bergman, 1977).

Guinea pig

Guinea pigs of either sex injected with lincomycin subcutaneously for seven days develop pigmented stones. The composition of these stones included 25% calcium, 23% carbonate, 14% bilirubin and 7.7% cholesterol. This model provided more insight into gallbladder mucosal injury than actual stone formation. The stones formed contained a higher percentage of cholesterol than pigment stones. (Malet, 1985).

Mice

Mice with hereditary hemolytic anemia developed pigmented stones while ingesting a standard rat chow diet. The stones formed within 7-10 months in 77% of females but by 10-14 months only 56% of the males had developed stones. The concretions formed were similar to pigmented stones of man. This model may be suitable for studying the pathogenesis of pigment stones associated with anemia (Malet, 1985).

Cholesterol gallstones

Monkeys

Several species of subhuman primates on long term,

high cholesterol diets, are known to be resistant to cholesterol gallstone formation, notably the rhesus and African green monkey. Although chimpanzees and other species may show susceptibility to cholesterol stone formation, cost of acquisition is prohibitive. Squirrel monkeys fed a diet of 25.5% butter and 0.5% cholesterol added to casein and sucrose developed gallstones within nine months in 83% of the animals (Osuga et al., 1974). However, the long term feeding process (9 months) and access to primate facilities often makes holding large numbers of animals for study at one time unfeasible (Holzbach, 1984).

Rat

The rat, an animal which lacks a gallbladder, takes up cholesterol rapidly when fed a high cholesterol diet. The increased cholesterol level stimulates the enzyme cholesterol 7 α -hydroxylase which converts cholesterol to bile acids. In this species, the administration of cholesterol does not induce the formation of supersaturated bile (Van der Linden and Bergman, 1977).

Mouse

In the mouse model, both 1% cholesterol and 0.5% cholic acid is fed to the animals and gallstones are formed

within two months. The cholic acid blocks the induction of bile acid synthesis and cholesterol increases in the cholesterol pool, resulting in more cholesterol secreted into the bile. The bile acid ingestion is a necessity for gallstone formation and hence is a disadvantage for comparison with human gallstones (Holzbach, 1984; Malet, 1985).

Guinea pigs

Guinea pigs fed 0.5% cholesterol diet devoid of vitamin C developed cholesterol gallstones within five weeks. This major dietary deficiency, when compared to humans, suggested this model was not useful in the study of gallstone formation. However, due to the mechanism involved in stone formation, this model is useful to study the hepatic 7 α -hydroxylase enzyme system (Malet, 1985).

Gerbils

A cholesterol-cholic diet similar to that used in the mouse model also induced gallstone formation in this species. However, because of the diet used, the stone formed is not comparable to humans (Van der Linden and Bergman, 1977).

Rabbits

Gallstones have been induced in rabbits by two different methods. One model involves feeding the animals a cholesterol analog, dihydrocholesterol or cholestanol. The other uses a 40% protein rich diet combined with 20% oleic acid (Van der Linden and Bergman, 1977; Lee et al., 1980). The stones formed were rich in glycochenoic acid, a major bile acid in rabbits. Cholesterol constituted only about one-fourth or less of the dry weight of these concretions. These stones differed significantly from humans which have a high cholesterol content of between 70-85% (Malet, 1985).

Hamsters

Two of the most popular models utilize rodent species: the hamster and prairie dog. The hamster model has been in use for many years. Dam and Christensen (1962) demonstrated that the hamster is capable of forming cholesterol gallstones when fed a diet of refined sugar and no polyunsaturated fatty acids. However, this diet has little similarity to the average human diet. Bile from several animals has to be pooled for chemical analysis because of the small size of the animal gallbladder. They also developed diarrhea and exhibited growth retardation.

(Chang et al., 1973). Despite these drawbacks, the hamster model has proved to be popular as acquisition and maintenance are relatively inexpensive and they form stones within 6-7 weeks (Van der Linden and Bergman, 1977). The work on this model has focussed more on cholesterol metabolism, prevention and/or dissolution of gallstones (Pearlman et al., 1979; Hoffmann, 1984).

Prairie dog

The herbivorous prairie dog is a model of unsurpassed popularity. Branneman et al. (1952) were the first to realize the true potential of this species. These animals, fed 1.25% cholesterol-enriched diet, developed cholesterol gallstones within two weeks. The caloric distribution of the diet is similar to that of humans and the stones formed contained 75-85% cholesterol by weight. The amount of bile produced by each animal was sufficient for chemical analysis of cholesterol, phospholipids, and bile acids, and the animals remained healthy on the lithogenic diet. Major problems as a model are that the animals are difficult to handle, seasonally unavailable and genetically heterogeneous. Its major advantages are that they are comparatively inexpensive to acquire and maintain and their bile is comparable to that of humans insofar as it contains the same four major bile acids. The two primary acids: (a)

cholic acid and (b) chenodeoxycholic acid and two secondary acids: (a) deoxycholic acid and (b) lithocholic acid (Van der Linden and Bergman, 1977; Chang *et al.*, 1973; Malet, 1985). In addition, the relative composition of the three main lipids are roughly comparable to those found in human bile (Van der Linden and Bergman, 1977; LaMont *et al.*, 1984).

The prairie dog model has been extensively used to provide information on a variety of parameters involved in gallstone formation: bile composition (DenBesten *et al.*, 1974), gallbladder mucus hypersecretion (Lee *et al.*, 1981b; Doty *et al.*, 1983a), prevention of mucus hypersecretion by the administration of aspirin (Lee *et al.*, 1981a), inhibition of bile stasis and stone formation with sphincterotomy and reversal with atropine (Hutton *et al.*, 1982), arachidonic acid and mucus secretion (LaMont *et al.*, 1984), effects of bile acids and axazolines (Cohen *et al.*, 1984), prevention of stone formation by hyodeoxycholic acid (Singhal *et al.*, 1984), and the role of cyclic nucleotides and glycoproteins during stone formation (Zak *et al.*, 1984).

Ground squirrels

The scarcity and protected status of prairie dogs in



Canada led Davison et al. (1982) and Fridhandler et al. (1983) to further develop Patton et al.'s (1961) ground squirrel model for cholelithiasis. The Richardson's ground squirrel, when fed a 1% commercially prepared cholesterol-enriched rat chow diet, exhibited bile with an increased lithogenic index close to theoretical saturation values after two weeks. These authors did not observe the precipitation of crystals but described defective gallbladder contractility during this time interval. Prolonged exposure of animals to the enriched diet gave a lithogenic bile and resulted in either cholesterol microcrystals or macroscopic stones after six months.

Richardson's ground squirrels are plentiful in Alberta and are considered to be a pest by farmers. The classification of this species is:

- Kingdom----- Animal
- Phylum----- Chordata
- Class----- Mammalia (vertebrates which possess hair and suckle their young).
- Order----- Rodentia (gnawing animals; enamel only on front incisors)
- Suborder----- Sciuromorphs (post orbital process, four cheek teeth above



and below). Squirrels,
beavers, gophers,
marmots, kangaroo rat,
chipmunk, prairie dog
and groundhog.

Genus-----Spermophilus

Species-----richardsonii

Objectives

This model had been used previously to study bile lithogenicity and gallbladder stasis during the early stages of cholesterol formation (Patton et al., 1961; Fridhandler et al., 1983). A thorough systematic investigation of this model in the cholelithiasis process however was lacking. The current study was designed to :

- (a) describe the morphology of normal ground squirrel
gallbladder
- (b) identify the chronology of crystal and stone formation
and method of formation
- (c) describe the morphology of these biliary concretions
- (d) describe intra-epithelial and mucosal changes
occurring prior to, during and after stone formation.

MATERIALS AND METHODS

The bile and gallbladders of 238 Richardson's ground squirrels (Spermophilus richardsonii) of both sexes were studied. Ground squirrels weighing between 350-450 gm were trapped from the wild around the Edmonton, Alberta area and housed individually in plastic wired-topped cages at the Surgical Medical Research Institute (S.M.R.I.) Animal Holding Facility, University of Alberta. They were kept on a 12:12 hour (6 p.m.-6 a.m.) light:darkness photoperiod at a temperature of 23°C and humidity of 35-40%. The animals were maintained on a diet of rat chow (Wayne Lab-bloc, Allied Mills Inc., Chicago, Illinois) and water ad libitum. Animals were held for one month during which time they were checked for parasites, loss of hair, weight and diarrhea.

Animals considered to be healthy were divided into control and experimental groups. Experimental animals were fed a 2% cholesterol-enriched rat chow diet (U.S. Biochemicals, Cleveland, OH) and water ad libitum. Control animals were maintained on the same commercial rat chow diet and water ad libitum. Each group consisted of four animals. Sampling intervals of 6, 12, and 18 hours; 1, 3, 5, and 7 days; 2, 3, 10, and 20 weeks; 3 weeks on on cholesterol diet followed by three week on normal diet were

used. Animals in the shorter time intervals, 6 hours through 1 day, were fed known quantities of food which were monitored before killing to ensure that they had actually eaten the cholesterol-enriched diet. These animals were not fasted overnight before killing.

Animals were fasted overnight and killed by cervical dislocation between 0900 and 1000 hours. The majority of bile was withdrawn from the gallbladder by a 1cc syringe and stored at -20°C for assay later. The bile was examined by polarizing microscopy to determine the presence of crystals or microliths. Biochemical assays of the bile to determine cholesterol, bile acids and phospholipids was performed by the Biochemistry Unit of S.M.R.I. From these parameters the lithogenic index of bile was calculated (Carey, 1978; Thomas and Hoffmann, 1973).

The same volume of fixative, 2.5% glutaraldehyde in Millonig's buffer pH 7.2 was injected into the gallbladder. The organ was then excised and immersed in the same fixative for one hour at room temperature, split along its longitudinal axis and rinsed of its luminal contents.

The luminal rinsings were examined by direct light and polarizing microscopy, photographed and stored in 10% neutral buffered formalin. Luminal rinsings from gall-

bladders that did not contain macroscopically visible stones were filtered through a 0.22 μ m Millex GS filter (Millipore Corp., Bedford, MA) which was subsequently air-dried, mounted on a stub and sputter-coated with gold. Luminal rinsings that contained macroscopic stones were filtered through a Whatman (England) #1 filter paper and left to air-dry. The dried stones were transferred onto stubs coated with electron conducting paint and sputter coated with gold. Crystals and stones isolated by either technique were examined using a Philips 505 SEM. Larger stones were fractured after surface observations were recorded, recoated and the internal architecture examined.

Macroscopically visible stones of some animals were washed in distilled water to remove any bile and debris and then dried in a vacuum desiccator until a constant weight was achieved. Stones were dissolved in a mixture of ethanol/ether (3:2 vol/vol) at 40°C for 72 hours in the dark with vigorous mixing. The mixture was then centrifuged at 1500g (Smith and LaMont, 1985a). The colorless supernatant was decanted and stored while the residue was washed again and re-centrifuged. On average, the ratio of stone weight to dissolution solvent was 15mg/ml. The supernatant and washings were combined and assayed for cholesterol content using the method of Carr and Dreker (1956). Analysis was done by the Biochemistry Unit of S.M.R.I.

The gallbladder of the ground squirrel is small and the various techniques listed below were not all performed on each organ. Similar experiments were repeated and tissue used as determined by procedure. One longitudinal strip of the organ was diced into 1mm² pieces for transmission electron microscopy and immersed in the same fixative for two hours at room temperature, postfixed in 1% osmium tetroxide for one hour, blocked stained in saturated aqueous uranyl acetate for one hour, dehydrated in an ascending series of ethanol and propylene oxide and embedded in LX-112 resin (Appendix I). Three of these blocks were randomly selected for electron microscopy. Ultrathin sections of 600-900Å⁰ were cut on a Reichert Ultracut microtome, mounted on uncoated 200 mesh copper grids, stained with saturated aqueous uranyl acetate for 10 minutes and lead citrate (Reynolds, 1963) for 2 minutes and examined with a Philips 410 electron microscope at an accelerating voltage at 30kv. Micrographs were taken on Kodak Fine Grain Positive 35mm film.

For morphometry of mucus secretory granules, sections from coded blocks where columnar epithelial displayed a nucleus, basal and apical regions were randomly selected and photographed at the same magnification of 4400 on 35mm fine grain positive film and the negatives were enlarged 2 times when printed. Eight to ten cells were photographed.

from each block. From the 24-30 prints from each animal, ten were randomly selected for planimetry. For each group of animals (n=4), 40 prints were digitized. Morphometric study was performed using a Nikon Microplan II semi-automatic image analyser to determine the area occupied by the mucus secretory granules and cytoplasm. The volume density (Vd) of the mucus granules was expressed as a percentage in which the total area of granules per cell was divided by the total cytoplasmic area multiplied by 100. Data was expressed as a percentage of means and standard error of the mean (SEM). Analysis of data was performed using the one-tailed unpaired Student's t test (Wahlin et al., 1976; Pradal et al., 1984; Weibel and Elias, 1967). The section thickness and compression factor (Holme's effect) were ignored because they did not affect the statistical treatment of the data (Wahlin et al., 1976; Pradal et al., 1984).

Another longitudinal strip of the gallbladder was immersed in the 2.5% gluteraldehyde in Millonig's buffer pH 7.2 for four hours at room temperature, postfixed in 1% osmium tetroxide for one hour, block-stained in saturated uranyl acetate for one hour, pinned on a cork with no tension and dehydrated in an ascending series of acetone. The tissue was critical-point dried in liquid carbon dioxide using a Seevac critical-point-drier and mounted on

aluminum stubs using colloidal silver paint (Appendix III). These dried specimens were sputter coated with gold using an Edwards S150B sputter coater, examined and photographed with a Philips 505 scanning electron microscope using Kodak Plus-X Pan 35mm film.

Another longitudinal strip of the organ was processed for light microscopy. The specimen was refixed in 10% buffered formalin for 24 hours, washed overnight in running water, and dehydrated in an ascending series of ethanol to 95%. Each strip of the specimen was further divided longitudinally into two parts. One part was dehydrated to 100% ethanol, cleared in xylene and embedded in paraffin (Luna, 1968); while the other was processed through to embedding in glycol methacrylate (Polysciences Inc. data sheet #123, -1982). Paraffin, methacrylate and histochemical slides were examined with a Leitz Orthoplan photomicroscope and selected areas photographed using Kodak Panatomic-X film (Appendix II).

To establish a mitotic index (MI), groups of animals (n=8) from sampling intervals of 1, 2, 10 and 20 weeks were killed, the organ excised and processed into methacrylate. Two micrometer sections were stained with Lee's methylene blue basic-fuschin (Luna, 1968). Slides were examined and the total number of cells and mitotic figures counted.

Nuclei which appeared between late prophase and telophase were counted as mitotic figures. The number of nuclei counted per animal (n=8) ranged from 2000 to 3000. % MI = number of mitotic figures counted multiplied by 100, divided by the total number of nuclei counted.

For light microscopy autoradiography, animals (n=4) from sampling intervals of 1, 2, 10 and 20 weeks were used. Prior to killing of animals, they were pulse injected intraperitoneally with 1.0 microcurie of tritiated thymidine/g body weight (specific activity 59ci/mole ICN Canada Ltd) at two one-hour intervals, killed and processed as above for glycol methacrylate. Two micrometer methacrylate sections were dipped into undiluted Ilford K.5D emulsion. The slides were drained and dried in a vertical position for one hour at room temperature, placed in a black box containing drierite, tape sealed and stored in the dark at 4°C for 3 weeks. Slides were developed in Dektol (Eastman Kodak, Rochester, NY) for two minutes, washed in water for 30 seconds, fixed in Kodak fixer for 5 minutes, washed in water for 15 minutes and counterstained with either methylene blue basic-fuschin or Gill's hematoxylin and eosin for two minutes (Budd, 1971) (Appendix V). To establish a labelling index (LI), the amount of background labelling determined the minimum grain count necessary to score a cell as labelled. In this study, the background

labelling was moderate and nuclei that had 15 grains or more overlying the nuclei were considered labelled. The number of labelled cells counted multiplied by 100, divided by the total number of cells counted. Analysis of mitotic and labelling indices was performed using the one-tailed unpaired Student's t test.

Eight micrometer thick paraffin sections of control (n=4) and one week treated animals (n=4) were deparaffinized and stained with high iron diamine/alcian blue pH 2.5 (Spicer 1965), and potassium hydroxide/alcian blue pH 1.0/ PAPS (Reid et al., 1985). The results of these stains are:

high iron diamine/AB pH 2.5

- Sulphomucins: grey-purple-black
- Sialic acids: blue (aqua)

KOH/AB1.0/PAPS:

- Sialic acids with side chain substitutions: red
- tissue vicinal diols: red
- O-sulphate esters: blue (Appendix VI)

For lipid histochemistry, control (n=4) and one week experimental (n=4) animals were killed and gallbladder tissue was fixed in Baker's formal solution for 24 hours,

frozen in isopentane immersed in liquid nitrogen, sectioned in a cryostat and stained with oil red O (Luna, 1968).

For localization of cholesterol at the electron microscopic level, digitonin-complexing experiments were conducted using control (n=4) and one week experimental (n=8) animals. Tissue was fixed in 2.5% gluteraldehyde for one hour at room temperature. The gallbladder was then split along its longitudinal axis, rinsed of its luminal contents and placed in fresh fixative for an additional 2 hours. The tissue was then washed with phosphate buffer for one hour, changing the solution every 15 minutes, and placed in a 2% digitonin solution dissolved in 0.1M Millonig's phosphate buffer for 4 hours at room temperature (Okros, 1967; Williamson, 1968; Koga et al., 1975). The specimen was post-fixed in 1% osmium tetroxide and then processed routinely for electron microscopy (Appendix IV).

For electron microscopic mucin autoradiography, control (n=4) and one week experimental (n=4) animals were matched by weight, injected with H³galactose, 1.0 microcurie/g body wt. (specific activity 5-20ci/mole, ICN Canada, Ltd.) intraperitoneally, and killed by cervical dislocation at 25 and 40 minutes interval thereafter. The gallbladder was removed and processed as above for electron microscopy. Ultrathin sections of 600-900A⁰ were cut on a

Reichert Ultracut microtome and mounted on 200 mesh copper grids attached to glass slides by 0.5% paralodion. Slides were dipped in Ilford L4 emulsion diluted 1:6 in water, allowed to dry for one hour, placed in a black box, taped sealed, and stored at 4°C for 4 weeks. Slides were developed in Kodak D-19 for 3 minutes, fixed in 2% sodium thiosulphate for 6 minutes, washed in distilled water for 6 minutes and stained in uranyl acetate for 10 minutes and lead citrate for 5 minutes (Appendix IV). Grids were then examined with a Philips 410 electron microscope at an accelerating voltage of 30kV. Micrographs were taken on Kodak fine grain positive film.

RESULTS

Control

Electron microscopic examination of the gallbladder wall of the Richardson's ground squirrel revealed that it was composed of three layers: mucosa, muscularis and adventitia or serosa. The mucosa was composed of a layer of simple columnar epithelial cells and lamina propria. The lamina propria was a well defined layer under the basal lamina. It was composed of collagenous fibrils, capillaries, arterioles, venules and fibroblasts.

Capillaries were observed in close proximity to the lining epithelium especially in mucosal folds (fig. 1). The endothelium was fenestrated, each fenestration closed by a diaphragm (fig. 2). Pinocytotic vesicles were observed in the endothelium. A continuous basal lamina surrounded the endothelium which was distinct from that of the overlying epithelium.

Beneath the lamina propria the muscularis was composed of smooth muscle bundles arranged in thin sheets of varying extent. The spaces between layers were occupied by characteristic connective tissue fibers and cells as well as blood vessels. In the lamina propria, unmyelinated nerve fibers were observed in close proximity to larger

blood vessels (fig. 3). Piriform swellings, or varicosities of postganglionic neurons were seen intramuscularly and in the lamina propria beneath the basal lamina (figs. 4, 5). Membrane specialization of these varicosities was not observed. They contained granules of various electron density, each of which exhibited a prominent surrounding membrane, a peripheral electron lucent halo and a dense central core similar to those observed in non-direct adrenergic nerves. External to the muscularis the adventitia, or serosa, consisted of lobules of fat, collagenous and elastic fibers, blood vessels, fibroblasts and lymphoid cells.

Three types of cells were observed in the lining epithelium: light, dark or pencil and edematous. Cell classification was based on the shape of the cell and nucleus as well as density of the cytoplasmic matrix.

Light cells

The majority of the cellular population in the lining epithelium were light cells (fig. 1). The cytoplasmic density of these cells varied depending on the functional activity and the organelles present. Non-active, or resting cells, contained few organelles and hence the cytoplasm appeared less dense than active cells. Active

cells had a heterochromatic, serrated nucleus that contained a prominent nucleolus. These cells ranged from 19 to 21 micrometers in height and 4.5 to 5.5 micrometers in diameter. A distinct apical zone devoid of cellular organelles, 0.8 to 1.5 micrometers in depth, was present in the cell. The shape of this zone varied from a slight convexity to an inverted U, both exhibiting intact microvilli (figs. 1, 6).

Electron dense mitochondria with transverse cristae were seen in the basal and subapical region of the cell, more numerous in the latter. Other organelles in the subapical cytoplasm were rough endoplasmic reticulum, lysosomes, residual bodies and centrioles (figs. 1, 6, 7). The residual bodies were membrane-bound, of different sizes and contained a variable amount of lipid. A few lipid droplets were occasionally observed in the basal region of the cell (fig. 8). No lipid droplets were seen in the lamina propria. Microfilaments were scattered throughout the cytoplasm of the cell but more concentrated near the centrioles (fig. 7). The Golgi apparatus was a prominent supranuclear feature in most cells. It generally consisted of 3 to 5 layered saccules with vesicles of various sizes seen near the maturing face (fig. 9).

Mucus secretion

Light microscopic histochemistry revealed that the gallbladder epithelium of control animals secreted both sialylated and sulphated mucin at a basal level (figs. 10, 11). The scanning electron microscope provided evidence of mucus secretion as thin viscid strands issuing from the luminal aspects of these cells (fig. 12). Secretory activity was not simultaneous through wide areas of the epithelial sheet but appeared restricted to groups of cells scattered over the luminal surface.

Autoradiographic studies at the ultrastructural level of control and seven day experimental animals, using a labelled glycoprotein precursor H^3 galactose, demonstrated the mucin granules to be membrane bound. These granules contained a flocculent material of moderate electron density (fig. 13). Twenty five minutes after intraperitoneal injection of the precursor, those mucus granules which contained the label were found predominantly in the supranuclear and subapical regions of the cell (fig. 14). Forty minutes after injection, labelled mucus was commonly observed in the lumen of the gallbladder (fig. 15).

Examination of epithelial cells of control.

gallbladder at the ultrastructural level showed mucus-containing granules of varying diameter in the supranuclear region of cells that contained prominent Golgi complexes. These granules were a characteristic feature of the subapical zone where they appeared to coalesce into larger granules prior to extrusion of their contents into the gallbladder lumen (figs. 16, 17).

The apical plasma membrane exhibited prominent microvilli that ranged in length from 0.8-1.6 micrometers with a diameter of 0.15 micrometers. The terminal web was poorly developed below the microvilli. In a few instances, cytoplasmic bullae were observed to arise between microvilli and contained particulate material but were devoid of cellular organelles (fig. 18).

Mitotic activity was rarely observed in the epithelial sheet but figure 19 shows a cell in the prometaphase stage. Mitochondria in the basal and apical regions, microvilli, mucus granules in the apical zone, desmosomes between adjacent cells, a centriole and microfilaments were observed in the dividing cell. Cells undergoing mitoses were larger than those adjacent, the chromosomes were at the same or higher level than the interphase nuclei.

Dark cells

The dark rod-shaped, or pencil cells, had a higher electro. density than the principal light cells (fig. 1). They ranged in height from 19 to 21 micrometers but had a narrower diameter of 3 to 3.5 micrometers at the nuclear level that became wider at the apical surface. The dark cells made contact with the basal lamina and lumen of the gallbladder (figs. 20, 21). The apical surface was populated with microvilli of normal density and dimension. There was a distinct apical zone devoid of cellular organelles but containing granules (fig. 20). Residual bodies and numerous mitochondria with transverse cristae were observed in the subapical and basal region of these cells but a Golgi apparatus was not seen. Dark cells appeared to occur singly, their lateral interdigitating processes standing out strongly against the less electron dense cytoplasm of the light cells. Desmosomes remained intact between light and dark cells (figs. 20, 21).

Edematous cells

Light barrel-shaped edematous cells were infrequently observed in the lining epithelium (figs. 22, 23). These cells were wider than the surrounding light cells and displayed a pyknotic or karyolytic nucleus. The

apical membrane was generally ruptured with cytoplasmic organelles extruded into the lumen (fig. 22). Numerous hydrated and vacuolated mitochondria with disrupted and distorted cristae and a lower electron density than normal were observed. Vesicular profiles of degenerated rough endoplasmic reticulum and lysosomes were also observed in the edematous cells (fig. 23). No other cellular organelle was observed.

A prominent basal lamina lay under all three cell types. It was continuous and followed the contour of the basal plasma membranes. The attachment of the plasma membrane to the basal lamina was by numerous peg and socket interdigitations rather than hemi-desmosomes (fig. 24). These interdigitations were more prominent in organs not actively involved in water resorption at the time of fixation.

The lateral cell membranes showed finger-like interdigitations, or microfolds, between adjacent cells. In the apico-lateral region the plasma membranes formed a prominent junctional complex between neighbouring cells. Extending down the lateral membrane to the basal plasma membrane, prominent desmosomes were observed. The lateral membranes between cells often exhibited various degrees of separation with dilation of the intercellular space. The

apical regions were held closely apposed by the junctional complexes while the basolateral regions displayed a separation of the lateral interdigitations to become widely distended (fig. 25). The desmosomes in these regions remained intact anchoring the finger-like projections across the dilated intercellular space (fig. 26). The basal plasma membrane remained apposed to the basal lamina although the peg and socket interdigitations common to this region were no longer observed (fig. 27).

Small round infiltrating leucocytes were observed migrating through the basal lamina into the intercellular spaces (fig. 28). Leucocytes were generally observed near the basal lamina and occasionally at higher levels approximating the junctional complex (fig. 29). The most frequently encountered cell type was the lymphocyte.

The scanning electron microscope demonstrated mucosal folds, or rugae, on the luminal surface of the gallbladder. The number and height of these folds was dependent on relative volume of fluid in the organ at time of fixation (figs. 30, 31). Semi-filled organs exhibited pocket-like depressions between mucosal folds. These pockets disappeared when the gallbladder was full of fluid, the surface showing only widely spaced, relatively small bumps. Sections through these projections failed to

demonstrate any underlying structure responsible for their formation.

Higher resolution scanning microscopy revealed the cobble-stone appearance of the epithelial sheet. The apical surface of these cells were dome-like and protruded to variable degrees into the lumen (fig. 12). Examination of fractured edge revealed the extensive lateral membrane interdigitations (fig. 32). A deeper fracture showed the large oval nuclei located near the base of the cells (fig. 33). Surface morphology of the basal lamina showed projections that may interdigitate in a peg and socket arrangement with the overlying epithelial cell. Small defects in the basal lamina were also noted and may be the result of the thixotropic nature of this layer (fig. 34).

Experimental animals

Mucus secretion

The 2% cholesterol-enriched diet stimulated an increase in mucus secretion by the gallbladder epithelium as early as 18 hours following ingestion, clearly demonstrated by scanning electron microscopy (fig. 35). This hypersynthesis and secretion of mucus was confirmed quantitatively by morphometry on the ultrastructural level

(table I, page 64). Mucus hypersecretion occurred when the lithogenic index was 0.742 (table II, page 65), significantly higher than control animals. In one and five day treated animals, SEM studies revealed a thick sludge-like layer covering the epithelial surface (figs. 36, 37, 38). TEM studies showed numerous mucus granules in the apical and subapical regions of the epithelial cells. The secretory granules maintained their discrete shape but the luminal surface of the cell changed from a slight convexity to an inverted U (fig. 39). Scanning EM studies continued to demonstrate a thick sludge-like layer during the one and two week intervals which was observed throughout the experimental period (figs. 41, 42). The continued hypersecretion of epithelial glycoprotein, coupled with other bile constituents such as bilirubin, formed the sludge layer. The extent of this layer, both in thickness and area increased throughout the experimental period. This intraluminal environment appeared to be suitable for the continued growth of these crystals into platy units, microliths and stones.

In experimental animals and occasionally in controls, cytoplasmic bullae were observed on the luminal surface of epithelial cells. These bullae were devoid of microvilli (figs. 40, 43). Goblet cells were not observed either in control or experimental animals.

Morphometric studies confirmed mucus hypersecretion throughout the experimental period (table I, page 64), although at a lower level in the 10 and 20 week treated animals. Animals fed a lithogenic diet for 3 weeks and then control diet for 3 weeks, indicated that the rate of mucus secretion returned to control values (fig. 44).

Crystal precipitation and stone formation

Scanning electron and polarizing microscopy failed to demonstrate the presence of cholesterol monohydrate crystals on the luminal surface or in the bile of control animals. Biochemical analysis of the bile components from control gallbladders indicated the lithogenic index (L.I.) averaged 0.356 while that of animals on the experimental diet, with evidence of ingestion, for 6 hours was 0.337, thus exhibiting no significant increase (table II, page 65). By 12 hours however, the lithogenic index had risen significantly to 0.568. Neither group exhibited alterations in epithelial morphology or physiological activity detectable by SEM. The first evidence of altered mucosal physiology occurred in animals after 18 hours on the lithogenic diet.

One day after ingestion of the diet the lithogenic index of the bile had risen to 0.974. Scanning electron

microscopic examination of the mucosal surface showed large numbers of rhomboidal cholesterol monohydrate crystals precipitating from the bile, many of which had the notched appearance noted in humans by Juniper and Burson (1957). The crystals were observed stuck between the microvilli on the luminal surface of the epithelial cells (fig. 45). Appearance of the precipitated crystals was indicative of cholesterol saturation in the bile, a physiologic feature supported by biochemical analysis. Animals on the diet for 3 days had a lithogenic index of 1.133 and continued to exhibit cholesterol monohydrate crystal precipitation. Animals on the diet for 5 days, with a lithogenic index of 0.989, continued to demonstrate crystal precipitation by SEM. The occurrence of platy units was observed on the luminal surface in these animals (fig. 38).

Table II showed the variation in lithogenic indices of bile during the remainder of the experimental period. It indicated the significant increase of the lithogenic index during the early experimental period which levelled off after the first seven days to a value in the 0.651-0.842 range through the first 10 weeks. The lithogenic index by 20 weeks averaged 0.615, still significantly higher than controls. Animals in the 20 week group that had their cystic ducts filled with stones had lower lithogenic indices than those whose ducts were not

occluded. The difference in values however, was not significant at this point.

One week animals continued to demonstrate cholesterol monohydrate crystal precipitation observable by SEM (fig. 46). After two weeks on the diet, the number of aggregated crystals seen on the mucosal surface was diminished.

Examination of luminal contents by direct light microscopy revealed the presence of concrements. Luminal rinsings filtered and examined by SEM demonstrated continued aggregation and growth of crystals through parallel lamination into larger platy units (figs. 47, 48). After three weeks, luminal rinsings contained refractive microliths, pure white in color and observable by light microscopy. The SEM showed these concrements to be clusters of platy band units (fig. 49). These platy bands are regarded as the basic unit required for the formation of gallstones in this model. These 3 week microliths had an irregular external surface formed predominantly by a random subparallel aggregation of the smaller platy subunits. This configuration gave the appearance of being arranged radially:



At ten weeks, concrements removed from the luminal washings were macroscopically visible and appeared to be of varying size (figs. 50, 51). This array of varying configuration was illustrative of the aggregative, growing

process of stone formation. The largest stones observed at 10 weeks exhibited a yellowish color and measured roughly 1mm. in diameter by direct light microscopy. Examination of these stones by SEM showed them to be composed of an aggregation of a number of cholesterol microliths. The surface was not smooth and the aggregate-like appearance gave these stones a typical mulberry shape (fig. 52). Higher resolution scans revealed that often these clusters were free of any matrix-like material in the grooves between them, adhering to one another through interdigitation of the crystals and platy units near each surface (fig. 53). In other areas of the stone however, component subunits were observed embedded in a thick layer of sludge on the surface of the stone (fig. 54).

Visual examination of the cystic duct and gallbladders of 20 week animals revealed many of the cystic ducts to be severely congested with a yellowish material while the bile was watery and turbid. The lumen of many organs was filled with these concrements. Light microscopic examination of the material rinsed from the organs and ducts demonstrated concrements that ranged from a fine sandy material to macroscopically visible stones. The largest of these stones was approximately 2mm. in diameter and those over 1mm. were generally brownish-yellow in color. Examination of these stones with the SEM showed a

smoother surface with occasional areas still exhibiting the parallel array of crystals and platy units comprising each lobe of the mulberry shaped stone (figs. 55, 56). Fracture of the stones revealed the formation of a much smoother, homogeneous, capsule-like outer layer which at higher resolution was observed to be composed of cholesterol plates that extended down into the central region of the stone in a radial fashion (fig. 57). These stones were not solid enough to allow a smooth fracture and the existence of a central cavity was not observed. The central region of the stone was composed of aggregation of leaf-like cholesterol crystals (fig. 58).

Biochemical analysis of the concrement aggregations revealed them to have a cholesterol content ranging from 61 to 74%, the amount increasing with prolonged exposure to the diet.

Mucosal changes

Cell proliferation and damage

Mitoses and labelled cells were observed throughout the epithelial sheet of control and also experimental, animals and did not show any preference for either the valleys or crests of the mucosal folds (figs. 59, 60).

Light, electron microscopic and autoradiographic studies revealed a low mitotic activity with a mean mitotic index (MI) of 0.027% and a labeling index (LI) of 0.169% (table III, page 66).



In animals exposed to the lithogenic diet for one week, the MI and LI were significantly higher than control values with a mean MI of 0.250% ($p < 0.05$) and LI of 0.394% ($p < 0.01$)⁸ (table III, page 66). The highest frequency of mitoses and labelled cells occurred in the two week-treated group which exhibited a mean MI of 0.384% ($p < 0.01$) and LI of 1.312% ($p < 0.001$). Transmission EM examination of tissue from the latter group revealed prominent mitoses on the crests of mucosal folds (fig. 59). Light microscope autoradiography demonstrated labelled cells on both the sides and valleys of the folds (fig. 60). Crystal and microlith formation was observed during these early stages of the experimental period but no macroscopic stones were seen.

Groups of light, barrel-shaped edematous cells with pyknotic or karyolytic nuclei were frequently observed in the 10 and 20 week experimental animals by TEM (fig. 62). The apical membranes of these cells were often ruptured with cytoplasmic organelles extruded into the lumen. SEM observations revealed gaps in the epithelial sheet (fig.

61) while TEM demonstrated that adjacent epithelial cells slid under the degenerated cells to protect the basal lamina (Fig. 62). During these later stages of the experimental period macroscopically visible stones were commonly observed.

In 20 week cholesterol-fed animals areas of the epithelial sheet revealed hyperplasia and hypertrophic cells on the crests of mucosal folds examined by light and scanning electron microscopy (figs. 63, 64). The normal hexagonal configuration of the epithelial cells was lost and their boundaries were indistinct. Prominent mitoses were often observed near hyperplastic lesions (fig. 64). The nuclei of the columnar cells were no longer basal, the cells themselves exhibited a variety of shapes. This arrangement gave the appearance of being pseudostratified.

The muscle layer of the gallbladder in 20 week animals appeared thicker, especially where prominent diverticula configurationally similar to Rokitansky-Aschoff sinuses were seen extending down to the adventitia (fig. 65). Electron microscopic studies revealed the presence of plasma cells and other leukocytes in the lamina propria and between the basal lamina and epithelial cells of these animals (figs. 66, 67).



Examination of sections from 10 week cholesterol-fed animal continued to demonstrate a significant increase in the number of mitoses ($p < 0.005$) with a mean MI of 0.329%, while in the 20 week group, animals exhibited a mean MI of 0.289% ($p < 0.005$). Table III indicated that the MI values for both groups followed this general trend. The incidence of mitoses and labelled cells at this point were lower than the peak values of the two week group but remained significantly higher than in control animals. Labelled fibroblasts were repeatedly observed in the lamina propria and adventitia as early as two weeks in animals fed the lithogenic diet, but were infrequent in the controls (figs. 68, 69).

Cholesterolosis-like lesion

In the twelve hour treated animals, the intercellular spaces were distended and contained electron lucent material with dense particulate material and osmiophilic bands among them (fig. 70). Similar material was also observed intracellularly, especially in the apical and supranuclear regions of the cells. The apico-lateral membranes remained firmly intact.

One, three, five and seven day treated animals exhibited numerous residual bodies within the epithelial

cells (fig. 71). The cells continued to accumulate lipid in massive amounts in the supranuclear region while basal regions contained discrete lipid droplets of varying electron density (figs. 72, 73, 76).

Frozen sections of control animals stained with oil red O failed to demonstrate lipid material in epithelial cells while in a five day-treated animal showed neutral lipid in the supranuclear region. (figs. 74, 75).

Electron microscopic observations on these tissues revealed that the supranuclear accumulations were non-osmiophilic and predominantly electron lucent exhibiting some flocculent material. At higher magnification discrete lipid masses were observed around the periphery of the accumulations. Centrally however, these droplets impinged upon one another, coalesced and became an ill-defined mass. Scattered among the lipid masses were lysosomes which appeared to be ingesting portions of the lipid mass to form residual bodies. Endoplasmic reticulum, mitochondria and Golgi of normal appearance were seen around the periphery of these accumulations (fig. 73).

Tissue from seven day treated animals, complexed with digitonin, revealed that the supranuclear accumulations contained free cholesterol incorporated into the overall

mass (fig. 77). Discrete lipid masses were observed in dilated smooth endoplasmic reticulum appeared to be membrane bound. Numerous ribosomes and a few lysosomes were often observed near these lipid accumulations.

Examination of the residual bodies at higher magnification revealed digitonin precipitation indicating the presence of free cholesterol (fig. 78). Digitonin-complexed cholesterol crystals were also observed on the luminal surface of the epithelial cells (fig. 79). The density and staining property of this precipitation was similar to that seen in the supranuclear accumulations and residual bodies.

One, two and three week treated animals also revealed supranuclear accumulations and distinct lipid droplets in the basal regions of epithelial cells. These droplets had distinct osmiophilic rings and central regions of varying electron density (fig. 76). Digitonin-complexed tissue failed to demonstrate the presence of any free cholesterol in the basal area of these cells.

The epithelial cells of ten and twenty week treated animals continued to demonstrate accumulation of lipids in the supranuclear and basal regions, but now also in the lamina propria. The electron density of the lipid in the lamina propria ranged from electron lucent to highly osmiophilic. Many of these lipid droplets had a myelinoid

appearance (fig. 10). Macrophages exhibiting dense osmiophilic bodies were also observed in the lamina propria (Fig. 11). Foam cells however, were not observed.

TABLE I: Morphometric analysis of mucus secretion in the gallbladder epithelium.

Intervals	Mean \pm SEM
Control	1.395 \pm 0.180
6 hours	1.716 \pm 0.234 [#]
12 hours	1.759 \pm 0.281
18 hours	2.367 \pm 0.260
24 hours	3.680 \pm 0.360
3 days	3.486 \pm 0.450
5 days	4.090 \pm 0.310
7 days	4.569 \pm 0.513
2 weeks	4.357 \pm 0.610
3 weeks	3.949 \pm 0.592
10 weeks	2.495 \pm 0.480
20 weeks	2.335 \pm 0.330
3W 3R*	1.593 \pm 0.335 [#]

¹ all values were compared to controls and unless indicated by '#' were statistically significant to $p < 0.05$ as assessed by the unpaired Student's t test.

* animals on the cholesterol-enriched diet for 3 weeks followed by 3 weeks on the control diet.

SEM refers to standard error of the mean

TABLE 41: Analysis of biliary lipids in gallbladder bile. ^{1,2,3} 65

	Cholesterol (mmol/l)	Phospholipid (mmol/l)	Bile acids (mmol/l)	Lithogenic Index
Control	8.18±2.41	23.9±2.3	237.0±11.0	0.356±0.036
6 hours	6.33±0.71	20.59±6.51	175.1±19.2	0.337±0.031
12 hours	11.11±0.86	26.17±4.37	211.2±13.8	0.563±0.079
18 hours	11.6±1.2	26.17±11.66	217.0±22.0	0.732±0.099
1 day	14.0±1.47	22.49±4.21	136.9±36.2	0.974±0.161
3 days	26.33±0.59	35.55±1.04	181.6±3.20	1.133±0.086
5 days	31.53±1.47	32.73±1.68	194.4±21.1	0.98±0.100
7 days	18.74±1.02	31.73±2.29	195.7±27.5	0.707±0.059
2 weeks	15.35±1.31	41.80±8.59	249.5±76.3	0.665±0.084
3 weeks	14.40±1.29	32.59±5.77	173.3±29.0	0.651±0.016
10 weeks	18.10±1.56	37.21±3.35	180.8±59.0	0.841±0.207
20 weeks	17.8±1.47	41.59±4.05	246.7±16.3	0.615±0.046

¹ n=6 in control group, n=3 in all other groups

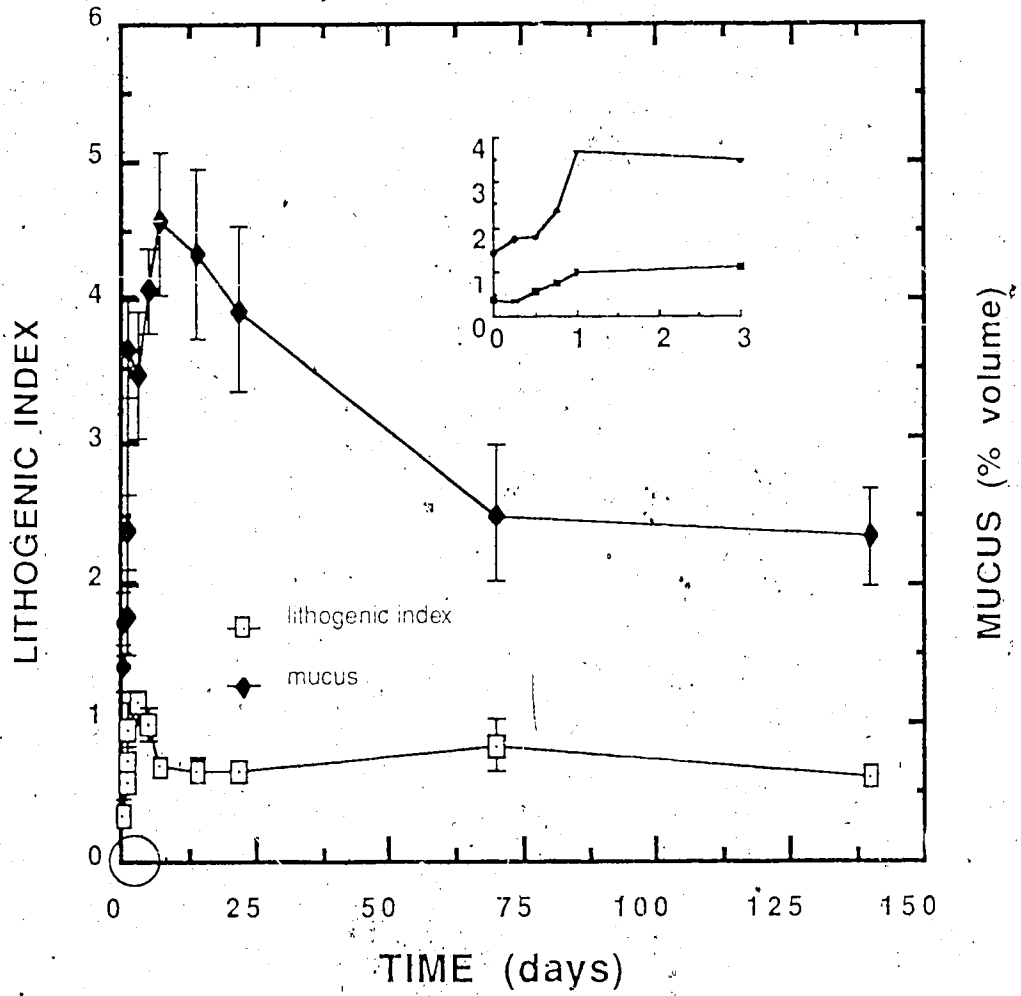
values are expressed as the mean ± standard error

unless indicated by '*', all lithogenic index values were statistically significant to p<0.05 as assessed by the unpaired Student's t test

TABLE III: Mitotic and labelling index values (0/00) during the various experimental intervals. Experimental values are compared to control and the level of significance is in parentheses below each.*

Condition	Mitotic Index(MI)	Labelling Index(LI)
Control	0.037 ± .013	0.169 ± .016
1 week-treated	0.250 ± .097 (p<0.05)	0.394 ± .084 (p<0.05)
2 week-treated	0.384 ± .093 (p<0.01)	1.312 ± .209 (p<0.001)
10 week-treated	0.329 ± .009 (p<0.005)	0.516 ± .093 (p<0.05)
20 week-treated	0.289 ± .083 (p<0.05)	0.317 ± .020 (p<0.05)

* values represent mean ± standard error
n = 4 to 8 animals per interval



Summary of crystal precipitation and stone formation.

	L.I.	Mucus hyper- secretion	Sludge	Crystals	Platy units & microliths	Stones
Control	-	-	-	-	-	-
6 hrs	-	-	-	-	-	-
12 hrs	-	-	-	-	-	-
18 hrs	↑	+	-	-	-	-
24 hrs	↑	+	-	+	-	-
3 days	↑	+	+	+	-	-
5 days	↑	+	+	+	-	-
7 days	↑	+	+	+	-	-
2 wks	↑	+	+	+	+	-
3 wks	↑	+	+	+	+	-
10 wks	↑	+	+	+	+	+
20 wks	↑	+	+	+	+	+

↑ denotes higher values than control

- denotes absent

+ denotes present

L.I. denotes lithogenic index

Summary of morphological changes

	Mitosis & L.I.	Hypertrophy & hyperplasia	Damage & extrusion	RA-sinus plasma cells	Cholesterosis-like lesion
Control	-	-	-	-	-
6 hrs	-	-	-	-	-
12 hrs	-	-	-	-	+
18 hrs	-	-	-	-	+
24 hrs	#	-	-	-	+
3 days	-	-	-	-	+
5 days	-	-	-	-	+
7 days	*	-	-	-	+
2 wks.	*	-	-	-	+
3 wks.	#	-	-	-	+
10 wks.	*	+	+	-	+
20 wks	*	+	+	+	+

- denotes absent

+ denotes present

* denotes higher values than control

denotes not done

L.I. denotes labelling index

DISCUSSION

Control animals

The gallbladder of the Richardson's ground squirrel was thrown into numerous mucosal folds or rugae, the height of which reflected the fullness of the organ at the time of fixation. Mueller et al. (1972) examined guinea pig gallbladder in empty and filled states and found that the folds or rugae disappeared when the gallbladder was fixed in the filled state. These authors suggested that the unstimulated filled gallbladder should be considered as the normal resting state of the organ. In addition they found that the residual elevations in a completely filled gallbladder were caused by large underlying vessels. The ground squirrel gallbladder exhibited these small mucosal humps when filled as well but further examination failed to reveal any underlying structures.

Fenestrated capillaries with diaphragms were observed in close proximity to the epithelium and were present in these folds. Hayward (1968) described fenestrated capillaries in the lamina propria in cats. Faye et al. (1966) showed fenestrated capillaries in the gallbladder of rabbits with different degrees of distention depending on the functional activity of the lining

epithelium. The capillaries below non-transporting cells were collapsed while those of active cells were distended.

Unmyelinated nerves were seen between muscle layers and in the lamina propria in close proximity to blood vessels. Cai and Gabella (1983, 1984) described ganglionated nerve plexuses in the serosa, near the cystic artery and its branches and in the lamina propria of the guinea pig gallbladder. Neurohistochemical observations by these authors (1983) revealed both acetylcholine-positive and catecholamine-containing fibers in the gallbladder of the guinea pig. In the present study, electron microscopic observations revealed prominent adrenergic varicosities intramuscularly and beneath the basal lamina. Cai and Gabella (1983) and Baumgarten and Lange (1969) did not observe any adrenergic varicosities intramuscularly in the guinea pig, rhesus monkey or cat, but saw a rich supply in the serosa and lamina propria where they form part of the mucosal plexus. Kyosola and Penttila (1977) observed adrenergic fibers in the human gallbladder, especially in the fibromuscular layer, and a few axons beneath the basal lamina. Bjorck et al. (1982) have shown that adrenergic nerves enhance the concentrating function of the feline gallbladder by stimulating water absorption from the lumen. In this study, the adrenergic varicosities reflected a non-direct system of nerves to the musculature and

epithelium of the ground squirrel gallbladder. However, neurohistochemical studies are required to identify the distribution of fiber types.

The lateral cell membranes exhibited microfolds that appeared to interdigitate with one another in TEM sections. Similar observations were made by Mueller et al. (1972) in the guinea pig and MacPherson et al. (1983) in the dog. They may also be similar to the microvilliform projections described by Hayward (1968), finger-like evaginations of Tormey and Diamond (1967), and elaborate digital processes of Wheeler (1971), all seen in cross section in a number of species with the transmission electron microscope. The microfolds of adjacent cells separated from each other and allow extensive distention of the intercellular space during active transport of solutes to the lamina propria. Spring (1983) postulated that some sodium was actively pumped into the lateral intercellular space while the rest was exocytosed through basal plasma membrane by the Na-F pump. The ATP for these pumps was supplied by mitochondria which were found concentrated in the basal region of the cell. Tormey and Diamond (1967) calculated that the basal region of the cells contained about 60-80% of the mitochondria present in the subapical region. Rough estimates indicated a similar ratio in the light cells of the ground squirrel gallbladder.

Prominent desmosomes were seen scattered along the lateral cell membranes of adjacent cells as far down as the basal plasma membrane. In a number of studies, (Kaye et al. 1966; Tormey and Diamond, 1967; Dietschy, 1966), desmosomes were not described between apposing cell membranes except in the apical zone. Kaye et al. (1966) considered desmosomes a rare occurrence in rabbit gallbladder. Mueller et al. (1972) have shown prominent desmosomes in the guinea pig gallbladder and postulated that the absence of desmosomes in the above studies may be the result of artifactual disruption due to manipulation and interruption of blood supply to the organ while the tissue was being obtained. The random distribution of desmosomes appeared to ensure a labyrinth of interconnecting channels between adjacent cells for the movement of solutes as postulated by Diamond and Bossert (1967) for the standing-gradient osmotic flow model. In the present study, basolateral desmosomes were not disrupted even when the intercellular space was extensively distended.

Dark, or pencil, cells were seen singly among the light cells. The dark cells exhibited the same features as the light cells only the cytoplasm was more electron dense and the organelles closely packed together. - Dark cells were described in humans (Evet et al. 1964), and rabbits (Hayward et al. 1968). Togari and Okada (1953) regarded

these cells as being effete while Yamada (1962) showed an increase in enzyme activity. Hopwood et al. (1980) suggested loss of cytosol might explain this increase in enzyme activity, prevented the free movement of organelles and impaired normal function of these cells. In the gallbladder of man, Bader (1965) proposed that the dark cell was an intermediate cell type in the course of development and differentiation from the undifferentiated basal cell to normal epithelial cell. The presence of mitosis in the lining epithelium showed that replacement epithelial cells are not derived from basal cells. Studies on the gallbladder epithelium of sheep (Hayward, 1965) and the dog (Johnson et al. 1962) suggested a declining functional activity for these cells. The dark cells observed in the present study were normal and lend support to the suggestion of Hopwood et al. (1980) that loss of cytosol impaired organelle movement and function. The functional significance of the dark cells needs further study.

A light edematous barrel-shaped cell was observed infrequently in the lining epithelium. The ultrastructural features of these cells suggested that they were aged and degenerative with a high degree of hydration. They appeared to be in the process of being extruded from the lining epithelium into the gallbladder lumen during normal

epithelial turnover. These cells exhibited the classical features of cell death as described by Trump and Arstila (1976). Apoptotic bodies were not observed in the gallbladder lumen or in neighbouring cells. Several authors (Kerr et al., 1972; Wyllie et al. 1980; Harmon et a., 1984) described apoptotic bodies as specific for cell death in which membrane bound organelles are extruded in the lumen of an organ or the degenerated cell is phagocytosed by neighbouring cells. Yamada (1968) observed light barrel-shaped cells with degenerated organelles in the mouse gallbladder and suggested that they were aged cells with declining activity. Dyban (1973) has shown that the normal turnover rate of the gallbladder epithelium of guinea pigs was 32 days. In the present study, the marked infrequency of mitotic figures and edematous cells, may also suggest a slow turn over rate for the ground squirrel gallbladder.

Leucocytes were seen migrating through the basal lamina and were found between epithelial cells near the basal lamina and occasionally in intercellular spaces at the level between the nucleus and junctional complex. Leucocytes were first described by Virchow (1857) and have been subsequently described in the literature as cask cells (Togari and Okada, 1953), and basal cells (Ferner, 1949). Kilburn et al. (1973) have shown random migration of leucocytes between epithelial cells in the trachea of

hamsters and guinea pigs exposed to toxic substances. In the present study a random transepithelial migration of leucocytes was observed but the functional implication remains to be elucidated.

Mucus

The gallbladder epithelium of control ground squirrels exhibited a basal level of both sialylated and sulphated glycoprotein secretion, a phenomenon similar to that described in the gallbladders of other models (Hayward, 1968; Lee, 1980; Lee and Scott, 1982; Yamada, 1962b; Lee, 1981; Wahlin, 1979; Esterly and Spicer, 1968; Smith and LaMont, 1985b).

Intercellular mucin granules have had their ultrastructural characteristics defined as membrane bound electron lucent granules with a dense core (Hayward, 1968; Lee, 1980; Koga, 1973) which led to contradictions. Hora and Schultz (1970) described lipid droplets in the supranuclear regions of epithelial cells of human gallbladder while Koga (1973) suggested these droplets were mucin granules. Light microscopy autoradiography failed to conclusively identify mucus granules but verified the incorporation of tritiated glycoprotein precursors as well as the pathway of mucus secretion (Wahlin, 1977; Ely et al

., 1971). In the present study, autoradiography at the electron microscope level demonstrated the occurrence of silver halide over these cellular inclusions following administration of radiolabelled galactose, a mucin precursor. This positive identification of mucin granules, rather than sole reliance on morphology, was integral to the interpretation and verification of observations made in this study.

Mucus, because of its visco-elastic properties, is extruded from the epithelial cells into the lumen in the form of strands. Scanning EM confirmed the transmission observations that not every cell was in a similar stage of the secretory cycle. Active secretion was observed to occur in groups of cells. Transmission EM showed these cells contained prominent rough endoplasmic reticulum, a Golgi complex, and microtubules, all features indicative of secretory potential and/or activity.

The mechanism of mucus release is still a matter of controversy. Hayward *et al.* (1968) proposed a holocrine mode for rabbit, others (Koga, 1973; Lee, 1980; Yamada, 1962b) described a merocrine secretion in the mouse and guinea pig, while Laito and Nevalainen (1972) advocated apocrine secretion in the human gallbladder. In the present study, mucin granules were observed in close proximity to

the apical surface, in some instances fusing with the plasma membrane and discharging their contents into the lumen of the gallbladder. This process was similar to that demonstrated electron microscopically in the rabbit (Lee, 1980), mouse (Wahlin et al. 1974, 1976; Wahlin, 1977), and guinea pig (Wahlin and Schieber, 1975), indicating a merocrine secretory mode.

The stimulus for and mechanism of mucus release and expansion is not fully understood. Lee et al. (1981b) demonstrated that ligation of the cystic duct before feeding prairie dogs a lithogenic diet prevented mucus hypersecretion and concluded the stimulus for hypersecretion was in the lithogenic bile.

The mechanism of mucin granule release is subjected to speculation. S.P. Lee proposed that there is a change in the ionic content of the granule which resulted in water absorption and an explosive extrusion of the granule content over the epithelial surface. This allowed the mucin to spread over non-secreting cells and formed a continuous layer (Personal communication).

The increased frequency in observation of apical cytoplasmic bullae by scanning electron microscopy in experimental groups, suggested an apocrine secretory

process similar to that observed in humans. Correlative transmission electron microscopy however, did not support this hypothesis. Sections through these apical bullae revealed that they contained few, if any, mucus granules. Apical regions of cells exhibiting various degrees of convexity contained masses of mucus secretory granules but the plasma membrane retained their microvilli, a feature not consistent with that of true apical bullae. Goblet cells were not observed in the mucosa of the ground squirrel. Apical bullae of similar morphology were observed in the gallbladder epithelium of newborn rabbits (Hayward, 1968) and dogs (MacPherson et al., 1983). None of these authors was able to attribute any definite function to bullae. Hopwood et al. (1980) claimed that the terminal web might be responsible for keeping organelles from entering the bullae. In the ground squirrel, the terminal web was poorly developed and as such would be unable to effectively ensure the absence of organelles in bullae. A poorly developed terminal web was also described in the mouse and rabbit (Yamada, 1955; Hayward, 1968). Trump and Arstila (1976) however, considered these structures to represent part of the cellular reaction to injury as they were common features in ischemic bowel syndromes. The absence of cellular organelles in the bullae and their function requires elucidation.

Experimental animals

Mucus secretion

Hypersecretion of epithelial mucins was observed in gallbladder epithelium of experimental animals as early as 18 hours after the ingestion of the cholesterol-enriched diet. Precipitation of cholesterol monohydrate crystals from the lithogenic bile was not observed until 24 hours in treated animals. Previous studies have demonstrated mucin to be a nucleating agent for crystal precipitation and its hypersecretion occurred prior to crystal precipitation (LaMont et al., 1984; Whiting and Watts, 1985; Hayward et al., 1968; Lee and Scott, 1979; Lee and Scott, 1982; Smith and LaMont, 1985b). In the present study, the ground squirrel-cholesterol model confirmed this pattern and has allowed quantitation of the phenomenon prior to and during cholelithiasis.

Previous studies have suggested that the stimuli for mucus hypersecretion was in the lithogenic bile (LaMont et al., 1984; Lee et al., 1981b). The latter authors demonstrated that ligation of the cystic duct in the prairie dog before cholesterol feeding prevented mucus hypersecretion. In the present study, bile lithogenicity increased significantly in the 18 hour treated animals and

responsible in whole or in part, for the stimulation of mucus hypersecretion. Florey (1970) postulated that mucous membranes in response to a noxious stimuli will increase mucus secretion and cell proliferation as a protective mechanism. Increased cellular proliferation was also observed in ground squirrels fed a lithogenic diet.

Quantitation of epithelial mucins demonstrated their continued increase in synthesis and secretion throughout the 20 week experimental period. These values peaked at the one-two week interval, an ideal time for the mucus to act as a nidus in the aggregation of crystals into platy units, microliths and stones. Continued hypersecretion facilitated the progressive growth of these smaller concretions into macroscopic stones.

Crystal precipitation and stone formation

Cholesterol gallstone formation was not merely a matter of producing supersaturated bile and was far more complex than the situation initially suggested by Admirand and Small (1968). Supersaturation of the bile with cholesterol was essential for stone formation but not everyone with supersaturated bile forms stones. The difference between stone forming and non-stone forming subjects appeared to be their ability to form cholesterol

crystals (Whiting and Watts, 1984). This was thought to be related to the presence of nucleation factors, their absence, or the presence of inhibitors in the bile.

Precipitation of cholesterol crystals from mildly supersaturated bile required the addition of particulate material, a process referred to as heterogenous nucleation (Bouchier, 1984). Whiting and Watts (1985) concluded the difference between stone and non-stone forming bile lay in the nucleation stage of crystal formation rather than in the presence of inhibitors. Initially many factors were thought to be able to initiate nucleation including bacteria, desquamated cells, epithelial glycoprotein mucins and mucus. Particular attention was focused on the role of epithelial glycoproteins in their many forms as mucins, mucus, and sludge (LaMont et al., 1984; Smith and LaMont, 1985b).

Most gallstones exhibited a core of mucus and these glycoproteins contributed to the lattice structure of the stone (Lee et al., 1979). Mucin can act as an area of epistatic contact in crystal growth (Bouchier, 1983), bound bilirubin (Smith and LaMont, 1983), and enhanced in vitro nucleation of cholesterol crystals (Levy et al., 1983). Strong indicators of the role of mucin in nucleation have been provided by in vitro studies (Levy et al., 1984) but particularly by in vivo animal models of cholelithiasis where excessive mucus secretion was the underlying common

observation (Doty et al., 1983a; Freston et al., 1969; Lee, 1981; Lee et al., 1981b). Hypersecretion of mucus has been noted to either accompany or precede stone formation in these models. Lee and Nicholls (1986) found a striking increase in the amount of mucus glycoprotein in gallbladder bile of patients with biliary sludge, even greater than those with gallstones. This high molecular weight glycoprotein is now considered a pronucleating agent in experimental and human gallstone disease (LaMont et al., 1984).

The ground squirrel model has demonstrated, through SEM observations, that even cholesterol crystal precipitation was preceded by increased mucus secretory activity. An increase in both the amount, and number of actively secreting cells was observed as early as 18 hours on the diet. The lithogenic indices revealed that the morphological documentation of increased mucus activity occurred just before, or in concert with, the supersaturating of the bile with cholesterol. Holan et al. (1979) was the first to demonstrate that accelerated nucleation of cholesterol monohydrate crystals was a distinguishing feature of lithogenic bile. LaMont et al. (1984) considered the stimulus for gallbladder mucus hypersecretion to be a component of the lithogenic bile. Prostaglandin regulation of mucin release from the

gallbladder has been demonstrated in the prairie dog using aspirin to block this process and thereby inhibited gallstone formation (Lee et al., 1981a).

The lithogenic index of the ground squirrel bile rose quickly to exceed 1.0, but then fell as low as 0.615 at 20 weeks. Gallstone formation however, continued during this period and analysis of biochemical components required to calculate the lithogenic index indicated the bile was not desaturated and contained a high proportion of cholesterol.

Biochemical analysis of the bile showed that the phospholipid level increased rapidly during the first 18 hours and dropped to normal level at 24 hours at which time cholesterol crystal precipitation occurred. Holzbach (1936) proposed that phospholipid vesicles maintained cholesterol in solution in the metastable zone and above this saturation level, cholesterol crystallized out of solution. During the same experimental period, bile acids level dropped below normal while cholesterol level increased thereby facilitating the saturation of bile. The increased lithogenic index may be due to decrease secretion of bile, dilution of secreted bile or failure of the gallbladder to absorb water adequately.

Scanning electron microscopic observations on the

mucosal surface of the ground squirrel gallbladder during the pathogenesis of cholelithiasis, revealed accumulation of a thick sludge-like layer. This became evident following the initial stages of cholesterol monohydrate crystal precipitation and continued throughout the experimental period. Gallbladder sludge, observed by sonography in humans; has been defined as thick bile that may either contain, or consist of, a fine suspension of pigment granules, mucin, calcium bilirubinate, cholesterol crystals and small stones of less than 3mm. diameter (Allen et al., 1981; Smith and LaMont, 1985a). Juniper and Burson (1957) described the presence of cholesterol crystals in a microscopic examination of gallbladder sediment. The crystals appeared colorless, transparent, and thin, with parallel edges often having a notched corner resembling pieces of broken window glass. Scanning electron microscopy of the cholesterol monohydrate crystals precipitated from ground squirrel bile confirmed these earlier observations. This indicated a similarity in configuration between these and human crystals.

Sludge occurred in gallbladders where stasis was evident and often disappeared after return of normal contractility. Doty et al (1983b) concluded that gallbladder stasis was an important link between hepatic secretion of cholesterol saturated bile and listed a number

of factors that might impair gallbladder emptying. Several workers have shown that sludge is an integral part of both cholesterol and pigment stone formation (Allen et al., 1981; Been et al., 1979; Bernhoft et al., 1983; Soloway et al., 1977). The thick sludge-like layer observed in the ground squirrel by SEM occurred at an ideal time to become involved as an accessory nucleation agent and aiding in the aggregation of small platy band subunits into larger concretions. Lee and Nicholls (1986) determined this sludge to be a sediment composed of cholesterol monohydrate crystals and bilirubin granules embedded in a matrix of mucus gel.

Smith and LaMont (1985a) identified the chemical nature of a brown-black material that composed the matrix of human cholesterol gallstones. This material was a non-lipid component identified as a mucin-bilirubin complex and had a composition similar to that of biliary sludge. Ground squirrels on the lithogenic diet for 10 weeks exhibited stones where the sludge-like material was embedding cholesterol crystals into its growing surface. After 20 weeks the larger cholesterol gallstones began to take on a brownish-yellow coloration when examined macroscopically. The SEM showed this matrix-like material on the surface of these stones. It helped to fill in the crevices between larger subunits in the stone, smooth out

the surface and continued to embed cholesterol crystals. Morphological observations on this model leave little doubt that mucus hypersecretion played a role in the initial stages of nucleation followed by the formation of biliary sludge which then aided in the aggregation of smaller subunits into concretions of increasingly larger size.

Osuga and his colleagues (1974) used the scanning electron microscope to investigate experimentally-induced gallstone development in the squirrel monkey and compare it with observations made on luminal contents of human gallbladders resected for cholecystitis (Osuga et al., 1975). Summarizing their findings they claimed that although the sequence of stone formation was similar, there were significant differences between the concretions of man and squirrel monkeys (Osuga et al., 1975).

When the pattern of stone development observed in the ground squirrel gallbladder are compared to the schematic diagrams provided by Osuga et al. for monkey (1974) and human (1975), the observations made in this study most closely fit those for the human. Neither the "wagon wheel" concretions nor the central cavity in simple stones of the monkey were common to either the ground squirrel or human. Similar configuration of ground squirrel microliths to those of human and the sand-like stones of the monkey,

indicated an underlying common growth pattern in the early phases of stone formation. The larger mulberry shaped stones, and the initiation of condensation, in the outer layers of stones from 20 week ground squirrels, when the organs were filled with concrements, indicated a pattern that will ultimately form mature stones with a configuration similar to those of the human.

The similarity in the pattern of stone formation and morphology of the resultant concrements to human stones is encouraging. When this is coupled with the similarity of bile chemistry, the reproducibility and frequency of incidence, the non-toxicity of the diet, and the relatively short time factor involved from introduction of the diet to gross stone formation, the ground squirrel is an excellent animal model for induction of experimental cholelithiasis.

Mucosal changes

Cell proliferation and damage

The data from this study demonstrated an increase in the rate of cell proliferation and progressive mucosal damage, both of which were intimately related to time on the diet and the presence of macroscopic stones. Some of

the changes observed were similar to those noted in previous studies (Scott, 1978; Putz and Willems, 1981; Scott, 1979; Müller-Beigler and Palme, 1982; Lee and Scott, 1982; Kaye et al., 1966; Felt, 1972). A number of those observed changes in cell morphology, were significantly different. The occurrence of mitoses throughout the epithelial sheet of control and experimental animals, without any pronounced valleys or crests, was similar to studies in the human (Putz and Willems, 1978; Putz and Willems, 1979) and guinea pig (Scott, 1974; Jacoby, 1958), but dissimilar to the rabbit (Kaye et al., 1966). The latter author suggested that proliferative compartments existed in the gallbladder of rabbits, the valleys more active in mitoses. Mueller et al. (1972) however, have shown that valleys and crests of mucosal folds were transient structures dependent upon the state of the gallbladder when fixed. The present study supported this finding.

Mitotic figures observed in the epithelial sheet of control animals were relatively rare. Previous studies in human (Putz and Willems, 1978; Putz and Willems, 1979), guinea pig (Scott, 1978; Jacoby, 1958; DeBorja, 1973), mouse (Scott, 1978; Lee and Scott, 1982) and rabbit (Scott, 1978; Kaye et al., 1966) gallbladder have demonstrated that the normal cell turnover rate in this organ was very slow.

Bargmann (1959) failed to observe mitosis in the human gallbladder and suggested this tissue was amitotic.

A significant difference between this and previous studies (Putz and Willems, 1978; Evett et al., 1964) centered on which cell was actually undergoing mitosis. Electron microscopic observations in the ground squirrel showed that columnar epithelial cells, and not the basal cells seen near the basal lamina, were involved in mitosis. Light microscopic studies of human gallbladder had earlier suggested the basal cells as the progenitors for this organ (Putz and Willems, 1978; Evett et al., 1964). The findings of this study clearly do not support this hypothesis.

In the one and two week experimental groups, the mitotic and labelling indices were significantly higher than those of control animals. These indices were considerably lower than those of other experimental models (Scott, 1978) but closer to the values obtained in human gallbladder epithelium (Putz and Willems, 1978; 1979). This increase in proliferative activity was observed before the occurrence of macroscopic stones, but during the period of crystal and microlith formation. Studies on the mouse (Scott, 1978, Putz and Willems 1981; Marsch-Zeigler and Palme, 1982; Lee and Scott, 1982) and other models (Scott, 1978) have also shown this rapid increase in the number of mitotic and labelled cells long before the presence of

stones. These authors suggested that abnormal bile might have been responsible for this increased proliferative activity and that mechanical irritation to the mucosa was secondary. Putz and Willems (1978) examined human lithiasic gallbladder and suggested that chronic mechanical irritation by gallstones might cause increased cell proliferation. This phenomenon was thought to be one form of response to irritation or injury (Florey, 1970). Cell proliferation may help increase the surface area to compensate for supersaturated bile (Marsch-Zeigler and Palme, 1982). In the present study, cholesterol-fed ground squirrels demonstrated modified gallbladder bile as early as eighteen hours, crystal precipitation within 24 hours, and microliths at 2 weeks.

Previous studies in guinea pig (Scott, 1974; Jacoby, 1958), mouse (Putz and Willems, 1981), and man (Putz and Willems, 1979) have shown that distended gallbladders also exhibited an increase in proliferative activity. The presence of stones in human (Putz and Willems, 1978) and mouse (Lee and Scott, 1982) gallbladder on the other hand, did not cause distention and therefore did not stimulate the increase proliferative activity. The crystals and microliths present early in the cholesterol-fed ground squirrel did not block the cystic duct, nor were the organs distended. The increase in mitotic activity in this model

was also clearly not related to distention. The gallbladders of animals from the early experimental period also failed to show any inflammatory response, another mitotic stimulant.

In the 10 and 20 week experimental groups, cellular damage and extrusion, hypertrophy, hyperplasia, Rokitansky-Aschoff sinuses, inflammatory cells and continued presence of significantly higher mitotic and labelling indices were phenomena similar those observed in the mouse (Marsch-Zeigler and Palme, 1982; Lee and Scott, 1982) and guinea pig (Scott, 1976). The presence of inflammatory cells in the lamina propria, thickening of the muscular layer and occurrence of Rokitansky-Aschoff sinuses were standard criteria used for microscopic diagnosis of chronic cholecystitis (Halpert, 1961; Edlund and Olsson, 1961). These earlier studies in the cholesterol-cholic acid mouse model showed cellular damage and extrusion as early as two days on the diet, hypertrophy and hyperplasia by the sixth day, the changes occurring long before the presence of macroscopically visible stones (Marsch-Zeigler and Palme, 1982; Lee and Scott, 1982). In the ground squirrel however, a significantly different time frame was involved, the changes were only observed in the presence of stones. This suggested that the increase in cellular damage might be due to either the continued toxicity of supersaturated bile or

a direct mechanical effect. This discrepancy between models may be either species or diet-related. The gallbladder of the ground squirrel appeared to have reacted slower to the cholesterol-enriched diet and may reflect more accurately the changes occurring in the human gallbladder.

A previous study using the mouse model suggested that dividing epithelial cells were extruded from the epithelial sheet (Marsch-Zeigler and Palme, 1982). In the ground squirrel, electron microscopic observations revealed that epithelial cells in preparation for division, on the crests of mucosal folds were larger than adjacent cells. They were distinctly different in morphology however, from the edematous cells that were actually extruded. Epithelial cell debris has been implicated as a nucleating factor for stone formation (Small, 1980; Sedaghat and Grundy, 1980; Lee and Scott, 1982). The extrusion of edematous cells during normal epithelial turnover in the ground squirrel may also act as a nucleating factor in the presence of saturated bile. Recent studies have implicated mucus hypersecretion as an important phenomenon contributing to stone formation (Lee et al., 1981b; LaMont et al., 1984).

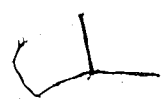
Transmission EM revealed that no actual defect in the epithelial sheet existed when one, or even two, cells were extruded. Correlative scanning and transmission EM showed

that neighbouring epithelial cells slid under those being extruded to protect the underlying layers. This may not be possible however, when large areas of the epithelium are denuded as in acute and chronic cholecystitis of human gallbladders (William and Smith, 1978). Other studies on human gallbladder (Hopwood et al., 1980; Myllarniemie and Nickels, 1977) also showed that damaged cells occurred singly or in groups. Scanning EM revealed actual defects in the epithelial sheet and the authors suggested that the holes represented empty goblet cells (Myllarniemie and Nickels, 1977). In the ground squirrel, goblet cells were not seen in either control or experimental animals.

Cellular damage may also be attributed to ischaemia (Trump and Arstila, 1976), but no any evidence of thrombi in mucosal blood vessels was observed in this study.

The battery of changes seen in the ground squirrel closely followed the chronological pattern described for premalignant lesions of the human gallbladder (Ojeda et al., 1985; Albores-Saavendra, 1986). The present study indicated that the Richardson's ground squirrel model is well suited to study the chronology of cholecystitis and malignant lesions.

Cholesterolosis-like lesion



The present study demonstrated a rapid increase in lipid accumulation in the mucosa of the ground squirrel gallbladder throughout the experimental period. Previous studies have shown the gallbladder epithelium to be capable of absorbing cholesterol and phospholipids from the bile (Neiderhiser et al., 1971; 1973; 1976; Hopwood et al., 1981; Kouroumalis et al., 1984; Ross et al., 1986). Lipid accumulation in ground squirrel gallbladder epithelium was observed intracellularly and intercellularly as early as 1 hour after ingestion of the lithogenic diet. Coupled with this was a significant increase in bile cholesterol levels. Neiderhiser et al. (1976) demonstrated a rapid increase of cholesterol absorption in the gallbladder of the guinea pig, the rate of absorption dependent on the absolute and relative cholesterol content of the bile.

Previous studies have proposed one way for these cells to rid themselves of the absorbed lipids was through release into the intercellular space. The lipids subsequently moved to the lamina propria and finally into either the venous or lymphatic system (Neiderhiser et al., 1976; Kouroumalis et al., 1984; Koga, 1985; Hora and Schulz, 1970; English and Hopwood, 1985). This mechanism appeared to facilitate transport of excess lipid in the gallbladder of the ground squirrel.

The accumulation of lipid in the supranuclear and basal regions of epithelial cells, as well as in dilated cisternae and residual bodies was observed in one, two, and three week old animals. A similar accumulation of lipids in the supranuclear and basal regions of the cells, as well as in tubular or vesicular reticula, has been described previously in human gallbladders with cholesterolosis (Koga, 1985; English and Hopwood, 1985; Miettinen and Tilvis, 1985). Several studies suggested that the free cholesterol absorbed from the bile was esterified in the smooth endoplasmic reticulum to form lipid droplets which were then released into the intercellular space and on into the lamina propria (Koga 1985; Nevalainen and Laito, 1972; Tilvis. et al. 1982; Subbiah and Dicke, 1977; Hora and Schulz, 1970). Support for this hypothesis was obtained in the present study by the localization of digitonin complexed free cholesterol in both dilated endoplasmic reticulum and lipid droplets in the supranuclear regions of the epithelial cells. Lipid droplets in the basal regions of these cells did not complex with the digitonin.

Residual bodies were found in the subapical and supranuclear region while lipid droplets appeared only in the basal aspect of the cells. Neiderhiser and colleagues (1971, 1973; 1976) have shown that uptake of lipids from

bile by the gallbladder epithelium was a normal phenomenon. These authors have demonstrated uptake of C^{14} -labelled oleic acid, cholesterol, lecithin and lyolecithin by the normal guinea gallbladder. The lipid droplet was either incorporated into residual bodies or transported into capillaries in the lamina propria. Lipid droplets observed in the ground squirrel may be on their way to capillaries in the lamina propria. The presence of residual bodies subapically, and lipid droplets basally, in these animals suggested that the lining epithelium of the gallbladder was capable of absorbing lipids from the bile and either incorporating them into residual bodies or transporting them to capillaries in the lamina propria.

Another mechanism available to the cell to rid itself of cholesterol was through heterophagocytosis, a process which results in the formation of residual bodies.

Epithelial cells from ground squirrels on the lithogenic diet exhibited numerous residual bodies in the supranuclear region of the cells, a situation similar to that described in human gallbladders with cholesterolosis (Nevalainen and Laito, 1972; Hora and Schulz, 1970). Digitonin-complexed experiments revealed free cholesterol in these organelles. The residual bodies may then be released into the intercellular space.

All changes observed in the present study occurred when the bile was lithogenic and cholesterol crystal precipitation or microlith formation were observed either on the epithelial surface or in bile washings.

In 10 and 20 week treated animals, there was continued presence of lipid in residual bodies, supranuclear and basal cell regions. In addition, dense osmiophilic droplets was observed in the lamina propria. Lipid appearance and density varied depending upon the degree of unsaturation of fatty acids present to form a complex with osmium tetroxide (Ghadially, 1984). In the present study, chronological examination of the ground squirrel gallbladder has shown that macroscopic stones, lithogenic bile and early morphological features of chronic cholecystitis also occurred during this time frame. This suggested that epithelial cells of the ground squirrel gallbladder continued to absorb lipid from the bile and excreted it into the lamina propria. These lipids were then engulfed by macrophages and removed by venous or lymphatic drainage in a pattern similar to that suggested for human gallbladder. Failure of these macrophages to enter the circulation resulted in cholesterolosis (Koga, 1985; Nevalainen and Laito, 1972; English and Hopwood, 1985, Hora and Schulz, 1970). In the present study, accumulation of foam cells in the lamina propria was not observed and the

lesion was different from that commonly described in cholesterolosis of human gallbladder (Koga, 1985; Miettinen and Tilvis, 1985). The alterations in gallbladder mucosa of ground squirrels fed a lithogenic diet were basically similar to those described in the cholesterol-cholic acid fed dog model (Holzbach et al., 1977).

The early presence of lipid intracellularly, at the time when gallbladder bile was mildly saturated, may be an adaptive mechanism of the gallbladder to prevent cholesterol precipitation. It was not dependent upon, or related to, the presence of gallstones (Holzbach et al., 1977; Salmenkivi, 1964) or cholecystitis (Womack and Haffner, 1944), and occurred much earlier than either of these phases of the cholelithiasis process.

SUMMARY AND CONCLUSIONS

Two hundred and thirty eight conditioned Richardson's ground squirrels (Spermophilus richardsonii) of both sexes weighing 350-450 grams were divided into control and experimental groups. Each group contained 4 animals. Control animals were maintained on a diet of rat chow and water ad libitum while experimental animals were fed a 2% cholesterol-enriched diet and water ad libitum. Animals were killed at intervals of 6, 12, 18, 24 hours, 5, 7 days, 2, 3, 10, 20 weeks and 3 weeks on cholesterol-enriched diet followed by 3 weeks on normal diet.

Animals were killed, bile withdrawn and examined by polarizing light microscopy and assayed for phospholipids, bile acids and cholesterol to establish a lithogenic index. Gallbladders were injected with the same volume of fixative, 2.5% glutaraldehyde in Miloning's buffer pH 7.2. Tissue was processed for transmission and scanning electron microscopy, electron microscopic autoradiography, electron microscopy digitonin experiment, electron microscopy quantitative study and light microscopic: lipid histochemistry, paraffin mucin histochemistry, and methacrylate autoradiography.

The results indicated that in control animals, folds

or rugae were transient structures dependent upon on the volume of bile present when fixed. The lining epithelium of the gallbladder was composed of three types of cells, light, dark and edematous cells. The edematous cells were degenerating cells that were extruded from the epithelial sheet. The dark cells were narrower than the light cells but had a similar morphology. Transmission electron microscopy revealed that normal columnar epithelial cells were undergoing mitoses that was different from basal cells. The basal lamina formed peg and socket interdigitations with the basal plasma membrane and desmosomes were seen throughout the lateral plasma membrane in actively transporting cells. Nor-adrenergic nerve fibers were seen beneath the basal lamina and in between muscle bundles. A basal level of both sialylated and sulphated mucins were stored in membrane-bound granules and exocytosed by merocrine secretion.

In experimental animals, mucus hypersecretion was observed as early as 18 hours before the precipitation of cholesterol monohydrate crystal. This hypersecretion continued throughout the experimental period and formed a thick sludge-like layer over the epithelial surface. Mucus secretion peaked in the 1-2 week sampling interval, an ideal time to act as a nidus for the aggregation of crystals into platy units, microliths and stones.

Biochemical assay of bile showed bile lithogenicity began to rise at 18 hours while cholesterol crystal precipitation occurred at 24 hours. Platy units and microliths grew by appositional growth by two-three weeks and aggregated into mulberry stones in 10 weeks. By 20 weeks, many stones were approximately 2mm in diameter and accompanied by large numbers of various concretions. The larger stones had a cholesterol content of 61-74%.

Morphological observations of the gallbladder epithelium revealed increased cellular proliferation in one week treated animals before the occurrence of macroscopic stones but in the presence of cholesterol crystals and microliths. Electron microscopic observation of 10 and 20 week treated animals demonstrated damaged epithelial cells occurred singly or in groups and that there was no defect in the epithelial sheet. Neighbouring epithelial cells slid under the basal aspects of cells being extruded to protect the basal lamina. Hyperplasia, hypertrophy, Rokitansky-Aschoff sinuses, muscular thickening, plasma cells in the lamina propria were observed about the same time when stones were visible.

Other mucosal changes observed were the presence of lipid accumulation intercellularly and intracellularly in 12 hours treated animals. Dig~~it~~onin experiments revealed

100

free cholesterol in dilated endoplasmic reticulum and in residual bodies. Neutral lipid was demonstrated by light microscopy histochemistry in the supranuclear and basal regions of cells. In the 10 and 20 week treated animals, dense osmiophilic lipid droplets were seen in macrophages and in the lamina propria.

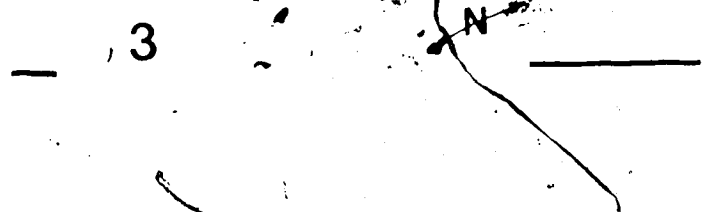
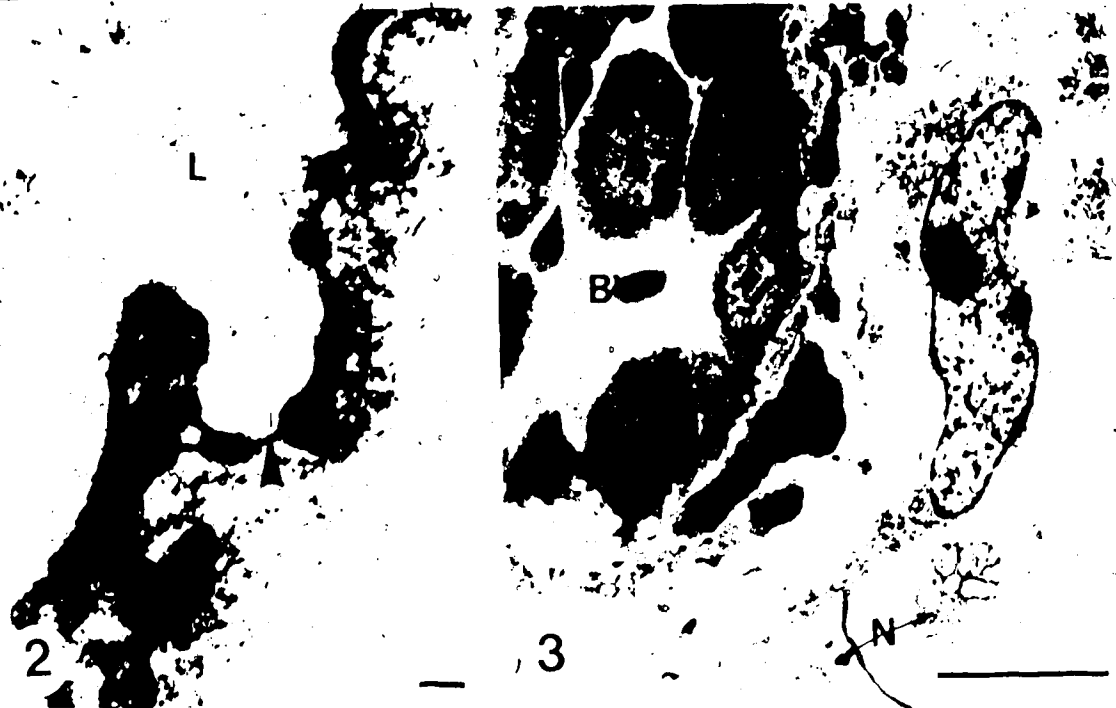
The present study demonstrated that the Richardson's ground squirrel fulfilled the criteria set out by Preston and Bouchier (1968) for a model to study cholelithiasis. Potential problems in directly applying results obtained from experimental studies to the human condition will always exist. However, constant comparison of data from both animal and human sources will help avoid pitfalls of extrapolation and contribute to solving the problems of human pathology in cholesterol cholelithiasis.

LEGENDS

Figure 1: A micrograph showing light and dark (white arrow) cells. A capillary (C) is seen in the lamina propria. Scale bar = 10 μ m.

Figure 2: A fenestrated capillary with diaphragm covering the fenestration (arrowhead). L- lumen. Scale bar = 0.1 μ m.

Figure 3: Unmyelinated nerves (N) in close proximity to a blood vessel (BV) of the lamina propria. Scale bar = 5 μ m.






Figure 4: An adrenergic nerve (Ad) is seen between muscle bundles (Mu). Scale bar = 5 μ m.

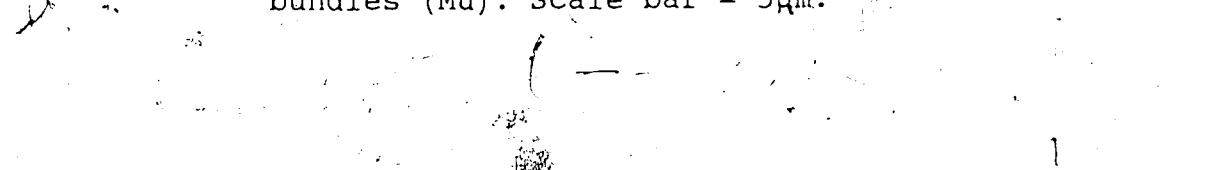


Figure 5: An adrenergic nerve (Ad) beneath the epithelial sheet (Ep). Scale bar = 5 μ m.




Figure 6: Junctional complex (Jc) between epithelial cells. Residual bodies (R) are seen in the supranuclear region. N- nucleus. Scale bar = 1 μ m.



Figure 7: A micrograph showing microfilaments (Mf) in close proximity to a centriole (Ce). Scale bar = 0.5 μ m.

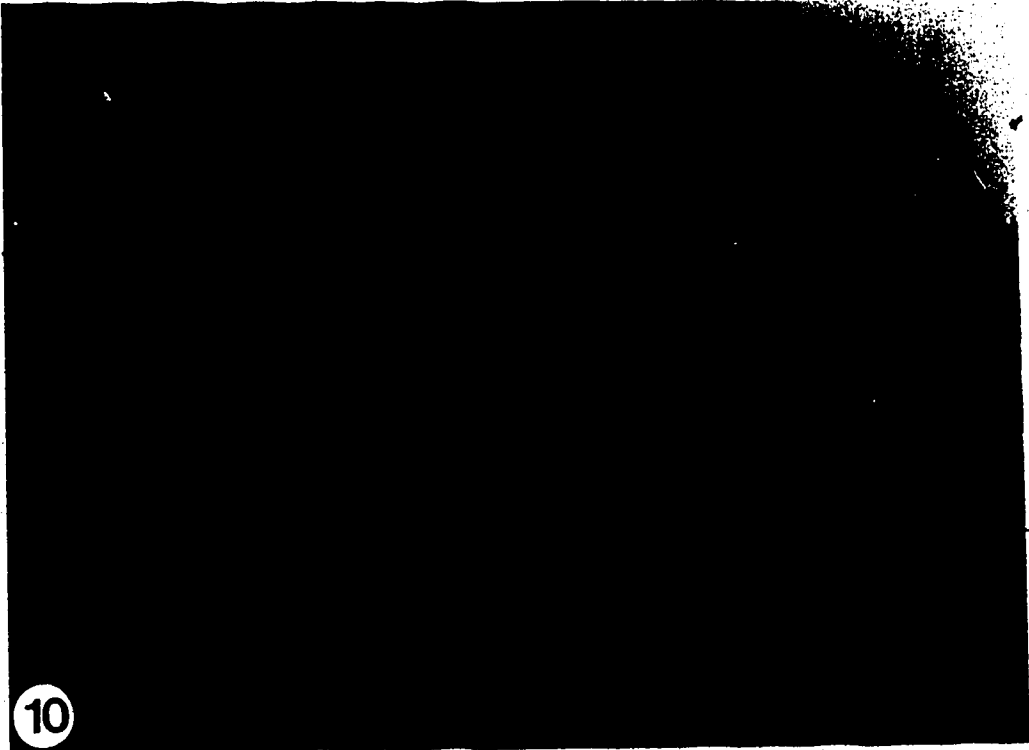
Figure 8: A lipid droplet (Li) in an epithelial cell near its basal plasma membrane, BL- basal lamina. Scale bar = 0.5 μ m.

Figure 9: An active Golgi complex (Gc) with secretory granules (Sg) near the maturing face. Note a microtubule (Mt) near the secretory granules. Scale bar = 0.5 μ m.



Figure 10: A light micrograph showing both sialylated (blue-aqua) and sulphated (brown-black) mucins on the surface of epithelial cells. High iron diamine-alcian blue pH 2.5 stain. Scale bar = 20 μ m.

Figure 11: A light micrograph of the gallbladder epithelium showing the supranuclear areas of a group of cells secreting sialomucin with side chain substitution (red). Potassium hydroxide/alcian blue pH 1.0/phenylhydrazine-Schiff stain. Scale bar = 20 μ m.



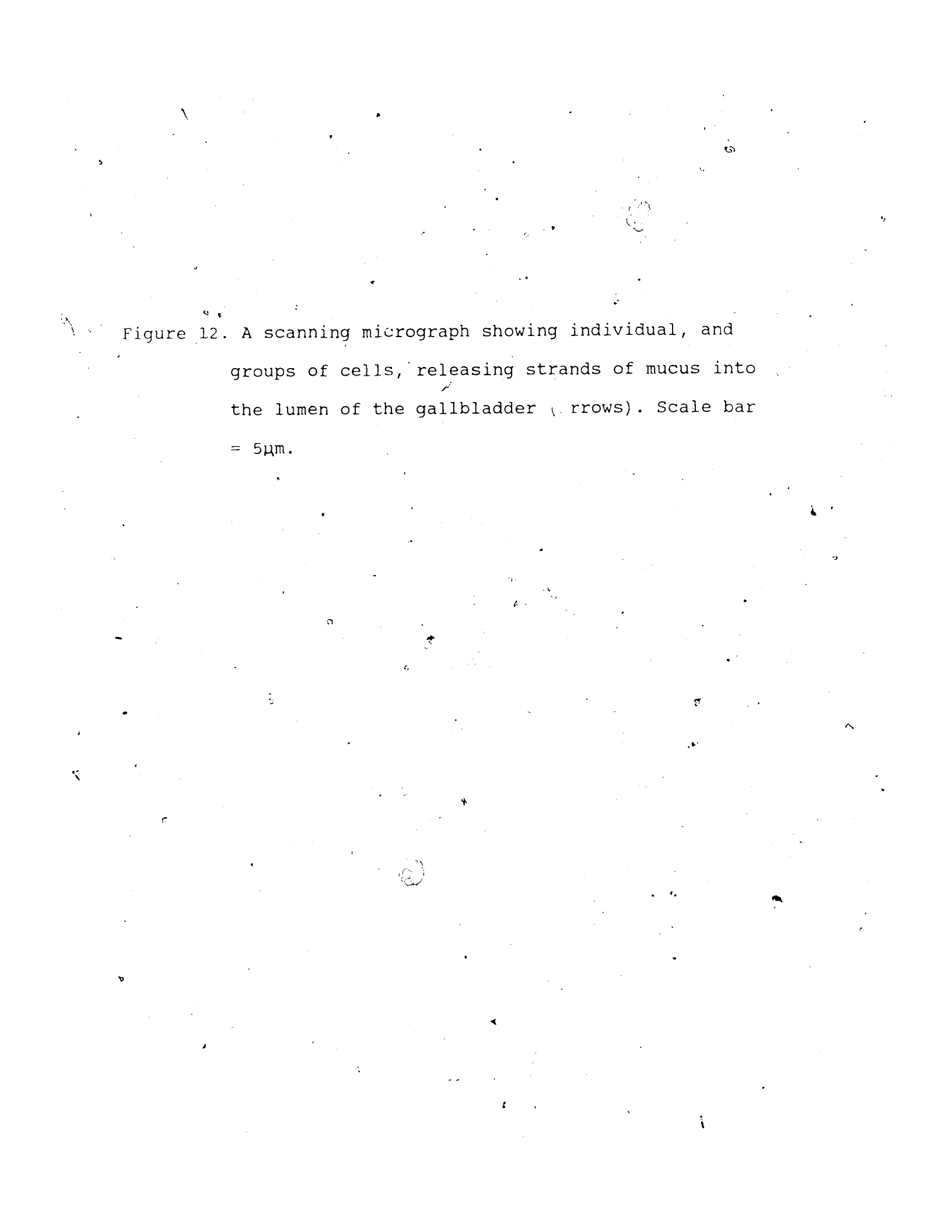
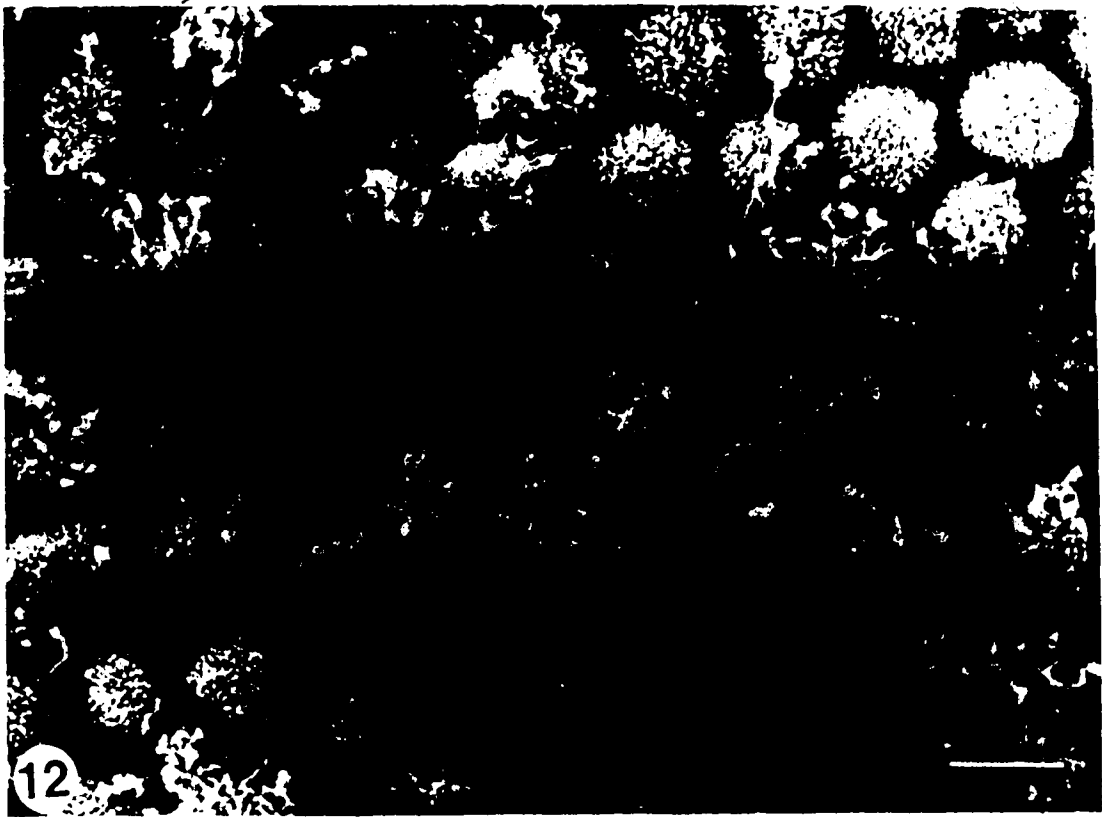
The image is a scanning micrograph showing a field of cells. Some cells are individual, while others are in small groups. From these cells, thin, dark strands of mucus are being released into the lumen of the gallbladder. Several small black arrows point to these mucus strands. A scale bar is present in the lower-left area of the image, indicating a length of 5 micrometers.

Figure 12. A scanning micrograph showing individual, and groups of cells, releasing strands of mucus into the lumen of the gallbladder (arrows). Scale bar = 5 μ m.






Figure 13: An electron microstopic autoradiograph of a control animal gallbladder 25 minutes after intraperitoneal H^3 galactose injection showing developed silver halide grains over a mucus granule. MV- microvilli. Scale bar = $0.2\mu m$.

Figure 14: An electron microscopic autoradiograph showing labelled material over mucus granules and endoplasmic reticulum in the supranuclear regions of cells. Seven day treated animal, 25 minutes after intraperitoneal H^3 galactose injection. Scale bar = $1\mu m$.

Figure 15: An electron microscopic autoradiograph showing labelled mucus on the luminal surface and subapical regions of epithelial cells. M- mitochondrion, Lu- lumen, MV- microvilli, arrowhead- labelled mucus granule. Control animal 40 minutes after intraperitoneal H^3 galactose injection. Scale bar = $0.5\mu m$.

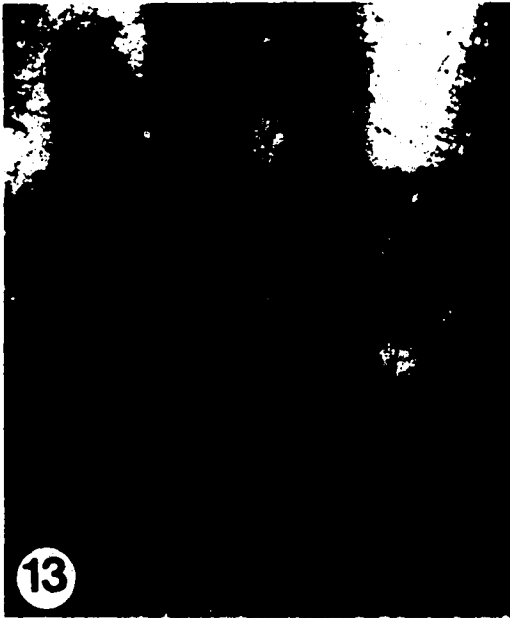


Figure 16: Mucus secretory granules (Sg) in the subapical region of the cell. Note the absence of cellular organelles in the region. M- mitochondria, Jc- junctional complex. Scale bar = $1\mu\text{m}$.

Figure 17: A micrograph showing a secretory granule (Sg) with an irregular profile. Note the contents of one granule being extruded into the lumen (arrow). Scale bar = $1\mu\text{m}$.

Figure 18: An apical bulla (B) containing only particulate matter. Scale bar = $1\mu\text{m}$.



Figure 19: A micrograph showing mitotic activity within the epithelial sheet. M- mitochondria, Ce- centriole, N- nucleus. Scale bar = 1 μ m.

Figure 20: An underdeveloped micrograph of a dark cell to demonstrate the presence of mitochondria (M) and residual body (R) in the apical region. Note the prominent junctional complex (JC) and desmosome (D) between light and dark cells. Scale bar = 1 μ m.

Figure 21: An underdeveloped micrograph of a dark cell showing the presence of mitochondria (M) in the basal region. Scale bar = 1 μ m.



19



20



21

Figure 22: An edematous cell with a pyknotic nucleus (N) and cellular contents being extruded into the lumen (L). Scale bar = 5 μ m.

Figure 23: An edematous cell with a karyolytic nucleus (N), lysosomes (Ly) and vacuolated mitochondria (M). Scale bar = 5 μ m.

Figure 24: A micrograph showing a prominent basal lamina (BL) forming peg and socket interdigitations with the basal plasma membrane of the overlying epithelial cells. Scale bar = 1 μ m.



20

20

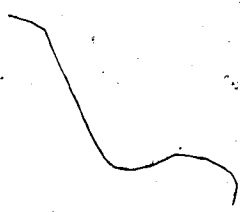


Figure 25: A micrograph showing various degrees of distention of the basal intercellular spaces (Is). Scale bar = $10\mu\text{m}$.

Figure 26: A prominent desmosome (D) still intact despite the distention of the intercellular space (Is). Scale bar = $1\mu\text{m}$.

Figure 27: The basal lamina (BL) under actively transporting epithelium demonstrates a reduction in the degree of peg and socket interdigitations with the overlying cells. D- desmosome. Scale bar = $1\mu\text{m}$.

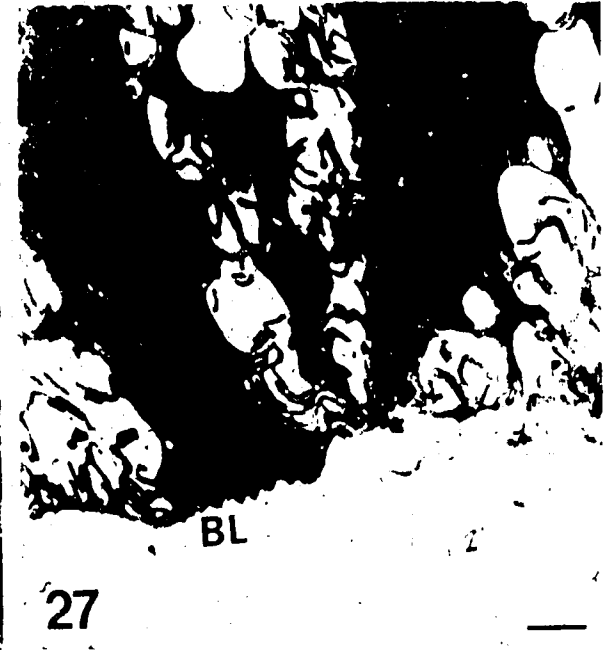
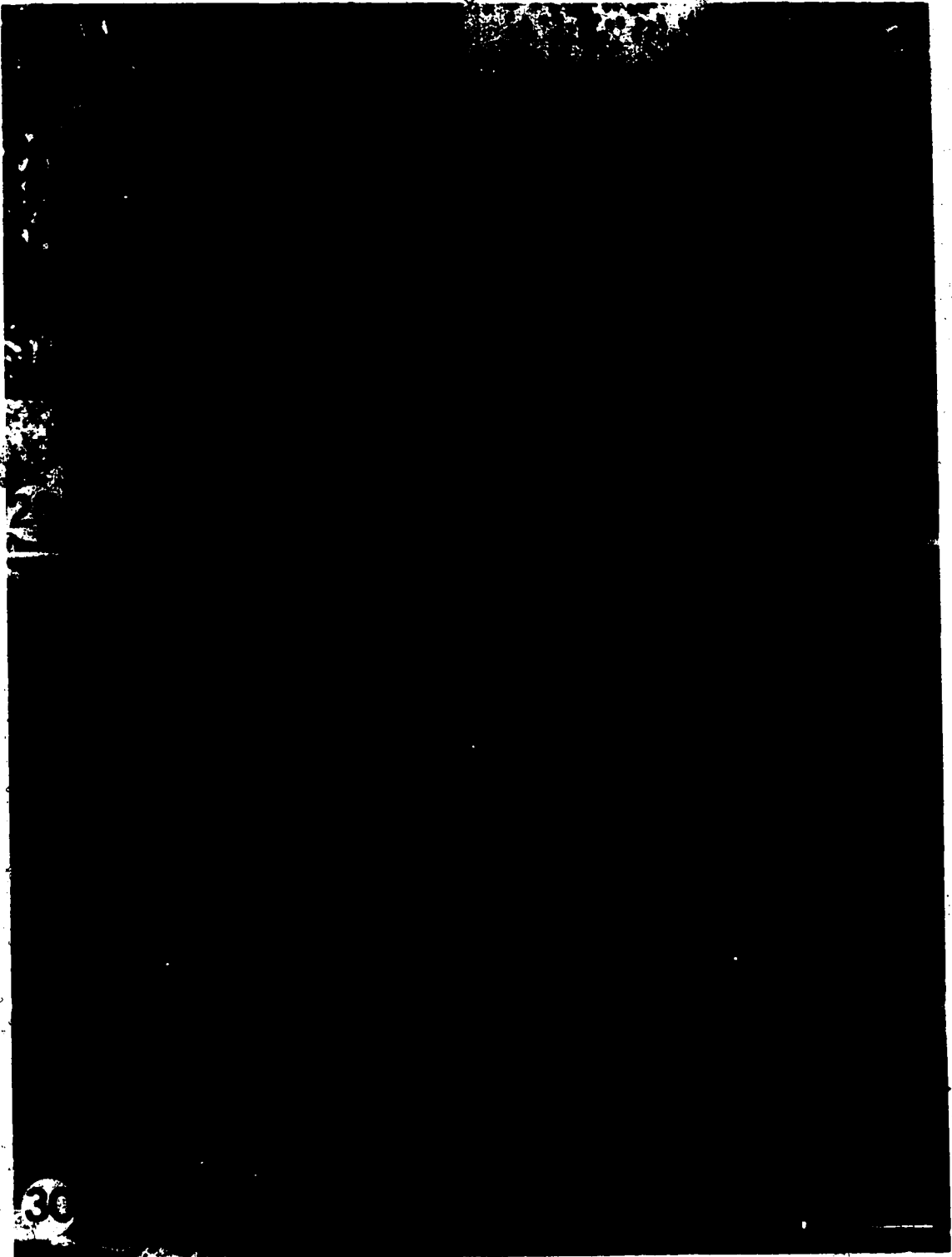


Figure 28: A leucocyte (Lu) migrating through the basal lamina (BL). Note a pseudopod (arrow) in the intercellular space. Scale bar = $1\mu\text{m}$.

Figure 29: A leucocyte (Lu) in the intercellular space near the junctional complex (Jc). L- lumen, arrows- lateral plasma membranes. Scale bar = $1\mu\text{m}$.

Figure 30: A scanning micrograph showing the degree of mucosal folding in an organ containing little or no bile. Scale bar = 0.1mm.



36




Figure 31: A scanning micrograph demonstrating the reduction in height and number of the mucosal folds when the organ is filled with bile. Scale bar = 0.1mm.



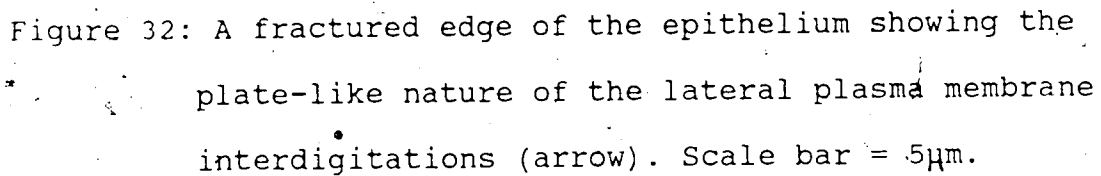


Figure 32: A fractured edge of the epithelium showing the plate-like nature of the lateral plasma membrane interdigitations (arrow). Scale bar = 5 μ m.

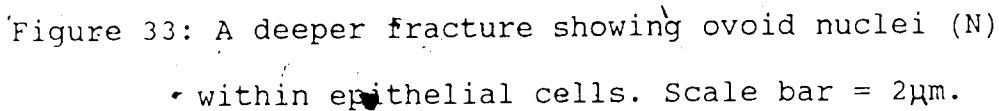


Figure 33: A deeper fracture showing ovoid nuclei (N) within epithelial cells. Scale bar = 2 μ m.

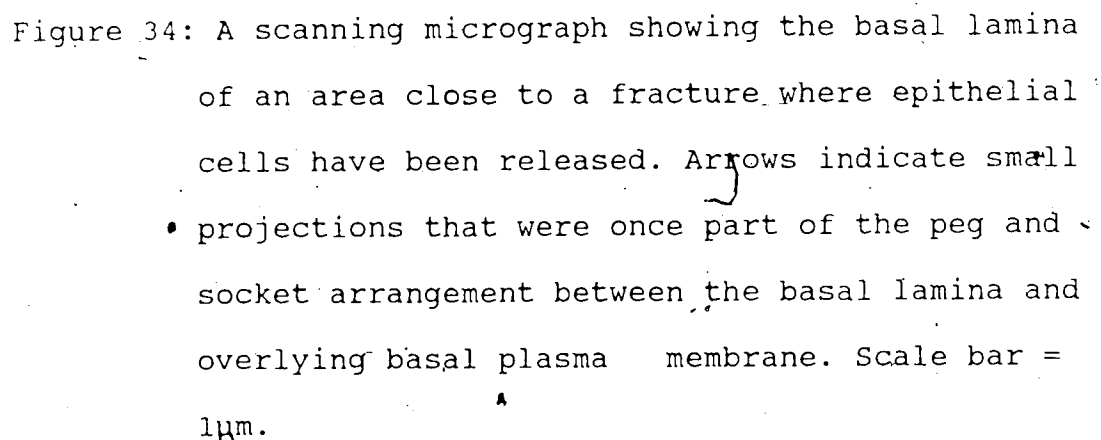


Figure 34: A scanning micrograph showing the basal lamina of an area close to a fracture where epithelial cells have been released. Arrows indicate small projections that were once part of the peg and socket arrangement between the basal lamina and overlying basal plasma membrane. Scale bar = 1 μ m.



32



33



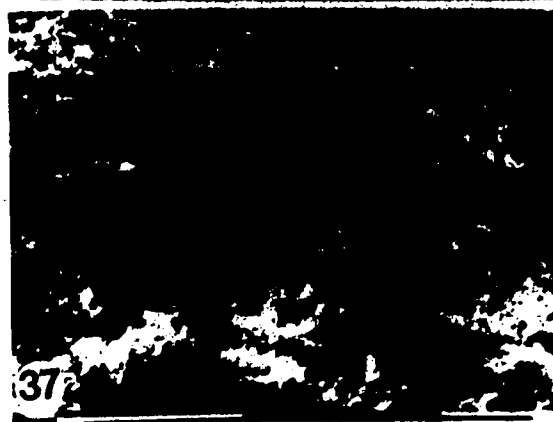
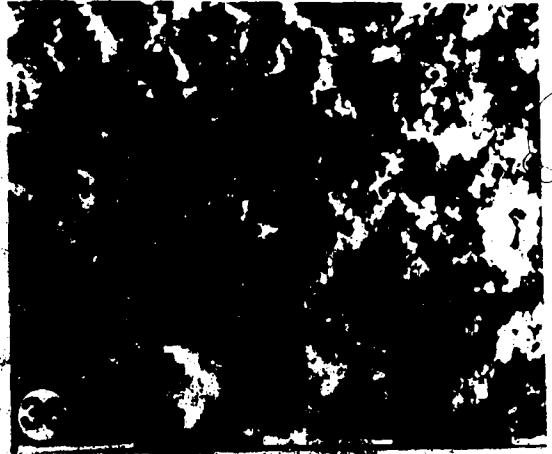
34

Figure 35: Increased mucus secretion at 18 hours. Scale bar
= 10 μ m.

Figure 36: Increased mucus secretion at one day. Scale bar
= 10 μ m.

Figure 37: Sludge-like material coalescing into a thick
layer covering large areas of the epithelial
surface at 3 days. Scale bar = 10 μ m.

Figure 38: Accumulation of mucus and initial lamination of
cholesterol crystals (arrow) at day 5. Scale bar
= 1 μ m.



Handwritten scribbles or markings on the right side of the page.

Figure 39: An electron micrograph showing numerous mucus secretory granules (Sg) in the apical region of a 7 day-treated animal. Note the presence of microvilli on the apical convexity. Jc- junctional complex, M- mitochondria, Scale bar = 1µm.

Figure 40: An apical bulla devoid of microvilli and contained cytoplasmic material. Scale bar = 10µm.






Figure 41: A thick sludge-like layer covering the epithelial surface of a two week-treated animal. Scale bar = 10 μ m.

Figure 42: Continued mucus hypersecretion in later sampling interval as demonstrated in a 20 week-treated animal. Scale bar = 10 μ m.

Figure 43: Surface morphology of a five day-treated animal showing prominent cytoplasmic bullae protruding into the gallbladder lumen. Note the presence of mucus and absence of microvilli on the surface of bullae. Scale bar = 10 μ m.

Figure 44: Epithelial cells of an animal fed a lithogenic diet for 3 weeks followed by normal diet for 3 weeks showing patchiness of mucus secretion similar to controls. Scale bar = 10 μ m.

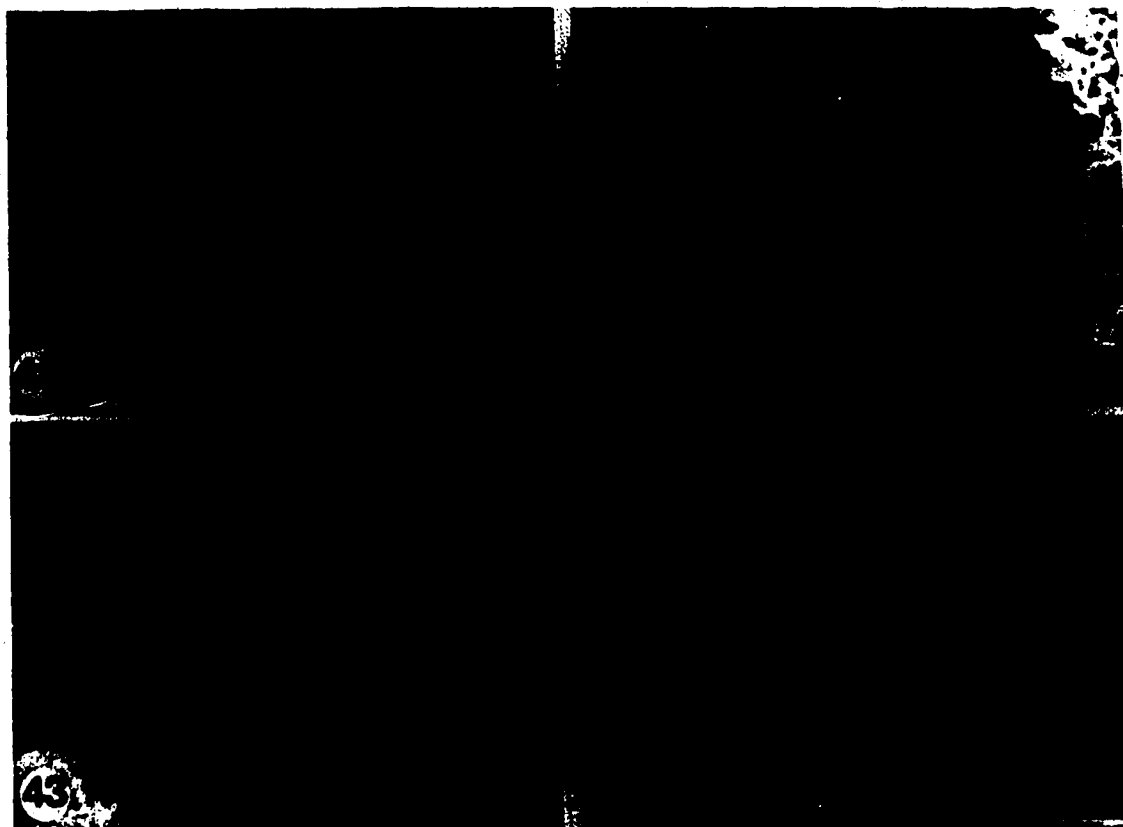


Figure 45: Cholesterol monohydrate crystals (arrows) stuck between microvilli at one day. Note the hypersecretion of mucus (arrowhead). Scale bar = $1\mu\text{m}$.

Figure 46: Continued precipitation of rhomboidal cholesterol monohydrate crystals at day 7. Note that some appear notched (arrow). Scale bar = $1\mu\text{m}$.

Figure 47: Crystal growth into platy subunits by parallel lamination common at 2 weeks. Scale bar = 0.1mm.

Figure 48: Surface of a platy subunit covered with biliary material. Scale bar = 0.1mm.

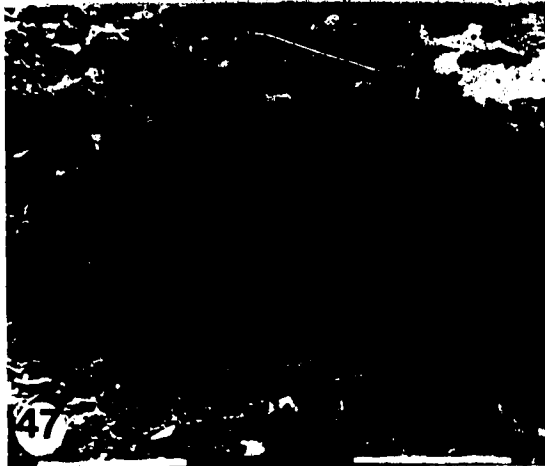


Figure 49: A 3 week microlith composed of a number of platy subunits arranged in an initial radial configuration. Scale bar = 0.1mm.

Figure 50: A number of concrements from a 10 week animal exhibiting various stages of growth. Scale bar = 1mm.

Figure 51: A concrement of intermediate size from a ten week animal. Note early evidence of lobular subunit aggregation. Scale bar = 0.1mm.

Figure 52: One of the largest stones from a 10 week animal exhibiting a multilobular shape. Scale bar = 1mm.

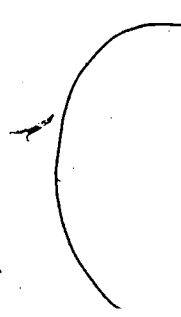


Figure 53: Higher resolution of a portion of figure 15 showing the component lobules. Scale bar = 0.1mm.

Figure 54: Another region of figure 15 showing biliary sludge embedding laminated cholesterol plates into the surface of the stone. Scale bar = 10 μ m.

Figure 55: A large mulberry shaped stone from a 20 week animal. Note the relative smoothness of its surface. Scale bar = 1mm.

Figure 56: Higher resolution of figure 20 showing polished regions where crystals are oriented parallel to the surface. Scale bar = 0.1mm.



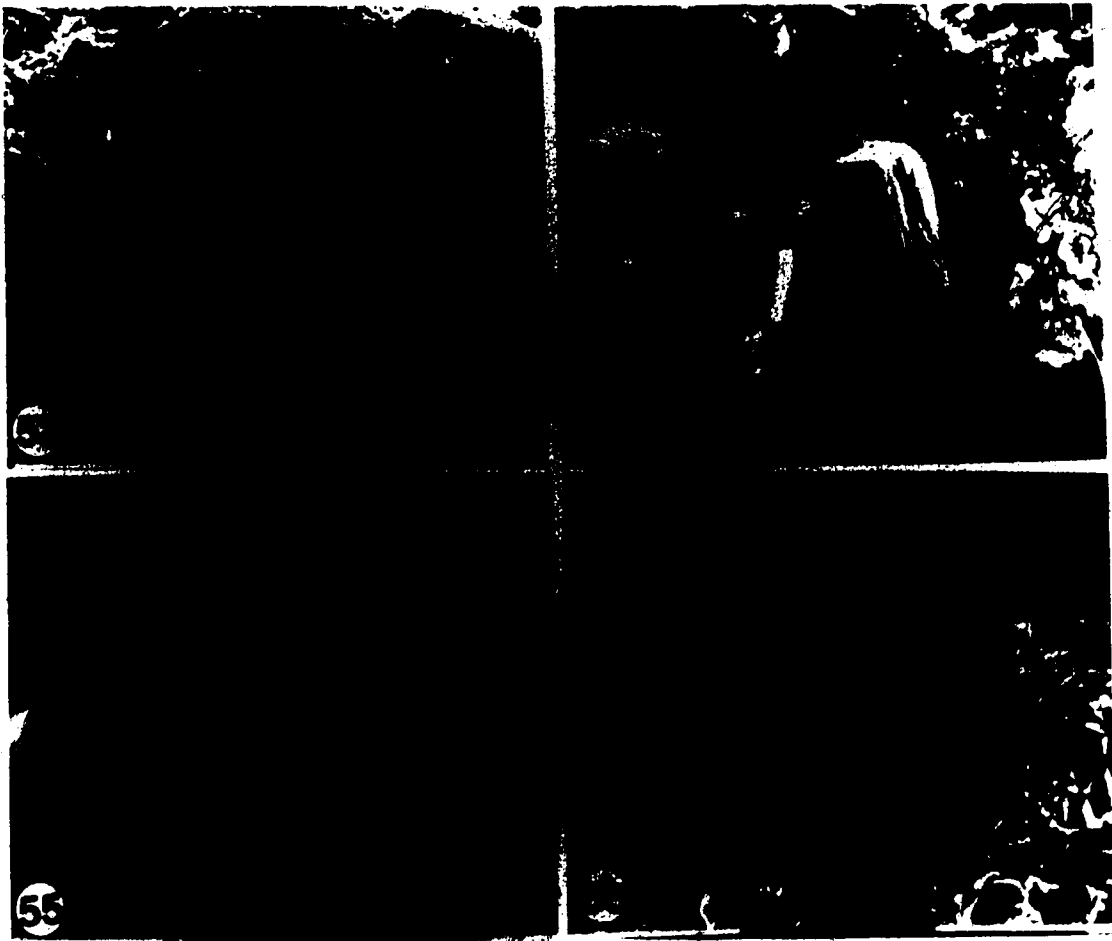


Figure 57: Fractured edge of a 20 week stone showing condensation of peripheral crystals into a capsule-like arrangement. The arrow indicates a septum radiating into the center of the stone. Scale bar = 0.1mm.

Figure 58: Central region of a fractured 20 week stone showing the aggregation of large numbers of laminated crystals. Scale bar = 0.1mm.



Figure 59: A two week-treated animal showing columnar epithelial cells undergoing mitosis (Mc) on the crest of a mucosal fold. Scale bar = 5 μ m.

Figure 60: Autoradiograph of a two week-treated animal showing labelled cells in the valley and sides of mucosal folds. Scale bar = 20 μ m.



Figure 61: A scanning electron micrograph of a ten week-treated animal revealing defects in the epithelial sheet (arrows). Scale bar = 10 μ m.

Figure 62: A transmission electron micrograph of a ten week-treated animal showing two edematous cells with ruptured apical membranes and karyolytic nuclei (N). Note the adjacent cells sliding under the basal aspect of the extruding cells. Scale bar = 2 μ m.

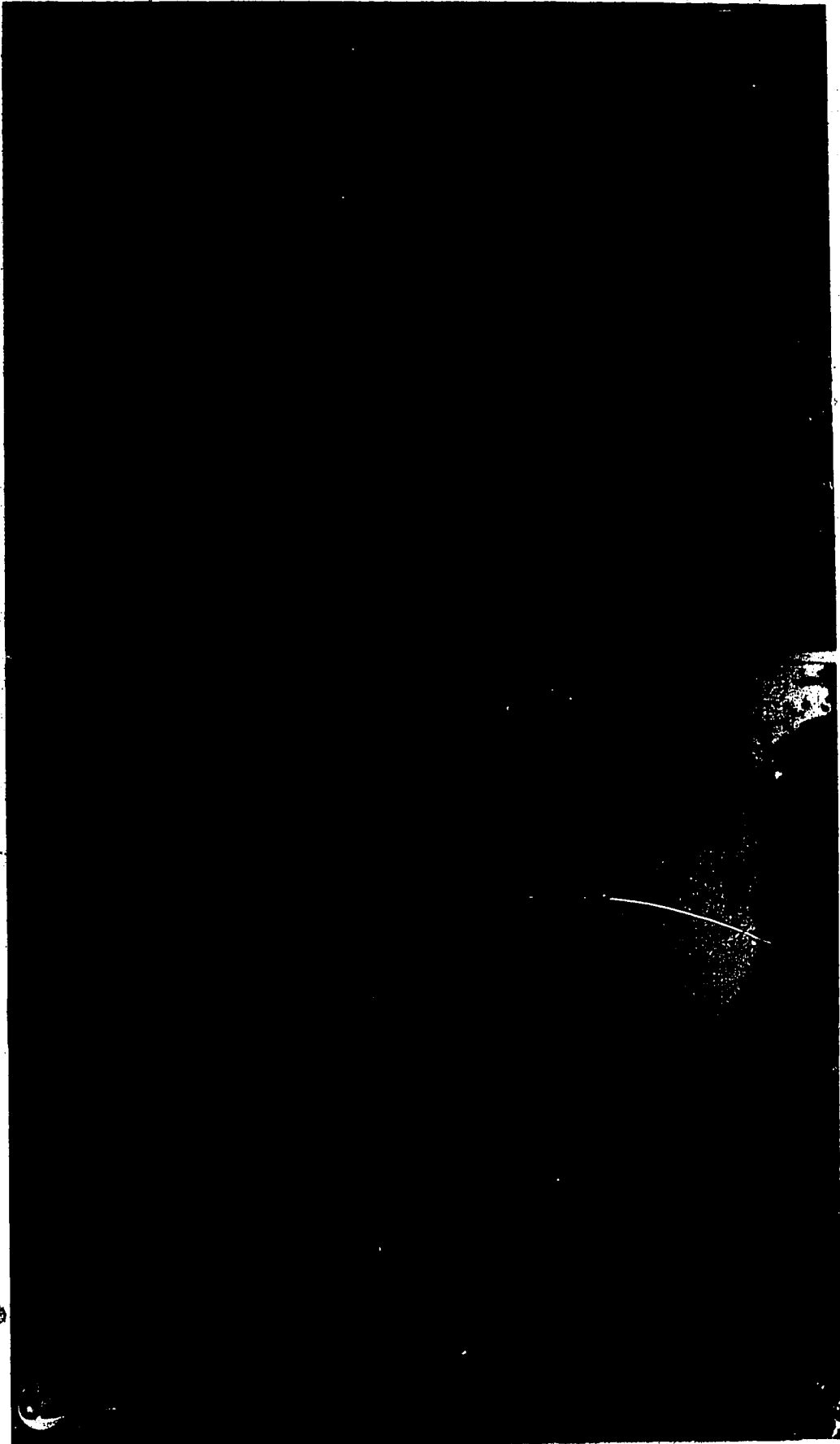
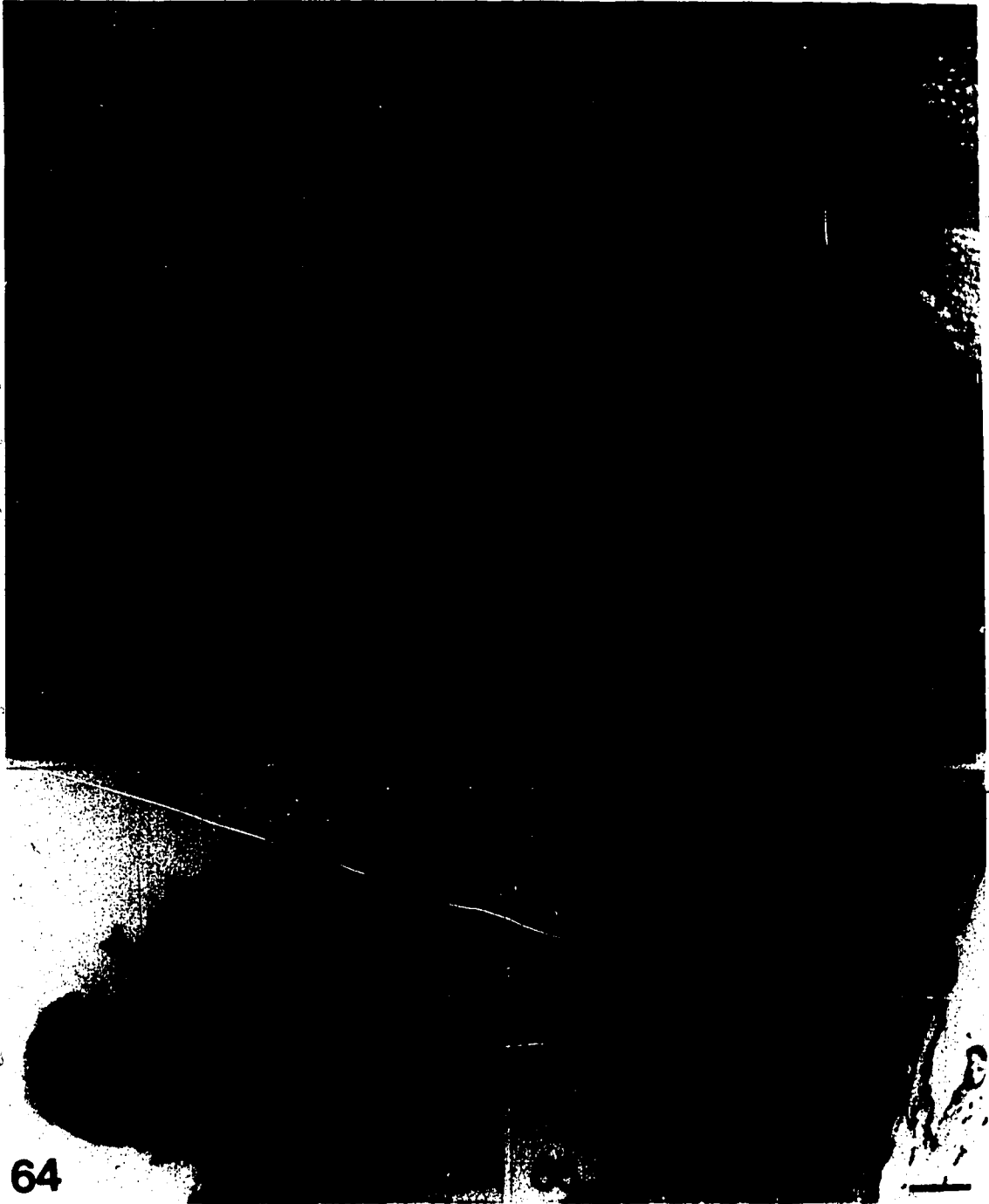


Figure 63: A scanning electron micrograph of a ten week-treated animal showing hypertrophic cells (arrowheads). Note normal epithelial cells in adjacent areas (curved arrow). Scale bar = 10 μ m.

Figure 64: Light micrograph of a 20 week-treated animal showing a hyperplastic lesion (arrow). Note two epithelial cells (arrowheads) close by in the process of mitosis. Scale bar = 20 μ m.

Figure 65: A 20 week-treated animal showing Rokitansky-Aschoff sinuses in the hypertrophied muscle layer. Scale bar = 40 μ m.



64

Figure 66: A transmission electron micrograph of a 20 week-treated animal showing inflammatory cells in the lamina propria. Epithelial cell (Ep), plasma cell (P), fibroblast (F). Scale bar = 3 μ m.

Figure 67: An electron micrograph of a 20 week-treated animal showing inflammatory cells (IC) between the basal lamina and epithelial cells (Ep) and in the lamina propria. C- capillary. Scale bar = 5 μ m.

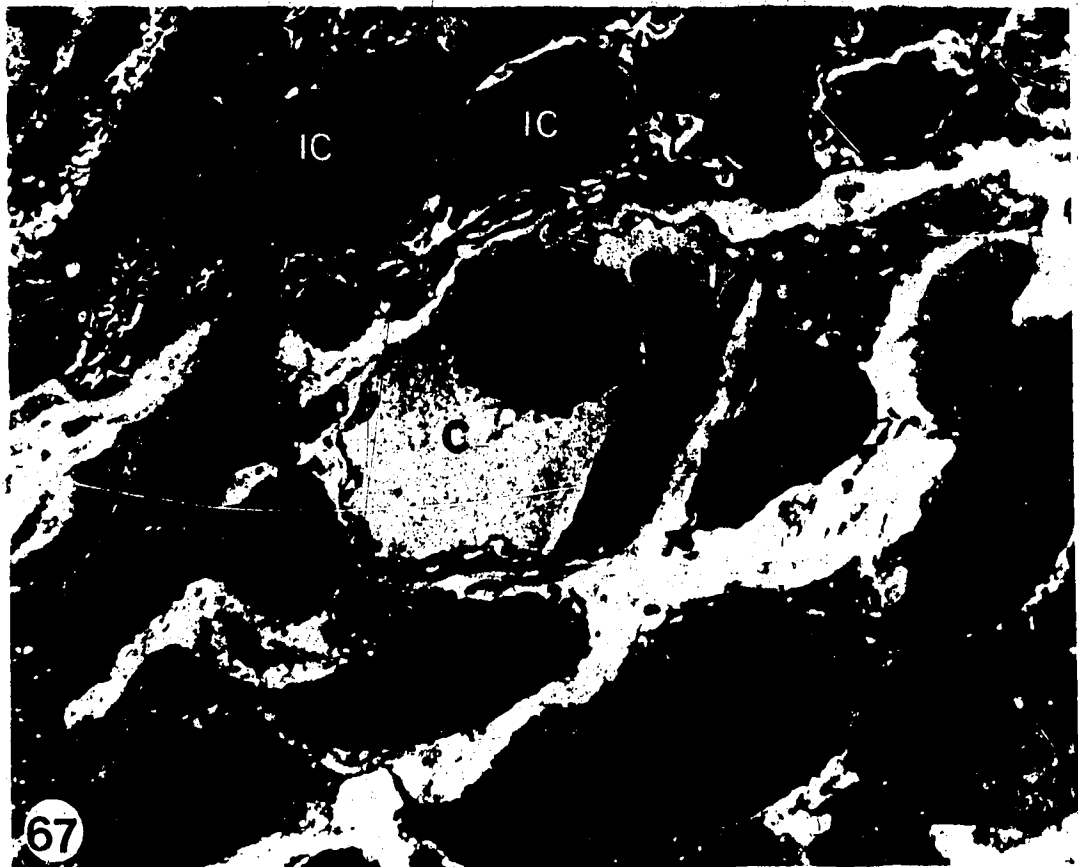
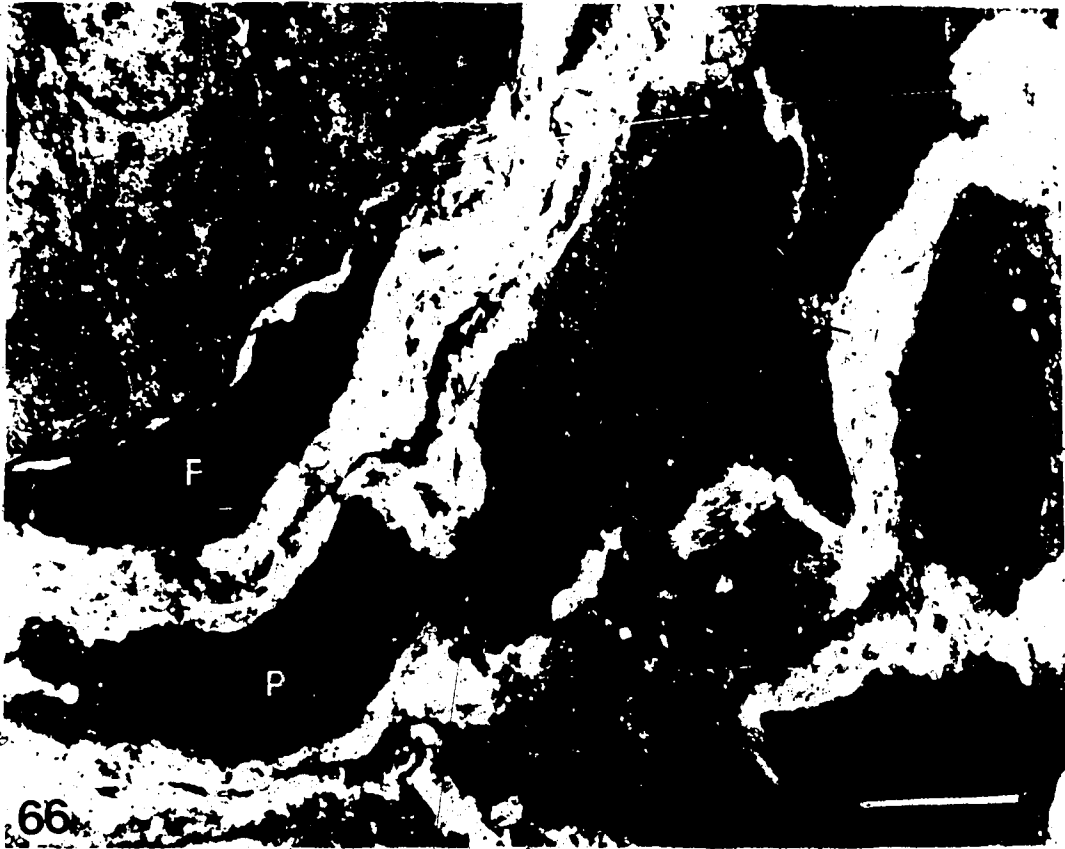
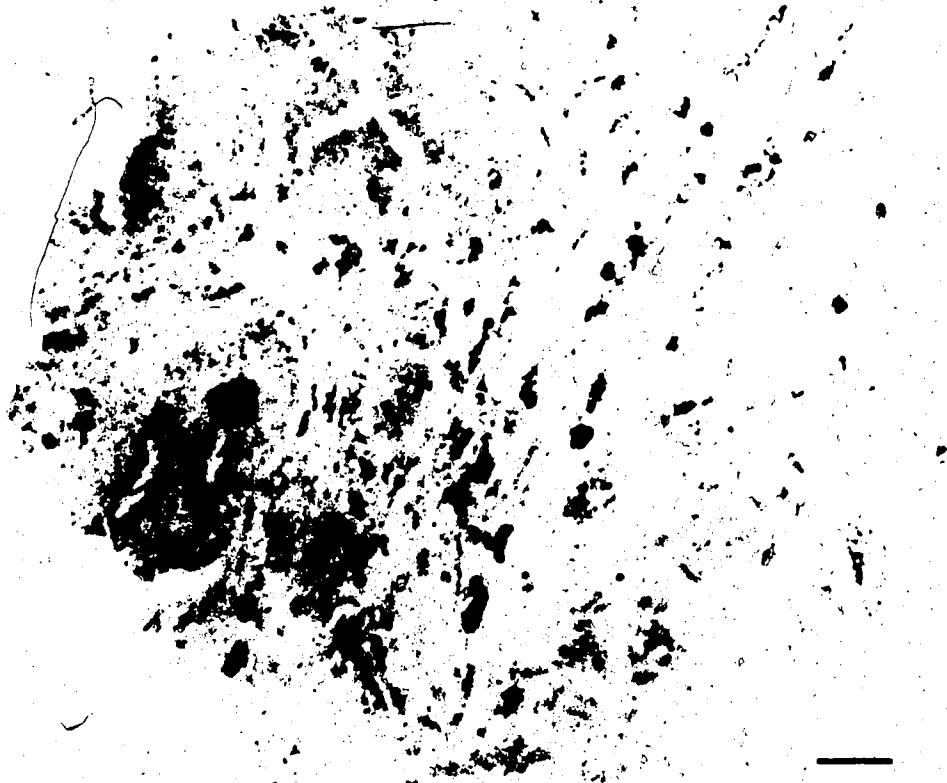


Figure 68: A light micrograph autoradiograph of a two week-treated animal showing numerous labelled fibroblasts in the lamina propria. Scale bar = 20 μ m.

Figure 69: A light micrograph of a two-week-treated animal showing numerous labelled fibroblasts in the adventitia. Scale bar = 20 μ m.



68



69



Figure 70: Lipid accumulation both intercellularly and intracellularly in 12 hour treated animals. N- nucleus, Lu- lumen. Scale bar = $3\mu\text{m}$.

Figure 71: Numerous residual bodies in the epithelial cells of one day treated animals. Scale bar = $2\mu\text{m}$.

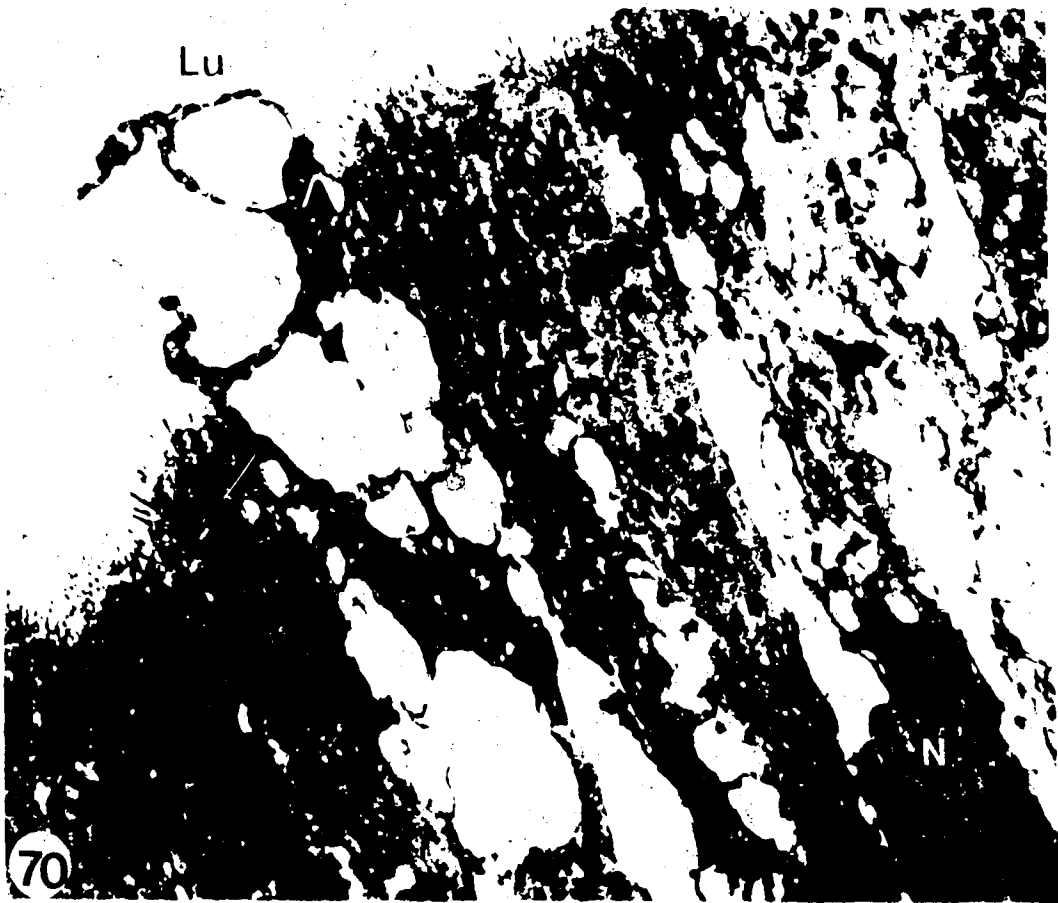


Figure 72: Lipid accumulation in the supranuclear region and lipid droplets (L) in the basal region of epithelial cells of seven day treated animals. Scale bar = 2 μ m.

Figure 73: Lipid accumulations (L) in the supranuclear region of an epithelial cell from a seven day treated animal. R- residual bodies, G- Golgi apparatus, rough endoplasmic reticulum (arrow), lysosome (arrowhead). Scale bar = 1 μ m.

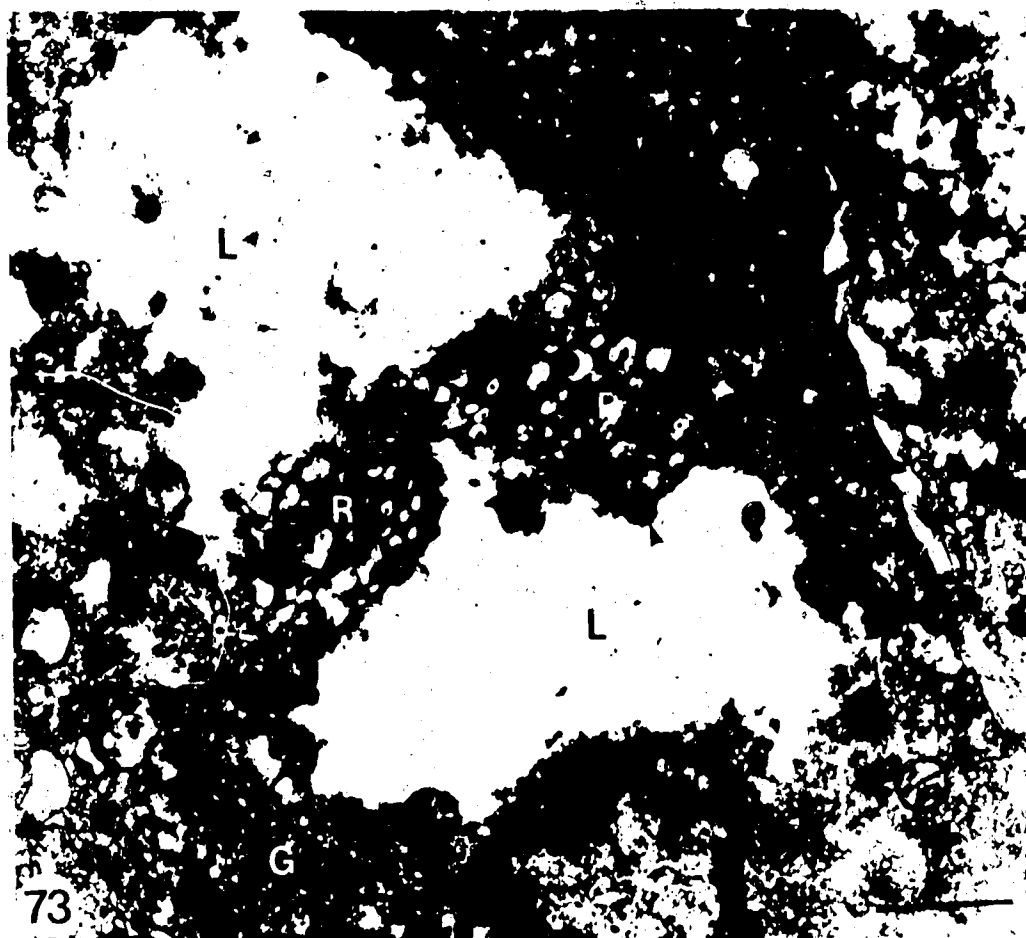
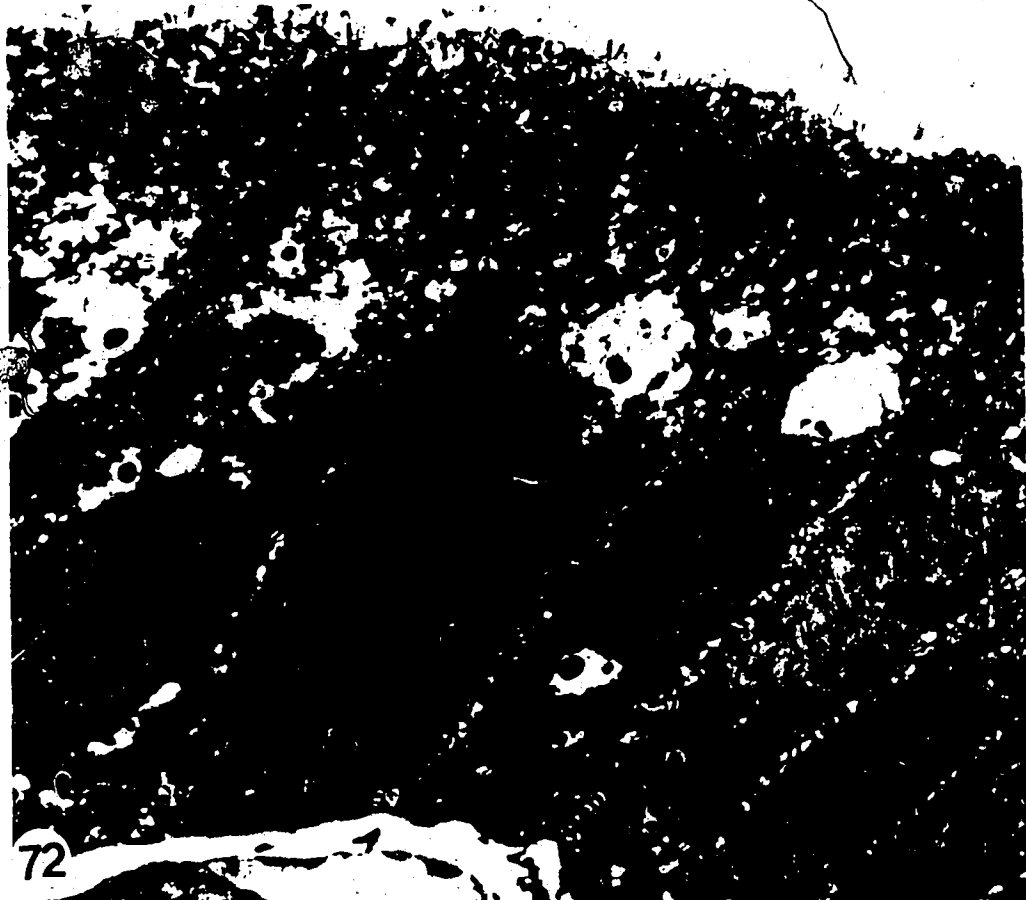
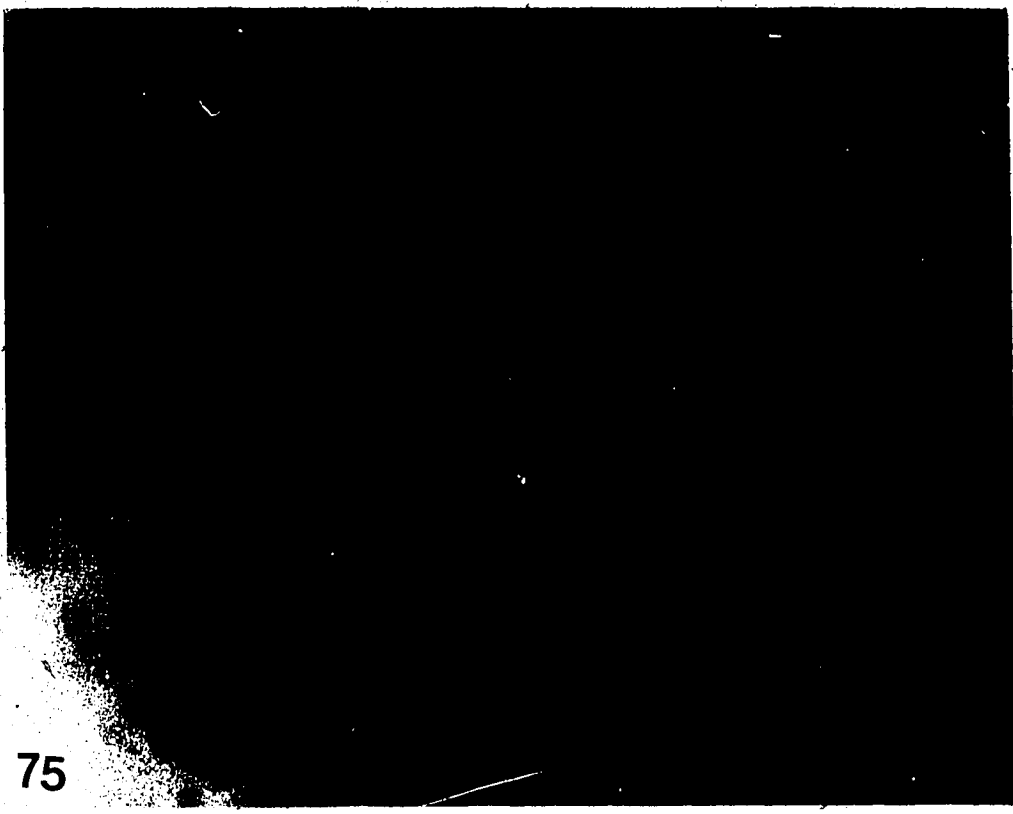
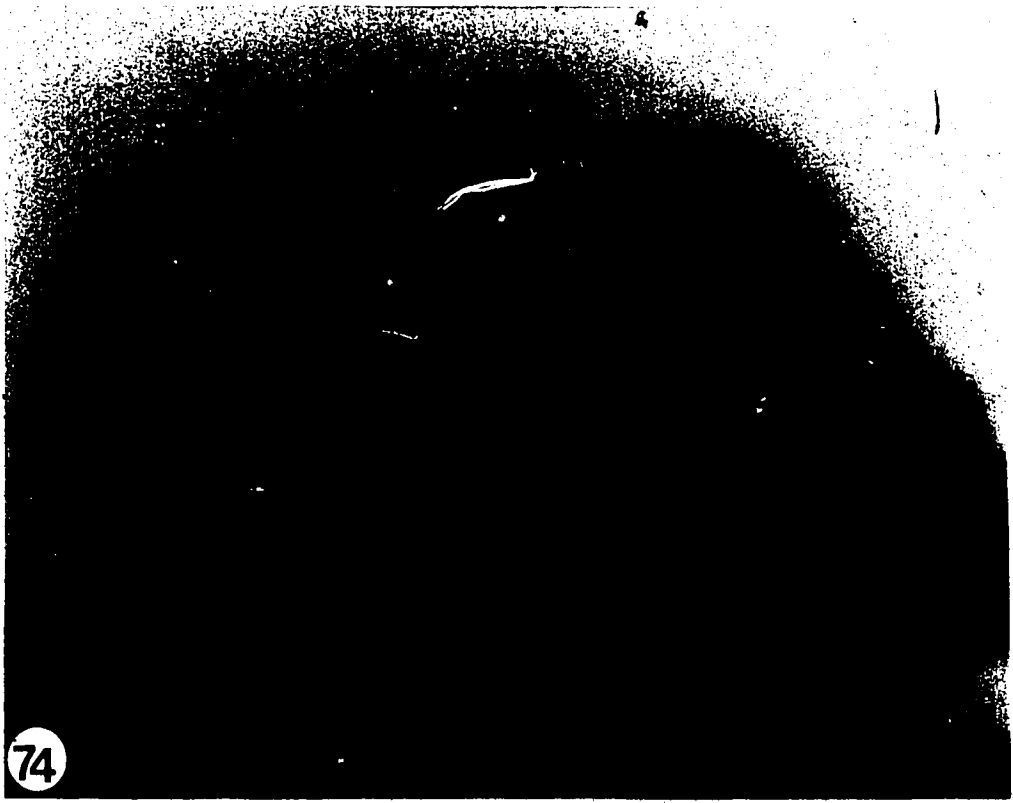


Figure 74: A frozen section of a control gallbladder stained with oil red O. Note the absence of any colored precipitate. Scale bar = 20 μ m.

Figure 75: A frozen section from a five day-treated animal stained with oil red O. Neutral lipid is demonstrated in the supranuclear regions of cells. Scale bar = 20 μ m.




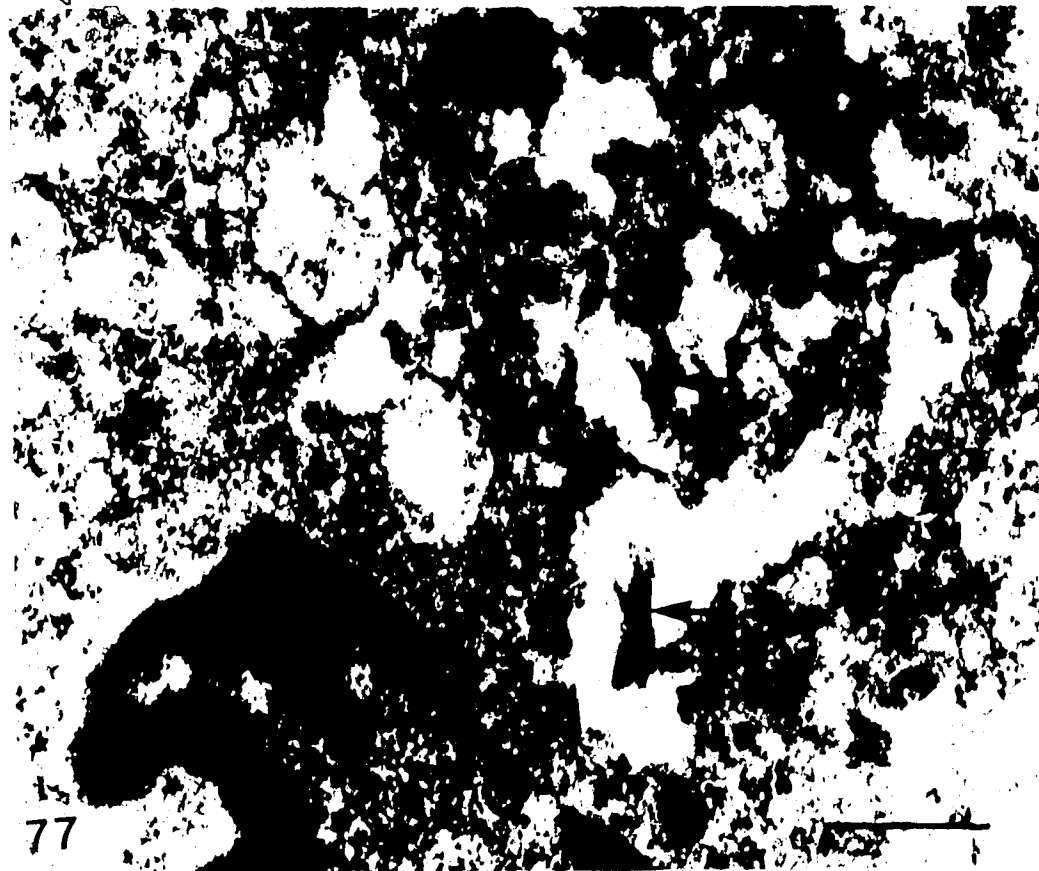
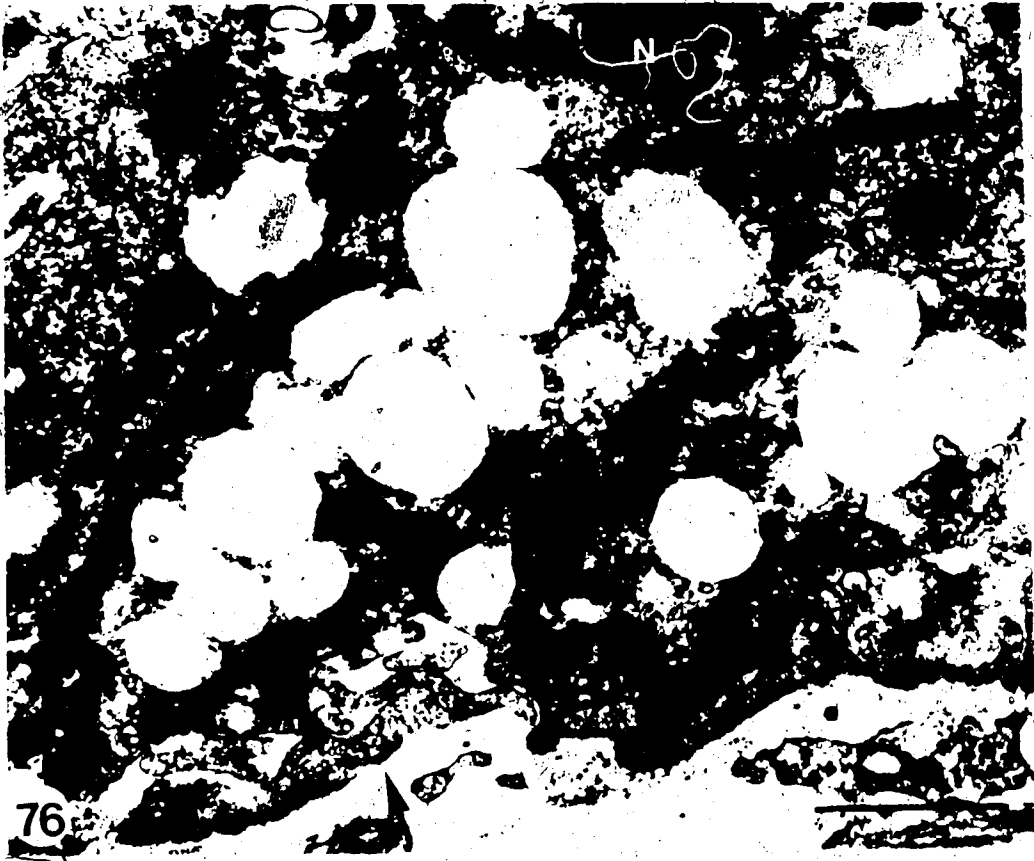


Figure 76: An electron micrograph of a two week-treated animal showing lipid droplets in the basal regions of epithelial cells. Arrow- basal lamina, - nucleus. Scale bar = 1 μ m.

Figure 77: Tissue from the gallbladder of a seven day treated animal complexed with digitonin to demonstrate free cholesterol (arrows) in dilated cisternae. Scale bar = 0.5 μ m.






Figure 78: Digitonin complexing with free cholesterol to demonstrate its deposition within a residual body (arrows) of a seven day treated animal. M- mitochondrion, L- lipid. Scale bar = 0.2 μ m

Figure 79: Tissue from a seven day treated animal complexed with digitonin demonstrating cholesterol crystals on the surface of epithelial cells. Scale bar = 1 μ m.

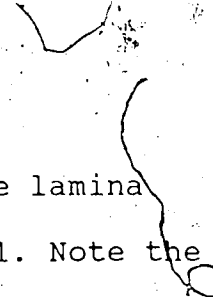
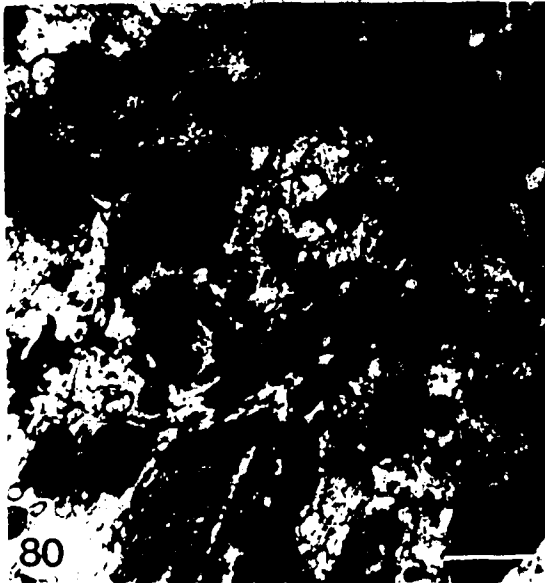
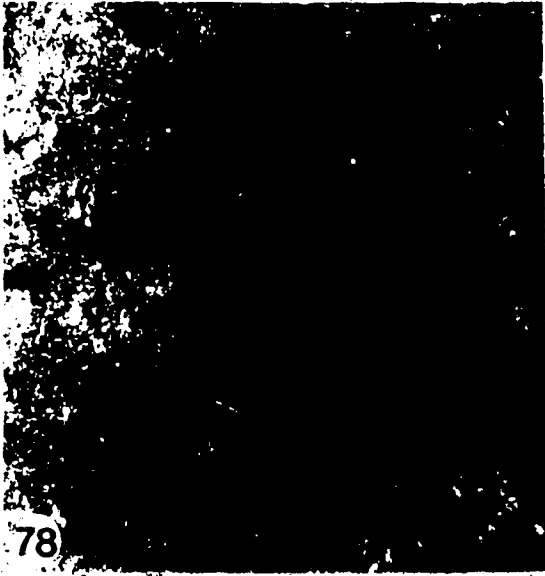


Figure 80: Dense osmiophilic droplets in the lamina propria of a 20 week treated animal. Note the presence of a few electron lucent lipid droplets (arrows). Ep- epithelial cells. Scale bar = 1 μ m.

Figure 81: A macrophage in the lamina propria with numerous dense inclusions. Ep- epithelial cells, Pl- plasma cell, C- capillary. Scale bar = 2 μ m.



BIBLIOGRAPHY

Admirand WH, Small DM. The physiochemical basis of cholesterol gallstone in man. *J Clin Invest* 1968; 47:1043- 1052.

Albores-Saavendra J, Alcantra-Vazquez A, Cruz-Ortiz H, Herrera-Goepfert R. The precursor lesions of invasive gallbladder carcinoma. Hyperplasia, atypical hyperplasias and carcinoma-in-situ. *Cancer* 1986; 45:919-927.

Allain CC, Poon LS, Chan CGS, Richmond W, Fu PC. Enzymatic determination of total serum cholesterol. *Clin Chem* 1974; 20:470- 475.

Allen A. Structure and function of gastrointestinal mucus. In: *Physiology of the gastrointestinal tract*. Johnson LR ed. New York, Raven press 1981; chap 21:617-639.

Allen B, Bernhoft R, Blanckaert N, Svanvik J, Filly R, Gooding G, Way L. Sludge is calcium bilirubinate associated with bile stasis. *Am J Surg* 1981; 141:51-56.

Bader G. Die submikroskopische Struktur des Gallenblasenepithels und seine Regeneration. 1. Mitt.: karpfen (*Cyprinus carpio*, L.) and Frosch (*Rana esculenta*, L.). *Z mikr anat Forsch* 1965; 74:92-107.

Bargmann W. *Histologie und mikroskopische Anatomie des Menschen*, 3rd edition. Thieme: Stuttgart, 1959:500.

Barlett GR. Phosphorus assay in column chromatography. *J Biol Chem* 1959; 234:466-468.

Baumgarten HG, Lange WL. Extrinsic adrenergic innervation of the extrahepatic biliary system in guinea pigs, cats and rhesus monkeys. *Z Zellforsch*. 1969; 100:606-615.

Been JM, Bills PM, Lewis D. Microstructure of gallstones. *Gastroenterology* 1979; 76:548-555.

Bernhoft RA, Pellegrini CA, Broderick WC, Way LC. Pigment sludge and stone formation in acutely ligated dog gallbladder. *Gastroenterology* 1983; 85:1166-1171.

Bjorck S, Jansson R, Svanvik J. Adrenergic influence on concentrating function in the feline gall bladder. *Gut* 1982; 23:1019-1023.

Bouchier IAD. Biochemistry of gallstone formation. *Clin Gastroenterology* 1983; 12:25-48.

Bouchier IAD. Debits and credits: a current account of cholesterol gall stone disease. *Gut* 1984; 25:1021-1028.

Boyd W. Studies in gallbladder pathology. *Br J Surg* 1922; 10:337-342.

Brenneman DW, Conner WE, Forker EL, DenBesten L. The formation of abnormal bile and cholesterol gallstones from dietary cholesterol in the prairie dog. *J Clin Invest* 1952; 51:1495-1503.

Brown MS, Goldstein JL. How LDL receptors influence cholesterol and atherosclerosis. *Sci Am* 1984; 251:58-66.

Brown MS, Goldstein JL. A receptor-mediated pathway for cholesterol homeostasis. *Science* 1986; 232:34-47.

Budd GC. High resolution autoradiography. In: Gahan PB, ed. *Autoradiography for Biologists*, London and New York: Academic press, 1972:95-116.

Cai W-Q, Gabella G. Innervation of the gallbladder and biliary pathways in the guinea pig. *J Anat* 1983; 136:97-109.

Cai W-Q, Gabella G. Catecholamine-containing cells in the nerve plexus of the guinea pig gallbladder. *Acta anat* 1984; 119:10-17.

Carey MC. Critical tables for calculating the cholesterol saturation of native bile. *J Lipid Res* 1978; 19:945-955.

Carr JJ, Drekter IJ. Simplified rapid technic for the extraction and determination of serum cholesterol without saponification. *Clin Chem* 1956; 2:353-368.

Chang S-H, HO K-J, Taylor CB. Cholesterol gallstone formation and its regression in prairie dogs. *Arch Pathol* 1973; 96:417-426.

Cohen BI, Singhal AK, Stenger RJ, May-Donath P, Finver-Sadowsky J, McSherry CK, Mosbach EH. Effects of bile acids oxazolines on gallstone formation in prairie dogs. *Lipids* 1984; 9:515-521.

Conter RL, Roslyn JJ, Porter-Fink V, DenBesten L. Gallbladder absorption increases during early cholesterol gallstone formation. *Am J Surg* 1986; 151:184-191.

Dam H. Determinants of cholesterol cholelithiasis in man and animals. *Am J Med* 51:596-613.

Davenport HW. Physiology of the digestive tract. Davenport HW ed. 3rd edition, Year Bk Med Publ 1971; 197-210.

Davidson NO, Glickman RM. Lipid absorption in man. In: Progress in Gastroenterology. Glass GBJ, Sherlock P, eds. 1983; 1V:57-75.

Davison JS, Frickhandler TM, Kelly J, Shaffer EA. Reduced gallbladder contractility associated with increased bile lithogenicity in the ground squirrel. *J Physiol* 1982; 329:41.

DenBesten L, Safaie-Shirazi S, Connor WE, Bell S. Early changes in bile composition and gallstone formation induced by a high cholesterol diet in prairie dogs. *Gastroenterology* 1974; 66:1036-1045.

Diamond JM, Bossert WH. Standing gradient osmotic flow. *J Gen*

Physiol 1967; 50:2061-2083.

Diehl AK. Guest editorial. Epidemiology of gallbladder cancer: A synthesis of recent data. J Natl Cancer Inst 1980; 65:1209-1214.

Dietschy JM. Recent developments in solute and water transport across the gallbladder epithelium. Gastroenterology 1966; 50:692-707.

Doty JE, Pitt HA, Kuchenbecker SL, DenBesten LW. Impaired gallbladder emptying before gallstone formation in the prairie dog. Gastroenterology 1983a; 85:168-174.

Doty JE, Pitt HA, Kuchenbecker SL, Porter-Fink V, DenBesten LW. Role of gallbladder mucus in the pathogenesis of cholesterol gallstones. Am J Surg 1983b; 145:54-61.

Dyban PA. Autoradiographic investigation of cell renewal in the gallbladder epithelium. Bull Exp Biol Med 1973; 76:102-105.

Edlund Y, Olsson O. Acute cholecystitis; its etiology and course with special reference to the timing of cholecystectomy. Acta Chir Scand 1961; 120:479-494.

Ely JW, Hall RC, Tepperman J. Mucus production in gallstone formation- autoradiographs using tritiated galactose. Surg Forum 1971; 22:383-384.

Engert R, Turner MD. Problems in the measurement of bile acids with 3, -hydroxysteroid dehydrogenase. Anal Biochem 1973; 51:399-407.

English M, Hopwood D. Lipid in the human gallbladder mucosa. A histochemical study by light and electron microscopy. J Path 1985; 146:333-336.

Esterly JR, Spicer SS. Mucin histochemistry of human gallbladder: changes in adenocarcinoma, cystic fibrosis and cholecystitis. J Natl Canc Inst 1968; 40:1-11.

- Evett RD, Higgins JA, Brown AL. The fine structure of normal mucosa in human gallbladder. *Gastroenterology* 1964; 47:49-71.
- Ferner H. Uber das Epithel der menschlichen Gallenblase. *Zeitschr Zellf* 1949; 34:503-513.
- Florey HW. The secretion of mucus and inflammation of mucous membranes. In: HW Florey, ed. *General Pathology*. London: Lloyd-Luke. 1970; 195-225.
- Forstner JF, Forstner GG. Calcium binding to intestinal goblet cell mucin. *Biochim Biophys Acta* 1975; 336: 283-291.
- Fox H. Ultrastructure of the human gallbladder epithelium in cholelithiasis and chronic cholecystitis. *J Path* 1972; 108:157-164.
- Freston JW, Bouchier IAD. Experimental cholelithiasis. *Gut* 1968; 9:2-4.
- Freston JW, Bouchier IAD, Newman J. Biliary mucosa substances in dihydrocholesterol-induced cholelithiasis. *Gastroenterology* 1969; 57:670-678.
- Fridhandler TM, Davison JS, Shaffer EA. Defective gallbladder contractility in the ground squirrel and prairie dog during the early stages of cholesterol gallstone formation. *Gastroenterology* 1983; 85:830-836.
- Ghadially FN. *Ultrastructural pathology of cell and matrix*. 2nd. Butterworths, Toronto, 1984; 458-464, 716-719.
- Gollish SH, Burnstein MJ, Ilson RC, Petrunka CN, Strasberg SM. Nucleation of cholesterol monohydrate crystals from hepatic and gallbladder bile of patients with cholesterol gallstones. *Gut* 1983; 24:836-844.
- Gurl N, DenBesten L. Animal models of human cholesterol gallstone disease: a review. *Lab anim Sci* 1978; 28:428-432.

Halpert B. Significance of the Rokitansky-Aschoff sinuses. Am J Gastroenterol 1961; 36:534-539.

Harmon B, Bell L, Williams L. An ultrastructural study on the "meconium corpuscles" in rat fetal intestinal epithelium with particular reference to apoptosis. Anat Embryol 1984; 169:119-124.

Hayward AF. Aspects of the fine structure of the gallbladder epithelium of the mouse. J Anat 1962a; 96:227-236.

Hayward AF. Electron microscopic observations on absorption in the epithelium of the guinea pig gallbladder. Z Zellforsch 1962b; 56:197-202.

Hayward AF. The fine structure of the gallbladder of the sheep. Z Zellforsch 1965; 65:331-339.

Hayward AF. An electron microscopic study of developing gallbladder epithelium in the rabbit. J Anat 1966; 100:245-259.

Hayward AF. The structure of the gallbladder epithelium. Int Rev Exp Zool 1968; 3:205-239.

Hayward AF, Freston JW, Bouchier IAD. Changes in the ultrastructure of gallbladder epithelium in rabbits with experimental stones. Gut 1968; 9:550-556.

Hofmann AF. Animal models of calcium cholelithiasis. Hepatology 1984; 4:209S-211S.

Holan KR, Holzbach RT, Hermann RE, Cooperman AM, Claffey WJ. Nucleation time: a key factor in the pathogenesis of cholesterol gallstone disease. Gastroenterology 1979; 72:611-617.

Holzbach RT. Animal models of cholesterol gallstone disease. Hepatology 1984; 4:191S-198S.

Holzbach RT. Recent progress in understanding cholesterol crystal nucleation as a precursor to human gallstone formation. *Hepatology* 1986; 6:1403-1406.

Holzbach RT, Marsch M, Tang P. Cholesterolosis; Physiochemical characteristics of human and diet-induced canine lesions. *Exp Mol Path* 1977; 27:324-338.

Hopwood D, Kouroumalis E, Milne G, Bouchier IAD. Cholecystitis: a fine structural analysis. *J Path* 1980; 130:1-13.

Hopwood D, Ross P, Milne G, Bouchier IAD. Oleic acid transport by the gallbladder epithelium. *J Path* 1983; 140:128.

Hora F, Schulz H. Ultrastructure of the strawberry gallbladder. *Beitr Path Anat* 1970; 141:195-212.

Hutton SW, Sievert CE, Vennes JA, Duane WC. Inhibition of gallstone formation by sphincterotomy in the prairie dog: reversal by atropine. *Gastroenterology* 1982; 82:1308-1313.

Illingworth DFW. Cholesterolosis of the gallbladder: A clinical and experimental study. *Br J Surg* 1929; 17:208-229.

Imamoglu K, Perry JF Jr, Wangenstein OH. Experimental production of gallstones by incomplete stricture of the terminal duct. *Surgery* 1957; 42:623-630.

Jacoby F. Mitotic activity in the gallbladder epithelium of the guinea-pig after ligation of the common bile duct. *J Physiol (Lond)* 1958; 199:21P-22P.

Johnson FR, McMinn RM, Birchenough RF. The ultrastructure of the gallbladder of the dog. *J Anat* 1962. 96: 477-487.

Juniper K, Burson EN. Biliary tract studies. 11. The significance of biliary crystals. *Gastroenterology* 1957; 32:175-211.

Kaye GI, Maenza RM, Lane N. Cell replication in the rabbit gallbladder. *Gastroenterology* 1966; 51:670-680.

Kaye GI, Wheller HO, Witlock RT, Lane N. Fluid transport in the rabbit gallbladder -a combined physiological and electron microscopic study. *J Cell Biol* 1968; 30:237-268.

Kerr JFR, Wyllie AH, Currie AR. Apoptosis: a basic biologic phenomenon with wide-ranging implications in tissue kinetics. *Br J Cancer* 1972; 26:239-257.

Kilburn KH, Lynn WS, Tres LL, McKenzie WN. Leukocyte recruitment through airway walls by condensed vegetable tannins and quercetin. *Lab Invest* 1973; 28:55-59.

Koga A. Electron microscopic observations on the mucous secretory activity and the human gallbladder epithelium. *Z Zellforsch* 1973; 139:463-471.

Koga A. Fine structure of the human gallbladder with cholesterolosis with special reference to the mechanism of lipid accumulation. *Br J exp Path* 1986; 66:605-611.

Koga A, Todo, Nishimura M. Electron microscopic observations on the cholesterol distributed in the epithelial cell of the gallbladder. *Histochemistry* 1975; 44:303-306.

Kouroumalis E, Ross PE, Clarke A, Hopwood D, Bouchier IAD. Cholesterol esters in the gallbladder bile and mucosa from patients with cholecystitis. *Clin Chem acta* 1984; 144:145-154.

Kyosola K, Penttila O. Adrenergic innervation of the human gallbladder. *Histochemistry* 1977; 54:209-2117.

Laito M, Nevalainen T. Scanning and transmission electron microscope observations on the human gallbladder epithelium. 11. Foetal development. *Z Anat Entwickl Gesch* 1972; 136:326-335.

LaMont JT, Smith BF, Moore JRL. Role of gallbladder mucin in

pathophysiology of gallstones. Gastroenterology 1984;
4:51S-56S.

LaMont JT, Turner BS, DiBenedetto D, Handin R, Schafer AI.
Arachidonic acid stimulates mucin secretion in prairie
dog gallbladder. Am J Physiol 1983; 245:G92-G98.

LaMote J, Putz P, Francois M, Willems G. DNA synthesis
index: higher for human gallbladders with cholesterol
stones than pigment stones. J Natl Cancer Inst 1983;
71:449-453.

Langone R. Heart attack and cholesterol. Discover March
1984; 21-26.

Lee SP. The mechanism of mucus secretion by the gallbladder
epithelium. Br J exp Pathol 1980; 61:117-119.

Lee SP. Hypersecretion of mucus glycoprotein by the
gallbladder epithelium in experimental cholelithiasis.
J Pathol 1981; 134:199-207.

Lee SP, Carey MC, LaMont JT. Aspirin prevention of
cholesterol gallstone formation in prairie dog
gallbladder. Science 1981a; 211:1429-1432.

Lee SP, LaMont JT, Carey MC. Role of gallbladder mucus
hypersecretion in the evolution of cholesterol
gallstones. Studies in the prairie dog. J Clin Invest
1981b; 67:1712-1723.

Lee SP, Lim TH, Scott AJ. Carbohydrate moieties of
glycoprotein in human hepatic and gallbladder mucosa
and gallstones. Clin Sci 1979; 56:533-538.

Lee SP, Nicholls JF. Nature and composition of biliary
sludge. Gastroenterology 1986; 90:677-686.

Lee SP, Scott AJ. Dihydrocholesterol-induced gallstones in
the rabbit: Evidence for bile acid injury to cell
membrane. Br J exp Pathol 1979; 60:231-237.

- Lee SP, Scott AJ. Further observations in lincomycin-induced cholelithiasis in guinea pigs J Pathol 1980; 131:117-125.
- Lee SP, Scott AJ. The evolution of morphologic changes in the gallbladder before stone formation in mice fed a cholesterol-cholic acid diet. Am J Pathol 1982; 108:1-8.
- Lee SP, Tasman-Jones C, Carlisle V. Oleic acid-induced cholelithiasis in rabbits. Am J Pathol 1986; 124:18-24.
- Levy PF, Smith BF, Atkinson D, LaMont JT. Human gallbladder mucin enhances in vitro nucleation of cholesterol monohydrate crystals (Abstract). Gastroenterology 1983;84:1382.
- Levy PF, Smith BF, LaMont JT. Human gallbladder mucin accelerates in vitro nucleation of cholesterol in artificial bile. Gastroenterology 1984; 87:270-275.
- Lofland H. Animal model of human disease: cholelithiasis. Am J Path 1975; 79:619-622.
- Luciano L, Reale E, Wolpers C. Die Feinstruktur der Gallenblase und der Gallengänge. V. Histochemische Lokalisierung von Mukostanzen im menschlichen Gallenblasenepithel. Histochemistry 1974; 38:57-79.
- Luciano L, Wolpers. Die Feinstruktur der Gallenblase und der Gallengänge, 1V. Die Cholesterose der menschlichen Gallenbladschleimhaut. Virchows Arch Abt B Zellpath 1973; 14:147-158.
- Luna LG. Manual of histologic staining methods of the Armed Forces Institute of Pathology. 3rd edition, McGraw-Hill, Toronto, 1968; 1-250.
- Mackey WA. Cholesterolosis of the gallbladder. A further contribution to the histology of this condition. Br J Surg 1941; 28:462-467.

MacPherson BR, Scott GW, Lennon F. Morphology of canine gallbladder. Scanning electron microscope observations on the epithelium. Cell Tissue Res 1983; 233:161-174.

Maki T. Pathogenesis of calcium bilirubinate gallstones: role of E. coli, B-glucuronidase and coagulation by inorganic ions, polyelectrolytes and agitation. Ann Surg 1966; 164:90-100.

Malet PF. Animal models of gallstone formation, Contemporary Issues in gastroenterology 1985; 4:309-333.

Marsch-Zeigler U, Palme G. The influence of cholic acid and cholesterol on cell proliferation in the mucosa of the mouse. Virchows Arch (Cell Pathol) 1982; 39:217-228.

Mentzer SH. Cholesterolosis of the gallbladder. Am J Path 1925; 1:383-388.

Miettinen TA, Tilvis RS. Cholesterolosis. Contemporary issues in Gastroenterology 1985; 4:267-273.

Moynihan BGA. A disease of the gallbladder requiring cholecystectomy. Ann Surg 1909; 50:1265-1272.

Mueller JC, Jones AL, Long JA. Topographic and subcellular anatomy of the guinea pig gallbladder. Gastroenterology, 1972; 63:856-868.

Myllarniemie H, Nickels JI. Observations by scanning electron microscopy of normal and pathological human gallbladder epithelium. Acta path microbiol Scand Sect A 1977; 85:42-48.

Naunyn B. Die Gallenstein, ihre Entstehung und ihre Bau. Mitteil. Grenzgeb Med Chir 1921; 33:1-54.

Neiderhiser DH, Harmon CK, Roth HP. Absorption of cholesterol by the gallbladder. J Lip Res 1976; 17:117-124.

Neiderhiser DH, Morningstar WA, Roth HP. Absorption of

lecithin and lysolecithin by the gallbladder. J Lab Clin Med 1973; 82:891-897.

Neiderhiser DH, Pineda FM, Hejduk LJ, Roth HP. Absorption of oleic acid by the guinea pig gallbladder. J Lab Clin Med 1971; 77:985-992.

Neiderhiser DH, Thornell E, Bjork S. The effect of lysophosphatidylcholine on gallbladder function of the cat. J Lab Clin Med 1983; 101:699-707

Nevalainen T, Laito M. Ultrastructure of the gallbladder with cholesterolosis. Virchows Arch Abt B Zellpath 1972; 10:337-342.

Ogata T, Murata F. Scanning electron microscopic study of cholesterol gallstones. Tohoku J Exp Med 1971; 104:25-44.

Ojeda VJ, Shilkin KB, Walters MN-I. Premalignant epithelial lesions of the gallbladder: a prospective study of 120 cholecystectomy specimens. Pathology 1985; 17:451-454.

Okros I. Digitonin reaction in electron microscopy. Histochemie 1968; 13:91-96.

Osuga T, Mitamura K, Miyagawa S, Sato N, Kintaka S, Portman OW. A scanning electron microscopic study of gallstone development in man. Lab Invest 1975; 31:696-704.

Osuga T, Portman OW, Mitamura K, Alexander M. A morphologic study of gallstone development in the squirrel monkey. Lab Invest 1974; 30:486-493.

Patton OH, Plotner K, Cox GE, Taylor CB. Biliary cholesterol deposits in ground squirrels and prairie dogs. Fed Proc 1961; 20:248.

Palmér RH. Bile salts and the liver. In: Progress in liver diseases. Popper H, Schaffner F eds. Vol 7, New York, Grune and Stratton, 1984; 221-242.

Paumgartner G, Paumgartner D. Current concepts of bile formation. In: Progress in liver diseases. Popper H, Schaffner F eds. Vol 7, New York, Grune and Stratton, 1984; 207-220.

Paumgartner G, Sauerbruch T. Secretion, composition and flow of bile. Clinics in Gastroenterology 1983; 12:3-22.

Pearlman BJ, Bonorris CG, Philips MJ, Chung A, Vimadala S, Marks JW, Schoenfield LJ. Cholesterol gallstone formation and prevention by chenodeoxycholic and ursodeoxycholic acids. A new hamster model. Gastroenterology 1979; 77:634-641.

Pearse AGE. In: Histochemistry, theoretical and applied. Vol.1. London: A Churchill ltd., 1968:659-674.

Pikula JV, Dunphy JE. Some effects of stenosis of the terminal common bile duct on the biliary tract and liver. N Eng J Med 1959; 360:315-318.

Pradal G, Lefranc G, Mollat F, Vo H, Riet A. A quantitative assessment of the glandular activity of endocrine cells of gastrointestinal mucosae by computer-assisted analysis of ultrastructural images: methodology. Biol Cell 1984; 50:147-156.

Putz P, Willems G. Proliferative changes in the epithelium of the human lithiasic gallbladder. J Natl Cancer Inst 1978; 60:283-287.

Putz P, Willems G. Cell proliferation in the human gallbladder epithelium: Effects of distension. Gut 1979; 20:246-248.

Putz P, Willems G. Effects of a lithogenic diet on cell proliferation in the murine gallbladder epithelium. Digestion 1981; 22:16-23.

Rains AJH. Gallstones. Causes and treatment. Springfield, Ill. Thomas CC; 1964.

- Reid PE, Owen DA, Ramey CW, Dunn WL, Clay MG, Jones EA. Histochemical procedures for the simultaneous visualization of sialic acid, its side chain O-acyl variants and O-sulphate ester. *Histochem J* 1985; 17:113-117.
- Reynolds ES. The use of lead citrate at a high pH as an electron opaque stain for electron microscopy. *J Cell Biol* 1963; 17:208-212.
- Ross PE, Azman M, Hopwood D, Shepherd A, Ramsay A, Bouchier IAD. Lipid absorption by the human gallbladder. *Ann N Y Acad Sci* 1986; 463:344-346.
- Salmenkivi K. Cholesterolosis of the gallbladder: a clinical study based on 269 cholecystectomies. *Acta Chir Scand* 1964; 324 (Suppl):1-93.
- Schoenfield LJ. Animal models of gallstone formation. *Gastroenterology* 1972; 63:189-191.
- Scott AJ. Are there proliferative compartments in the gallbladder? *Gastroenterology* 1974; 67:1231-1237.
- Scott AJ. Lincomycin-induced cholecystitis and gallstones in guinea pigs. *Gastroenterology* 1976; 71:814-820.
- Scott AJ. Epithelial cell proliferation in diverse models of experimental cholelithiasis. *Gut* 1978; 19:558-562.
- Sedaghat A, Grundy SM. Cholesterol crystals and the formation of cholesterol gallstones. *N Engl J Med* 1980; 302:1274-1277.
- Shaffer EA. The pathogenesis of gallstone formation. *Ann Roy Coll Phy Surg Can* 1980; 13:18-20.
- Sheltawy MJ, Losowsky MS. Determination of faecal bile acids by an enzymatic method. *Clin Chim Acta* 1975; 64:127-132.

Singhal AK, Cohen BF, Mosbach EH, Upe M, Stenger RJ, McSherry
Max Donath P, Palaia T. Prevention of cholesterol-
ced gallstones by hyodeoxycholic acid in the
rie dog. J Lipid Res 1984; 25:539-549.

Small DM. Cholesterol nucleation and growth in gallstone
formation. N Engl J Med 1980; 302:1305-1307.

Smith BF, LaMont JT. Bovine gallbladder mucin binds bilirubin
in vitro. Gastroenterology 1983; 85:707-712.

Smith BF, Lamont JT. Identification of gallbladder mucin
bilirubin complex in human cholesterol gallstone
matrix. Effects of reducing agents on in vitro
dissolution of matrix and intact gallstones. J Clin.
Invest 1985a; 76:439-445.

Smith BF, LaMont. JT. Gallbladder mucin and gallstone
formation. Contemporary issues in gastroenterology
1985b; 4:101-111.

Soloway RD, Trotman BW, Ostrow JD. Pigment gallstones.
Gastroenterology 1977; 72:167-182.

Spicer SS. Diamine methods for differentiating
mucosubstances histochemically. J Histochem Cytochem
1965; 13:211-234.

Spring KR. Fluid transport by gallbladder epithelium. J exp
Biol 1983; 106:181-194.

Subbiah MTR, Dicke BA. Presence of cholesterol ester
synthetase in the guinea pig gallbladder epithelium.
Biochem Biophys Res Commun 1977; 74:1273-1279.

Sweet JE. The formation of gallstones. Ann Surg 1950;
150:624.

Tamura K. Consideration for the mechanism of formation of
cholesterol stones. Nippon Geka Gakkai Zasshi (Jap)
1943; 44:42-48.

Tepperman J, Weiner M. Experimental gallstones: an adventure in biological geology. *Yale J Biol Med* 1968; 41:107-119.

Thomas PJ, Hoffmann AF. A simple calculation of the lithogenic index of bile: Expressing biliary lipid composition as a rectangular coordinates. *Gastroenterology* 1973; 65:698-699.

Tilvis RS, Aro J, Strandberg TE, Lempinen M, Miettinen TA. Lipid composition of bile and gallbladder mucosa in patients with acalculous cholesterolosis. *Gastroenterology* 1982; 82:607-615.

Togari C, Okada T. The minute structure of the human gallbladder. *Okijamas Folio Anat Japan* 1953; 25:1-12.

Tormey J McD, Diamond JM. The ultrastructural route of fluid transport in the rabbit gallbladder. *J Gen Physiol* 1967; 50:2031-2060.

Trump BF, Arstila AU. Cell injury and cell death. In: *Principles of pathobiology*. Lavia MF and Hill RB, eds. Oxford University Press, London 1976; 9-95.

Turley SD, Dietschy JM. Cholesterol metabolism and excretion. In: *The liver: biology and pathobiology*. Arias I and Schachter D eds. chap 28, New York, Raven press 1982; 467-492.

Van der Linden W, Bergman F. Formation and dissolution of gallstones in experimental animals. *Int Rev Exp Path* 1977; 17:174-233.

Vayda E. Comparison of surgical rates in Canada and in England and Wales. *N Engl J Med* 1973; 289:1224-1229.

Virchow R. Ueber das Epithel der Gallenblase und uber einen intermediaren Stoffwechsel des Fettes. *Virchows Archiv*. 1857; 11:574-578.

Wahlin T. Synthesis of glycoproteins in the Golgi complex of the mouse gallbladder epithelium during fasting, refeeding, and gallstone formation. A light microscopic, autoradiographic and quantitative electron microscopic study. *Histochemistry* 1977; 51:133-140.

Wahlin T. Histochemical analysis of mucosubstances and cytochemical studies of the Golgi region and secretory granules of the normal gerbil principal cells. *Acta anat* 1979; 103:468-476.

Wahlin T, Schiebler TH. Zur entwicklung des Gallenblasenepithels des meerschweinchens. 11. Elektronenmikroskopische und enzymhistochemische untersuchungen. *Histochemistry* 1975; 44:253-275.

Wahlin T, Bloom GD, Carlsoo B. Histochemical observations with the light and electron microscope on the mucosubstances of the normal mouse gallbladder epithelial cells. *Histochemistry* 1974; 42:119-131..

Wahlin T, Bloom GD, Danielsson A. Effect of cholecystokinin-pancreozymin (CCK-PZ) on glycoprotein secretion from gallbladder epithelium. *Cell Tiss. Res.* 1976; 171:425-435.

Wahlin T, Bloom GD, Carlsoo B, Rhodin L. Effects of fasting and refeeding on secretory granules of the mouse gallbladder epithelium. A quantitative electron microscopic study. *Gastroenterology* 1976; 70:353-358.

Weibel ER, Elias H. Introduction to stereological principles. In: *Quantitative methods in morphology*. Berlin, Springer 1967; 89-98.

Weiser HB, Gray GR. Colloidal phenomena in gallstones. *J Phys Chem* 1932; 36:286-299.

Wheeler HO. Concentrating function of the gallbladder. *Am Med* 1971; 51: 588-595.

Whiting MJ, Watts JMCK. Supersaturated bile from obese patients without gallstones supports cholesterol

crystal growth but not nucleation. Gastroenterology
1984; 86:243-248.

Whiting MJ, Watts JMCK. Cholesterol gallstone pathogenesis: a
study of potential nucleating agents for cholesterol
crystal formation in bile. Clin Sci 1985; 68:589-596.

Williams AE, Smith J. A scanning electron microscope study of
the normal and pathological human gallbladder. Scanning
Electron Microscopy 1978; 11:713-719.

Williamson JR. Ultrastructural localization of free
cholesterol (3 B-hydroxysterols) in tissues. J
Ultrastruct Res 1969; 27:118-123.

Womack NA. The development of gallstones. Surg Gynecol Obstet
1971; 133:937-945.

Womack NA, Haffner H. Cholesterolosis: Its significance in
the badly damaged gallbladder. Ann Surg 1944; 119:392-
401.

Womack NA, Zeppa R, Irvin GL. The anatomy of gallstones. Ann
Surg 1963; 157:670-686.

Wyllie AH, Kerr JFR, Currie AR. Cell death: the significance
of apoptosis. Int Rev Cytol 1980; 68:251-306.

Yamada E. The fine structure of the gallbladder epithelium
of the mouse. J biophys biochem Cytol 1955; 1:445-458.

Yamada K. Chemocytological observations on two peculiar
epithelial cell types in the gallbladders of laboratory
rodents. Z Zellforsch mikrosk Anat 1962a; 56:180-187.

Yamada K. Morphological and histochemical aspects of
secretion in the gallbladder of the guinea pig. Anat
Rec 1962b; 144:117-123.

Yamada K. Some observations on the fine structure of light
and dark cells in the gallbladder epithelium of the

mouse. Z. Zellforsch. mikrosk Anat 1968; 84:463-472.

Zak RA, Frenkiel PG, Marks JW, Bonorris GG, Allen A, Schoenfield LJ. Cyclic nucleotides and glycoproteins during formation of cholesterol gallstones in the prairie dogs. Gastroenterology 1984; 87:263

Appendix I

0.2M Buffer solution

Solution A: 27.6 g sodium phosphate Monobasic/1 liter/DH₂O

Solution B: 28.4 g sodium phosphate Dibasic/1 liter/DH₂O

0.1M Buffer solution pH 7.4

Solution A: 190 ml/1000 ml

Solution B: 810 ml/1000 ml

Dilute in 1000 ml DH₂O

Adjust pH with 1% calcium chloride solution

100 ml of 2.5% gluteraldehyde in 0.1M phosphate buffer solution

5 ml of 50% aqueous gluteraldehyde

95 ml of 0.1M phosphate buffer

1% osmium tetroxide in 0.1M phosphate buffer

1 g Osmium tetroxide

100 ml 0.1M phosphate buffer

Epon 812

Epon 812 resin	23 g
Dodecenyl succinic anhydride	11.3 g
Nadic methyl anhydride	11.1 g
DMP 30	0.8 g

0.1% Toluidine blue

- 0.1 g toluidine blue/100 ml DH₂O
- 0.1 g sodium borate in above solution

Saturated uranyl acetate.

uranyl acetate dissolved in DH₂O

Lead citrate

- Lead nitrate 1.33 g
- Sodium citrate 1.76 g
- Dissolved in 50 ml of DH₂O
- 2 pellets of sodium hydroxide

Lee's methylene blue - basic fuchsin (MBBF).

Methylene blue stock solution

Methylene blue.....0.5 g
 Distilled water.....400 ml

Basic fuchsin stock solution

Basic fuchsin.....0.5 g
 Distilled water.....400 ml

Stock buffer

Solution A: Sodium phosphate monobasic.....27.5 g
 Distilled water.....1000 ml

Solution B: Sodium phosphate dibasic.....71.5 g
 Distilled water.....1000 ml

Stock buffer pH should be 6.2-7.2. Higher pH levels produce deep blue results. Lower pH values give a pink tinge to sections.

Working solution

Methylene blue..... 12 ml
 Basic fuchsin solution..... 12 ml
 Solution A (stock solution)..... 7 ml
 Solution B (stock buffer)..... 18 ml
 95% ethyl alcohol..... 15 ml

Filter solution

Appendix II

Methacrylate fixation and processing

10% neutral buffered formalin.....24 h
70% alcohol.....1 h
85% alcohol.....1 h
95% alcohol (2 changes).....30 mins. each
Catalysed sol. A 85% alcohol (1:1).....1 h

Solution

A.....overnight

Embed tissue in mold with sol. A+B.....

Leave to harden at room temperature.....

Catalysed solution A

Sol. A (JB 4) 100 ml

Catalyst..... 0.9 ml

Mixed thoroughly for uniform solution.

Embedding mixture

Catalysed solution A..... 25 parts

Solution B..... 1 parts

Stir rapidly and thoroughly to avoid hardening

Appendix III

Procedure for transmission and scanning electron microscopy

Fix tissue in 2.5% gluteraldehyde for 4 hours

Wash 3 x 15 minutes in Milloning's buffer

Place tissue in 1% osmium for 1 hour

Wash 3 x 10 minutes in distilled water

Place tissue in saturated aqueous uranyl acetate

Pin SEM tissue on cork with no tension

30%, 50%, 70%, 90% ethanol for 15 minutes in each solution

TEM tissue

100% ethanol for 1 hour

1:1 ethanol/propylene oxide for 20 minutes

1:3 ethanol/ propylene oxide for 30 minutes

100% propylene oxide for 1 hour

3:1 propylene oxide/ epon mixture for 20 minutes

1:1 propylene oxide/ epon mixture for 30 minutes

1:3 propylene oxide/ epon mixture for 1 hour

100% epon mixture - over night

Embed in moulds in fresh epon

Heat in oven for 48 hours at 55°C

SEM tissue.

100% ethanol 3x 10 minutes

Absolute acetone- 2x 15 minutes

Critical-point dry

Coat with colloidal gold in sputter-coater

Appendix IV

TEM Digitonin Experiment

Tissue fixed in 2.5% gluteraldehyde for 4 hours

Place tissue in 2% digitonin solution dissolved in buffer
for 4 hours

Rinse in buffer

Post-fixed in 1% osmium tetroxide and process as above for
TEM

TEM autoradiography

Dipping method

Grids coated with 0.5% parlodion dissolved in amyl acetate
Attached to slide by parlodion

Silver sections picked in loop placed on grids

Slides dipped in Ilford L-4 emulsion diluted with water

1:6

Dripped dried, stored in light proof box for 3-4 weeks at
4°C and then developed:

Kodak D 19 for 3 minutes

Dipped in distilled water for 30 seconds

Fixed in 25% sodium thiosulphate for 6 minutes

Washed in distilled water for 6 minutes

Stained in uranyl acetate and lead citrate for 10 minutes
each.

Appendix V

Light microscopy autoradiography

Two micrometer thick methacrylate sections were cut
Slides were dipped in undiluted Ilford K.5 D emulsion
Dripped dried for 1 hour
Stored in light proof black box sealed with black tape
at 4°C for 3-4 weeks

Developed as follows:

Dektol diluted 1:1 with water for 2 minutes

Washed in water for 2 minutes

Fixed in Kodak fixer for 5 minutes

Washed in water for 15 minutes

Appendix VI

High Iron Diamine - Alcian blue pH 2.5

Paraffin sections cleared in:

Xylene for 5 minutes

Xylene for 5 minutes

100% ethanol for 3 minutes

95% " " 3 "

85% " " 3 "

70% " " 3 "

Distilled water for 3 minutes.

Stain for 24 hours in a fresh solution of:

N,N- dimethyl-m-phenylenediamine di HCL.....1.68 g

N,N-dimethyl-p-phenylenediamine HCL.....0.28 g

Dissolve these two in 750 ml of distilled water

Immediately add 19.6 ml of 40% ferric chloride to activate
the solution

Rinse quickly in distilled water

Stained in Alcian blue pH 2.5 for 20 minutes

Alcian blue 8GX..... 1.00 g

Glacial acetic acid..... 100.0 g

Adjust the pH to 2.5 and filter solution. Add a few crystal
of thymol

Rinse quickly in distilled water

70%, 85%, 95%, 100% ethanol for 3 minutes each

Xylene (twice) for 5 minutes

Mount in permount.

Results

Sulphomucins - grey-purple black

Sialic acid - Blue (aqua)

Appendix VII

Potassium hydroxide/alcian blue pH 1.0/ periodic acid-
phenylhydrazine- Schiff

Cleared paraffin sections as above

Saponify in 0.5% KOH in 70% ethanol for 15 minutes

Wash slowly in running tap water for 5 minutes

Stain in 1% alcian blue in 0.1N HCL (pH 1.0)

Oxidize in 1% aqueous periodic acid for 2 hours

Wash slowly in tap water for 10 minutes

Treat with 0.5% aqueous phenylhydrazine hydrochloride for 2
hours

Wash in running water for 5 minutes

Stain with freshly prepared Basic Fuchsin-Schiff for 4 hours

Bring to water as above

Results

Sialic acids with side chain substitutions..... Red

Tissue vicinal diols..... Red

O-sulphate esters..... Blue